



저작자표시-비영리-변경금지 2.0 대한민국

이용자는 아래의 조건을 따르는 경우에 한하여 자유롭게

- 이 저작물을 복제, 배포, 전송, 전시, 공연 및 방송할 수 있습니다.

다음과 같은 조건을 따라야 합니다:



저작자표시. 귀하는 원저작자를 표시하여야 합니다.



비영리. 귀하는 이 저작물을 영리 목적으로 이용할 수 없습니다.



변경금지. 귀하는 이 저작물을 개작, 변형 또는 가공할 수 없습니다.

- 귀하는, 이 저작물의 재이용이나 배포의 경우, 이 저작물에 적용된 이용허락조건을 명확하게 나타내어야 합니다.
- 저작권자로부터 별도의 허가를 받으면 이러한 조건들은 적용되지 않습니다.

저작권법에 따른 이용자의 권리는 위의 내용에 의하여 영향을 받지 않습니다.

이것은 [이용허락규약\(Legal Code\)](#)을 이해하기 쉽게 요약한 것입니다.

[Disclaimer](#)

공학박사 학위논문

**Development of Anode Spot Plasma Ion
Source for High Current Beam Extraction**

고전류 인출을 위한 양전극 국부 플라즈마 이온원 개발

2017년 8월

서울대학교 대학원

에너지시스템공학부

이윤아

Development of Anode Spot Plasma Ion Source for High Current Beam Extraction

지도교수 황 용 석

이 논문을 공학박사 학위논문으로 제출함

2017년 4월

서울대학교 대학원

에너지시스템공학부

이 윤 아

이윤아의 공학박사 학위논문을 인준함

2017년 6월

위 원 장 김 곤 호 (인)

부위원장 황 용 석 (인)

위 원 정 경 재 (인)

위 원 김 중 국 (인)

위 원 홍 인 석 (인)

Abstract

Development of Anode Spot Plasma Ion Source for High Current Beam Extraction

Yuna Lee

Department of Energy System Engineering

(Fusion & Plasma Engineering)

The Graduate School

Seoul National University

Anode spot is an additional discharge in front of positively biased electrode exposed to pre-existing (ambient, bulk) plasmas. It is distinguished from the ambient plasma by a double layer, and sustained by the drifted electron accelerated by the double layer potential. The main application of anode spot is used as charged particle source based on its basic characteristics with high plasma density. The main application of anode spot might be a high brightness ion sources for Nano-applications

at Seoul National University. We have developed a high-brightness ion source with high power efficiency by generating an anode spot plasma near to extraction aperture, and it has been successfully utilized as ion sources for FIB (Focused Ion Beams) and Nano-MEIS (Nano-Medium Energy Ion Scattering).

Recently, it essentially needs the high current large-area ion source in ion implantation field to cover the large area of substrates. We will develop the plasma ion source utilized anode spot (ASPIS, Anode Spot Plasma Ion Source) for high ion beam current extraction to expand its application field. Enlarged the extraction aperture is limited by the size of anode spot that its variation can be a constraint to the ASPIS operating as a high ion current source. It is investigated the correlation between the plasma properties of anode spot including the size variations and the operating parameters of ASPIS. Based on the experimental results, we propose an optimum design parameter and operating range of the ASPIS in order to be used ASPIS as a high current ion source though solving the 0-D particle balance model of anode spot considering ion beam extraction from it.

As the diameter of extraction aperture enlarged in range of mm level, it is measured the extracted ion beam currents according to the operating parameters of ASPIS and examined the sustainment conditions of anode spot during the ion beam extraction. The beam currents are also measured with varied the design parameters of ASPIS such diameter of bias electrode and extraction aperture. It is well-known that the ion beam current is proportional to bias current in ASPIS used as high brightness

ion source. In contrary, there is the nonlinearity between bias current and ion beam current that the ion beam current is abruptly increased according to the diameter ratio of bias electrode to anode spot. As the diameter of bias electrode increases, the optimum operating pressure for extracted maximum ion beam is gradually decreased and so does beam current. In this manner, the size of the anode spot must be at least larger than the extraction aperture and be about the diameter of the maximum bias electrode to extract high ion beam current with sustainment of anode spot.

It is known that the anode spot size is a function of reciprocal of operating pressure, the ionization cross section determined by the double layer potential and mass ratio of electron to ion of operating gas species. However, it is observed that the anode spot size is varied with operating pressure as well as bias voltage. The plasma properties of anode spot as well ambient plasma are analyzed with the consideration on anode spot size variation. As increasing the operating pressure and bias voltage, the bias currents increase with decreasing the double layer potential. In contrary, the size variations of anode spots have different change trends with each operating variables. Because the anode spot controls its size to maintain the ionization rate inside anode spot with respect to the changes on plasma properties of ambient plasma or operating pressure. It suggests the modified formulae related to anode spot size by considered the correlation between the plasma properties including anode spot size and operating parameters of ASPIS.

The characteristics of anode spot plasma considered with ion beam

extraction is understood by developed the 0-D particle balance of anode spot. The electron is focused on analysis the anode spot properties so far, it is important to consider the generation and loss of ions at anode spot to be used as ion source. The 0-D particle balance model of anode spot is verified that the calculated plasma properties of anode spot with considered the additional ion loss due to beam extraction are compared with the experimental results. When the size of the bias electrode and the extraction aperture were changed, it is found that the maximum ion beam current is extractable at the area ratio of bias electrode to extraction aperture as 2. It is also predictable the size variation of anode spot with respect to bias current that the operating parameters as well as design parameters of ASPIS is suggested with target current.

In this study, it is confirmed that the appropriate operation conditions of ASPIS are restricted that the quasi-neutrality conditions of anode spot should be satisfied to sustain the anode spot extracted high current ion beams. In order to apply the anode spot plasma ion source as a large area ion source beyond the high current ion source, this research will be used as a key index to suggest guidelines for ion source design.

Keywords; Anode spot, ASPIS(Anode Spot Plasma Ion Source), High ion beam extraction, Anode spot size, Double layer, Particle balance model

Student Number: 2010-21043

Contents

Abstract	i
Contents	v
List of Figures	ix
List of Tables	xvii
List of Abbreviations	xviii
Chapter 1. Introduction	1
1.1. Anode Spot Plasma	1
1.1.1. Criteria of Transition from Electron Sheath to Anode Spot.....	5
1.1.2. General Characteristics of Anode Spot.....	8
1.2. Application of Anode Spot: High Brightness Ion Source.....	12
1.3. Motivation of this Research	18
Chapter 2. High Current Ion Beam Extraction form ASPIS with Larger Aperture	21
2.1. Experimental Details of Anode Spot Plasma Ion Source	21

2.2.	Discharge Characteristics of Anode Spot with Aperture	24
2.3.	Ion Beam Extraction for Anode Spot Plasma	29
2.3.1.	Optimum Operating Pressure Variations by Diameter of Bias Electrode.....	29
2.3.2.	Nonlinearity between Bias Current and Beam Current	34
2.4.	Summary: Effective Factors for Sustainment of Anode Spot with Ion Beam Extraction	37

**Chapter 3. Plasma Properties and Size of Anode Spot with
Operating Parameters..... 40**

3.1.	Experimental Details of Plasma Source and Diagnostics.....	42
3.1.1.	Plasma Source and Bias Probe	42
3.1.2.	Langmuir Probes for Measurement of Plasma Properties	46
3.2.	Stable Operational Regime of Anode Spot.....	61
3.3.	Analysis I-V Curves from Two Different Plasmas.....	66
3.3.1.	Probe I-V Curves with Varied Operating Parameters.....	67
3.3.2.	Plasma Properties Determinations of Anode Spot and Ambient Plasma	72
3.3.3.	Spatial Distribution of Plasma Properties	83
3.4.	Determination of Anode Spot Size by Operating Parameters	86
3.4.1.	Anode Spot Size Variations by Operating Parameters	87

3.4.2.	Correlation between the Plasma Properties of Two Plasmas and Operating Parameters	92
3.4.3.	Modification of Anode Spot Size Estimation	107
3.5.	Summary: Why Is the Anode Spot Size Varied?	110

Chapter 4. Prediction of Operational Conditions of ASPIS for

High Current Beam Extraction.....113

4.1.	Necessity of 0-D Particle Balance Model of Anode Spot	113
4.2.	Development of 0-D Particle Balance Model of Anode Spot	122
4.2.1.	Terminologies Used in Particle Balance Model of Anode Spot..	123
4.2.2.	Generation and Loss Processes in Anode Spot	125
4.2.3.	Determination of Plasma Potential with Varied Bias Current.....	134
4.2.4.	Detail Description of Particle Balance Model of Anode Spot	141
4.3.	Validation of 0-D Particle Balance Model with Experimental Results .	145
4.3.1.	Anode Spot Plasma Properties with Varied Bias Current.....	145
4.3.2.	Validation of 0-D Particle Balance Model in ASPIS	148
4.3.2.1.	Operating Criteria of ASPIS for High Current Beam Extraction.....	149
4.3.2.2.	Anode Spot Plasma Properties Variations with Ion Beam Extraction.....	150
4.4.	Expectation of ASPIS's Operating Parameters Range	153

Chapter 5. Summary and Conclusion	158
Bibliography.....	161
Abstract in Korean.....	168

List of Figures

- Figure 1. 1. Schematic diagrams for generation mechanism of anode spot plasma from electron sheath: The biased voltage to electrode, V_{bias} , is gradually increased in range from V_1 to V_3 ($V_1 < V_2 < V_3$). (a) The formation of electron sheath by accelerated electron from ambient plasma, (b) anode sheet generated by excitation reaction of electron-neutral collision at the center of electrode's surface and (c) the transition from electron sheath to anode spot by biasing more positive voltage to electrode than ionization potential of working gas. 3
- Figure 1. 2. General properties of anode spot measured by Song: (a) characteristic current-voltage curve of anode spot, (b) the spatial distribution of plasma potential indicating anode spot, double layer and ambient plasma, (c) the anode spot size in terms of inverse of operating pressure and the type of working gas. 9
- Figure 1. 3. (a) Electron energy probability function measured inside the anode spot that two different electron groups are existed as trapped and drifted electrons, and (b) the plasma density of anode spot plasma is proportional to bias current. 11
- Figure 1. 4. Anode Spot Plasma Ion Source (ASPIS) developed as high brightness ion source with micro extraction aperture: (a) schematic diagram of ASPIS, (b) recorded its configuration near to the extraction aperture by photograph, (c) photograph of anode spot near to extraction aperture. 14
- Figure 1. 5. Determination of optimum operating condition of bias current for

beam extraction: (a) comparison the trends of bias current and beam current changes in terms of bias voltage, (b) the variation of potential differences between anode spot and bias voltage with applying higher bias voltage to bias electrode.17

Figure 2. 1. Cross-sectional drawing of the experimental setup of ASPIS. The area of bias electrode exposed to ambient plasma is controlled by covering it using limiting insulators with inner diameter of 3, 4, and 5 mm.23

Figure 2. 2. (a) The current-voltage characteristic curve of anode spot plasma generated in front of a bias electrode with outer diameter of 4 mm at gas pressure of 50 mTorr. (b) The change in shape of anode spot plasma on the current-voltage curve.25

Figure 2. 3. (a) The variation of current-voltage characteristic curve of anode spot plasma with the operating pressure for a bias electrode with outer diameter of 4 mm. (b) The change in shape of anode spot plasma with the outer diameter of bias electrode and operating pressure.26

Figure 2. 4. (a) The variation of ion beam current extracted from anode spot plasma with the operating pressure for a bias electrode with outer diameter of 4 mm. (b) The change in shape of anode spot plasma with the operating pressure.30

Figure 2. 5. The variation of ion beam current extracted anode spot plasma with the operating pressure: for bias electrodes with different outer diameters (3, 4 and 5 mm) at fixed bias current of 600mA.
 32

Figure 2. 6.	The variation of the extracted ion beam current with the bias power operating at the optimum pressure for each case: 75 mTorr for 3 mm of bias electrode, 50 mTorr and 15 mTorr for 4 mm and 5 mm, respectively.	35
Figure 2. 7.	The control parameters of ASPIS including the design parameter for high ion current beam extraction from ASPIS.	38
Figure 3. 1.	The comparison between the estimation of anode spot size variations with different double layer potentials and the measured anode spot sizes expressed as varied the operating pressure and bias voltage.	41
Figure 3. 2.	Schematic diagram of plasma source, bias probe and diagnostics: The plasma properties are measured by Langmuir probes and the shapes of sizes change of anode spots are recorded by Digital camera.	43
Figure 3. 3.	(a) Schematic diagram of single Langmuir probe and related circuitry configuration. (b) A typical voltage-current curve achieved by single probe with cylinder tip. (c) 1 st derivative of the I-V curve and determination of plasma potential. (d) Semi-log plot of the I-V curve near to plasma potential and it shows the way to find electron temperature with linear fit.	49
Figure 3. 4.	Typical current-voltage curves and their first derivatives in case of the existence of electron beam component in plasma: drifted Maxwellian electrons represented as (a) I-V curve, (b) its 1 st derivative of I-V curves and isotropic mono-energetic electrons expressed as (c) I-V curve, (d) its 1 st derivative of I-V curves.	59

Figure 3. 5. (a) Discharge characteristic current-voltage curves obtained positively biased electrode in pressure range from 15 mTorr to 75 mTorr with fixed RF power as 150 W. (b) Images of anode spots operated at 25 mTorr: Stable spherical anode spot(left), unstable anode spot with unclear boundary(center), unstable anode spot with current spike(right).63

Figure 3. 6. I-V curves obtained at anode spot and ambient plasma by movable Langmuir probe: (a) The image represented the configuration of anode spot, ambient plasma and probe. The probe is varied it position within 30 mm. (b) the typical probe current variation according to the position changes of probe, (c) changed the bias voltage.70

Figure 3. 7. In case of operating at 15 mTorr of operating pressure, 42V /110mA of bias voltage and current. Inside the anode spot: (a) characteristic current voltage-curve, (b) changed the plot format as log plot for electron temperature. Outside the anode spot (ambient plasma): (c) characteristic current-voltage curve, (d) changed the plot format as semi log plot.73

Figure 3. 8. In case of operating at 15 mTorr of operating pressure, 42V /110mA of bias voltage and current: (a) inside anode spot: probe current 1st derivative to bias voltage, (b) outside anode spot (ambient plasma): probe current 1st derivative to bias voltage, and (c) comparison the EEPFs between achieved at anode spot and ambient plasma.74

Figure 3. 9. How to achieve the electron density fraction of trapped electron to accelerated electron from ambient plasma at EEDF of anode spot.79

Figure 3. 10.	(a) The image of anode spot and ambient plasma and spatial distributions of (b) plasma potential, (c) electron temperature, (d) plasma density with experimental conditions: 36 V/ 100 mA with sustained pressure as 50 mTorr.	84
Figure 3. 11.	(a) The anode spot size variations and (b) the bias current variations as increasing the operating pressure from 15 mTorr to 75 mTorr with fixed bias voltage and RF power of 150 W.	88
Figure 3. 12.	(a) The anode spot size variations and (b) the bias current variations as increasing the bias voltage from 25 V to 51 V with fixed RF power of 150 W and the operating pressure range as 15 -75 mTorr.	89
Figure 3. 13.	The anode spot size, L_{as} , is expressed as a function of bias current by combined the relationship among the bias current, bias voltage and the anode spot size as shown in Fig. 3.12.	90
Figure 3. 14.	The double layer potential is decreased with operated at high pressure or high bias voltage as the RF power is fixed as 150 W.	94
Figure 3. 15.	The electron temperatures of ambient plasma as well as those of anode spot are varied with bias voltage and operating pressure.	95
Figure 3. 16.	The electron temperature of anode spot is proportional to double layer potential regardless of the operating parameters such as the operating pressure and bias voltage.	97
Figure 3. 17.	(a) The electron density variations of accelerated electron entered into anode spot and (b) the electron density variations of thermal	

	electron in anode spot.	100
Figure 3. 18.	The density ratio of thermal electron to drifted electron into anode spot is decreased as increasing the bias current.	102
Figure 3. 19.	The product of thermal electron density and the electron temperature of anode spot is linearly proportional to the bias current.	103
Figure 3. 20.	(a) The calculated ionization reaction rate in anode spot and (b) the product of ionization reaction rate and the volume of anode spot.	105
Figure 3. 21.	The value as the ionization rate divided by the root of the electron temperature estimated as the plasma density of anode spot, is proportional to bias current regardless of the variation of operating pressure.	106
Figure 3. 22.	Comparison the anode spot size between measured results and estimated value with measured plasma properties of ambient plasma and anode spot by modified formulae.	109
Figure 3. 23.	The correlation among the operating parameters, plasma properties of anode spot and the size variation of anode spot.	110
Figure 4. 1.	Schematic diagrams of the originality of electrons components in anode spot to be interpreted the bias current flown into bias electrode by (a) Song, (b) Park.	116
Figure 4. 2.	A schematic diagram illustrating the relationship between the operating parameter and plasma properties and influence between plasma and ion beam extraction with generation and maintenance	

	of anode spot.	118
Figure 4. 3.	The schematic configuration of anode spot and ambient plasma expressed with the plasma properties and design parameters....	123
Figure 4. 4.	The schematic diagram for explanation of generation and loss terms of charged particles in anode spot and the circuit schematic connected to ion source for sustaining the anode spot and extracted ion beam current from anode spot.	126
Figure 4. 5.	(a) The schematic diagram of charged particle loss through the boundaries, (b) the space potential variation by the existence of ambient plasma, double layer, anode spot and bias electrode....	135
Figure 4. 6.	The plasma potentials of ambient plasma and anode spot are compared between measured and estimated by Eqs. (4.14) and (4.19).	140
Figure 4. 7.	The calculation result of ionization rate constant with varied the electron temperature of ambient plasma.	144
Figure 4. 8.	The comparison between the calculated and measured results: (a) bias current, (b) thermal electron density, (c) anode spot size, (d) double layer potential and (e) electron temperature of anode spot.	147
Figure 4. 9.	The estimated values that the plasma properties and extracted beam current density tendency with varied the diameter of bias electrode from 2.1 mm to 7 mm in case of fixed the extraction aperture as 2 mm in diameter.	151
Figure 4. 10.	The estimated ion beam currents are estimated with varied the extraction aperture size at fixed diameter of bias electrode as 3, 4,	

and 5 mm. 154

Figure 4. 11. The operational range of bias current and operating pressure are determined by the comparison among the anode spot size, diameter of bias electrode (3.5 mm) and aperture size (2 mm). 155

Figure 4. 12. The estimated operating pressure and extractable beam current are varied with the beam extraction aperture size. The extractable beam current is estimated with constant bias current. 157

List of Tables

Table 1.1.	Comparison of ion source performances among various plasma ion source in terms of beam current density and power efficiency [15, 31-32, 41-43]	16
Table 3.1.	Determination of plasma properties for ambient plasma as well as anode spot from probe characteristic I-V curves.	82
Table 4.1.	The terminologies used in 0-D particle balance model of anode spot.	125
Table 4.2.	The detail explanation of generation reaction in anode spot and charged particle loss terms through the boundaries of anode spot.	133

List of Abbreviations

- D_{bias} : Diameter of bias electrode [mm]
 a_{ext} : Diameter of extraction aperture [mm]
 A_{ext} : Area of extraction aperture [mm²]
 A_{bias} : Area of bias electrode [mm²]
 A_{wall} : Area of discharge chamber wall [mm²]
 N_{gas} : Neutral density [m⁻³]
 $n_{e,am}$: Ambient plasma density [m⁻³]
 $T_{e,am}$: Electron temperature of ambient plasma [eV]
 $V_{p,am}$: Plasma potential of ambient plasma [V]
 $n_{e,as}$: Anode spot plasma density [m⁻³]
 $T_{e,as}$: Electron temperature of anode spot [eV]
 $V_{p,as}$: Plasma potential of anode spot [V]
 V_{DL} : Double layer potential [V]
 L_{as} : Anode spot size [mm]
 I_{bias} : Bias current [mA]
 V_{bias} : Bias voltage [V]
 V_{ext} : Extraction voltage [kV]
 I_{ext} : Extracted ion current [mA]

1. Introduction

Anode spot is a small, localized plasma generated in pre-existing plasma. Instead of increasing the plasma density of the entire discharge chamber's volume to enhance the ion beam current extraction, it has been successfully developed the plasma ion source with high power efficiency by generated the anode spot plasma, which has high plasma density characteristics, near to the extraction aperture. Until now, the anode spot plasma ion source (ASPIS) with micro aperture has been used in Nano-applications, such as FIB (Focused Ion Beam) and Nano-MEIS (Medium Energy Ion Scattering) where needs high brightness ion source. In order to extend the application field of ASPIS, especially ion implantation field, it is necessary to develop the ASPIS as high current plasma ion source. Therefore, in this section, it is aimed to establish the purpose and the scope of this study based on understanding the discharge characteristics of anode spot and the application in high brightness plasma source utilizing anode spot.

1.1. Anode Spot plasma

Anode spot is a localized discharge occurred in electron sheath that is additionally generated in front of electrode immersed in pre-existing (ambient or bulk) plasma, in case that positive voltage applied on electrode's surface. The anode spot generally

forms as small and bright ball shape attached to electrode that is also called as plasma bubble, plasma ball, fireball or plasma contactor. It is known that plasma properties of anode spot, such as plasma density and electron temperature are higher than that of ambient plasma. The anode spot is distinguished to ambient plasma and sustained by double layer, which is expressed as a combination of ion and electron sheath with step-like potential structure.

The generation mechanism of anode spot plasma is dominantly electron-neutral (e-n) collisions for ionization inside the electron sheath. In case that the electrode is immersed in the surrounding plasma, the sheath, which is almost charge free space, is existed between the electrode surface and surrounding plasma. The sheath is commonly attracted ions so that the plasma potential of surrounding plasma is sustained higher value than that of electrode. Because electrons have high mobility than ions that the electron losses through the wall might be increased. Keeping electrode's potential lower than plasma potential maintains the plasma basic characteristic, quasi-neutral condition by repelling electron and accelerating ion toward electrode. Interestingly, an electron sheath, attracting electrons, forms in front of the electrode in some special cases as shown in **Fig. 1.1. (a)**. In order to generate the electron sheath in front of electrode, the area of electrode must be very small compared with that of conducted wall containing the ambient plasma and the electrode must have higher potential than ambient plasma by applied positive voltage.

After formed the electron sheath near to positively biased electrode, the

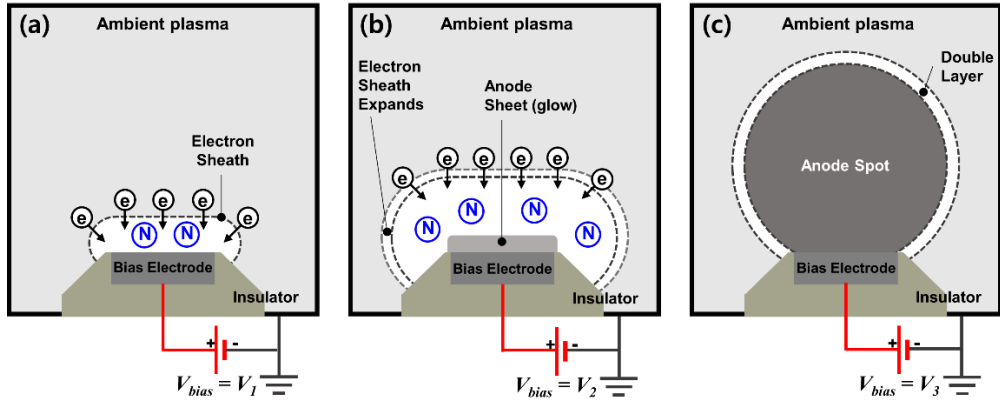


Figure 1.1. Schematic diagrams for Generation mechanism of anode spot plasma from electron sheath: The biased voltage to electrode, V_{bias} , is gradually increased in range from V_1 to V_3 ($V_1 < V_2 < V_3$). (a) Formation of electron sheath by accelerated electron from ambient plasma, (b) anode sheet generated by excitation reaction of electron-neutral collision at the center of electrode's surface and (c) The transition from electron sheath to anode spot by biasing more positive voltage to electrode than ionization potential of working gas.

incident electrons are accelerated into electron sheath by the potential difference between the electrode and the ambient plasma. If the potential difference is not enough to ionize the neutral particles, the neutral particles near to electrode are excited by e-n collisions. As shown in **Fig. 1.1. (b)**, it is observed that the glows, named as anode sheet, is existed at the center of electrode, and the light emitted from glow can be the evidence that the collisions between electrons and neutral particle lead to neutral particles' excitations.

With biasing higher voltage to electrode, V_3 , the ionization reaction by e-n

collisions is occurred dominantly in case that the accelerated energy of incident electron is higher than the ionization potential of working gas. **Figure 1.1. (c)** shows the schematic diagram of anode spot and its structure. The anode spot plasma can be understood as a kind of DC glow discharge that the ambient plasma and electrode are considered as virtual cathode and anode of DC glow discharge, respectively, the thickness of electron sheath is assumed as the gap distance between cathode and anode. The electron sheath thickness is followed the space charge limited theory that is increased as the applied voltage increases. The electron sheath is changed into anode spot plasma with satisfaction of transition conditions that the electron sheath thickness reaches to a certain value thickness at a given operating pressure and the accelerated energy of incident electrons exceeds ionization potential of operating gas species.

Constricted DC plasmas and arc plasmas are generated in basic structure of DC discharge by voltage difference between cathode and anode. In an arc plasma, an anode spot is generated in front of anode in case that the temperature of electrode surface is rapidly increased as high electron current flows into the anode [1, 2]. Generating anode spot in arc plasma is affected by anode's material and the heat flux induced by electron current flow into electrode. And constricted DC plasma is kind of DC glow discharge that operates with constricted size of anode, which is much smaller than the area of cathode, so that a small and bright plasma called as plasma ball is generated in front of the anode [3-5]. However, there is a significant difference between the plasma ball at constricted DC plasma and the anode spot mentioned in

this study that it is found in relationship between the ambient plasma and anode spot. Since the two types of plasmas (constricted DC plasma and arc plasma) do not require the ambient plasma to generate the anode spot while the anode spot are generated by considered the ambient plasma as virtual cathode, so that the ambient plasma must be existed for generating and sustaining anode spot. In addition, it is not affected to sustain the ambient plasmas whether anode spot is existed, and the anode spot and ambient plasma can be independently controlled, respectively. On contrary, it is impossible to be controlled independently from ambient plasma since the plasma ball of constricted DC plasma must be existed to sustain the discharge between cathode and anode.

In summary, the anode spot covered in this study is generated by the additional discharge in the electron sheath and its characteristics can be controlled independently from ambient plasma.

1.1.1. Criteria of Transition from Electron Sheath to Anode Spot

Formation of electron sheath in front of positively biased electrode is essential to generate anode spot. As mentioned above, the ion attracting sheath is generally found between plasma and conductor exposed to a plasma, but it is examined that the changes of the generated sheath type depends on the area ratio between the discharge chamber wall contained plasma and electrode exposed to plasma [6]. Baalrud [7, 8]

proposed an electrode area criterion for electron sheath generation to be formulated by using the fact that the net current flown in to the conducted wall is zero. The criterion for area ratio of discharge chamber to electrode is derived as Eq. (1.1) based on the assumption that ions and electrons escaped through the entire wall of discharge chamber and only electron can be lost by electrode.

$$A_{electrode} < \sqrt{2.3 \frac{m_e}{M_i}} A_{wall} \quad (1.1)$$

where $A_{electrode}$, A_{wall} are electrode area and wall area of discharge chamber, m_e and M_i are electron mass and ion mass, respectively. ($\sqrt{2.3 \frac{m_e}{M_i}}$ is defined as μ that is derived from ratio of electron thermal velocity, $v_{e,th} = \sqrt{\frac{8kT_e}{\pi m_e}}$, to Bohm velocity of ion, $u_B = \sqrt{\frac{kT_e}{M_i}}$. In case of using Argon as operating gas, μ is approximately 0.0059.) Electron sheath model is based on Child-Langmuir ion sheath, and the thickness of electron sheath is derived as Eq. (1.2) [9,12].

$$L_{es} = \frac{2\sqrt{2}}{3} \pi^{1/4} \left(\frac{\epsilon_0 T_e}{en_e} \right)^{1/2} \left(\frac{V_{es}}{T_e} \right)^{3/4} \quad (1.2)$$

where ϵ_0 is permittivity of free space, V_{ES} is electron sheath voltage, n_e and T_e are represented as electron temperature, plasma potential of plasma, respectively. The thickness of electron sheath, L_{es} , is a function of biased voltage to electrode and ambient plasma properties, such as electron temperature and plasma density. It is also

verified by a series of experiments [9, 11] and PIC simulations [12] that the thickness of electron sheath is increased with electron sheath voltage, but decreased as dense plasma with high electron temperature.

As the voltage applied to electron sheath is maintained above the ionization potential of the operating gas, the ionization process is dominant inside the electron sheath so that the electron sheath is changed into anode spot plasma. It has been investigated the breakdown voltage for generating anode spot by Conde [11] and Park [12]. By solving 1-D Poisson's equation, the biased voltage to the additional electrode should be higher than 1.9 times of plasma potential of the ambient plasma to generate the anode spot. Conde suggested that two different potential profiles calculated numerically near to electrode indicate the transition from electron sheath to anode spot. Park considered that the ambient plasma is worked as virtual cathode, and proposed the breakdown voltages by solving 1-D Townsend's DC discharge model, and the breakdown voltage for generating anode spot is estimated to be increased in case of operating at lower pressure, low density of plasma with low electron temperature and it is expressed as Eq. (1.3).

$$Ap \frac{2\sqrt{2}}{3} \pi^{\frac{1}{4}} \left(\frac{\varepsilon_0 T_e}{en_e} \right)^{\frac{1}{2}} \left(\frac{V_b}{T_e} \right)^{\frac{3}{4}} - \ln \left(1 + \frac{1}{\gamma_{eq}} \right) \exp \left[Bp \frac{2\sqrt{2}}{3} \pi^{\frac{1}{4}} \left(\frac{\varepsilon_0 T_e}{en_e} \right)^{\frac{1}{2}} \frac{V_b^{-\frac{1}{4}}}{T_e^{\frac{3}{4}}} \right] = 0 \quad (1.3)$$

where A and B are Townsend 1st and 2nd ionization coefficients, p is operating pressure and γ_{eq} is expressed bipolar electron coefficient as J_e/J_i , respectively.

In summary, the criteria for the transition from electron sheath to anode spot that the area ratio between discharge chamber and electrode, the thickness of electron sheath and breakdown voltage for generating anode spot are expressed in terms of the plasma properties of ambient plasmas, operating pressure and biased voltage to electrode.

1.1.2. General Characteristics of Anode Spot

Since the anode spot plasma has been mainly used as a tool to generate a double layer at laboratory plasma, the characterization of anode spot is not important to understand itself. The research of basic characteristics of anode spot is widely studied by Song [13, 14]. It is observed various phenomena such as characteristic current-voltage curves of anode spot, the breakdown voltage of generating anode spot in terms of operating pressure, the size of anode spot as a function of operating gas species and pressure and potential profile among anode spot, double layer and ambient plasma, as shown in **Fig. 1.2**. It is also discussed the stability of spherical anode spot plasma by circuit model [14].

Figure 1.2. (a) is depicted as the characteristic current-voltage curve of the positively biased electrode that it represent the status of anode spot[13, 15-21]. The interesting point in the current-voltage curve of positively biased electrode is that the current slopes are different in terms of biased voltage with existence of current jump,

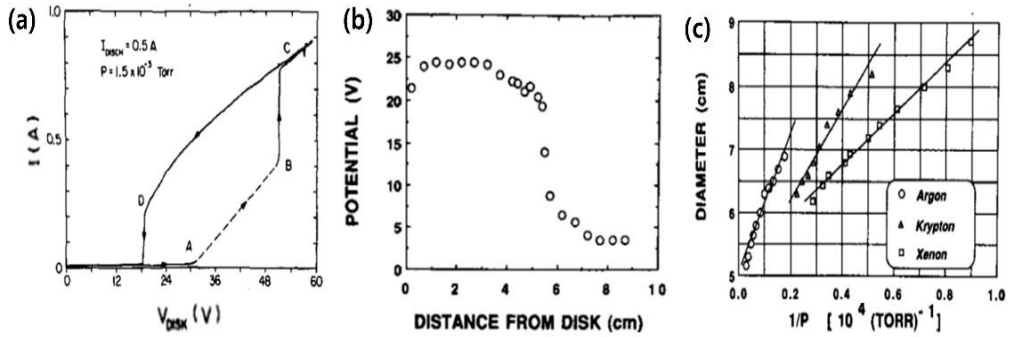


Figure 1. 2. General properties of anode spot measured by Song : (a) characteristic current-voltage curve of anode spot, (b) the spatial distribution of plasma potential indicating anode spot, double layer and ambient plasma, (c) the length of anode spot in terms of inverse of operating pressure and the type of working gas.

and hysteresis is observed like DC plasma. The electron sheath is existed in front of electrode at voltage range from 0 V to 30 V (0 – ‘A’ in **Fig. 1.2. (a)**). Increasing the biased voltage, V_{disk} , unstable anode spot is generated that the current spike is occurred regularly by transition from electron sheath to anode spot (‘A’ – ‘B’ regime of **Fig. 1.2. (a)**). Current spikes become more frequent as applied voltage is increased. When the biased voltage reaches to 50 V, a sudden current jump takes place that stable anode spot is sustained with constant current. A further increase of voltage applied to electrode produces only a moderate increment of current, and it reaches to saturated current that is determined by the plasma density of ambient plasma [15]. As biased voltage is decreased below 50 V, the characteristic follows the path indicated by ‘C’-‘D’ regime of **Fig. 1.2. (a)** without current spike that it is an evidence that anode spot plasma operates as self-sustain plasma.

Figure 1.2. (b) is the results of measured spatial distribution of plasma potential, it indicates the existence of double layer between two different plasmas, such as anode spot and ambient plasma, that double layer has a steep potential difference with narrow gap [13, 17-23]. The double layer potential has been found which has higher value than the first ionization potential of operating gas species [13, 17] and the biased voltage to electrode is slightly higher than the anode spot's potential that most of loss current through the electrode consists electron current [13, 16-17, 20, 25].

The anode spot shape is normally sphere, but cylindrical anode spot, called as "fire-rod" is also observed in case of the existence of magnetic field [26, 27] near to positively biased electrode, or the electrode adopted relatively large area [16, 17]. The size variations of anode spot has been experimentally examined as **Fig. 1.2. (c)** [13]. The experimental results about anode spot size correspond with the theoretical approach [13, 16] and it is derived from ion generation - loss balance inside anode spot expressed as Eq. (1.4).

$$L_{as} = \frac{1}{N_{gas}\sigma_{ioniz}(E_i)} \sqrt{\frac{m_e}{M_i}} \quad (1.4)$$

where N_{gas} is neutral particle density, $\sigma_{ioniz}(E_i)$ is ionization cross section by electron-impact with electron energy as ionization potential, E_i , and m_e , M_i are electron mass, ion mass, respectively. The anode spot size is a function of a reciprocal of the operating pressure and the mass ratio between electron and ions. It also affected by

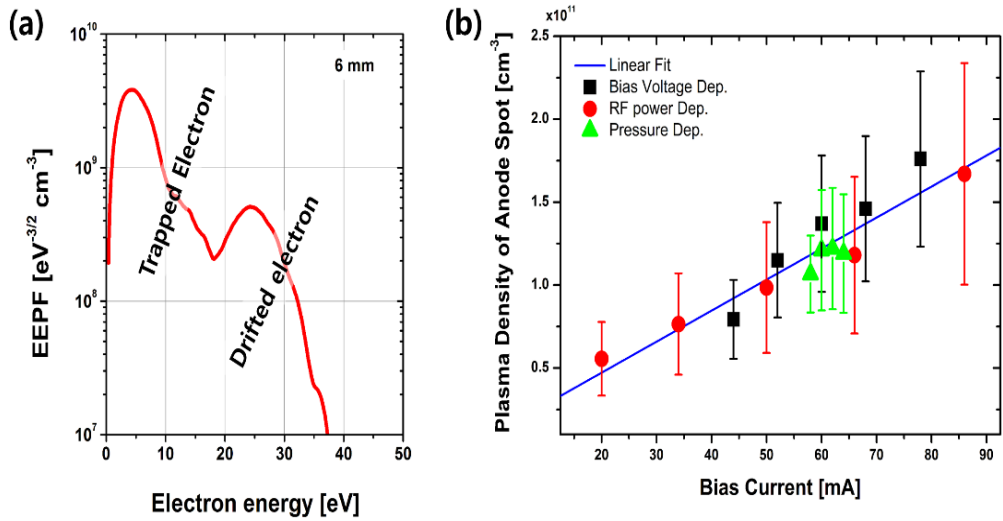


Figure 1. 3. (a) Electron energy probability function measured inside the anode spot that two different electron groups are existed as trapped and drifted electrons, (b) The plasma density of anode spot plasma is proportional to bias current.

ionization cross section in case with ionization potential of operating gas.

Park has conducted experimentally and theoretically the researches related to electrons of the anode spot [25]. It has been investigated the originalities of electrons in anode spot and figured out the current flown into electrode in terms of electron originality. The most of electron inside the anode spot is assumed as accelerated electrons from the ambient plasma [13]. **Figure 1.3. (a)** is represented the Electron Energy Probability Function (EEPF) that is derived by 2nd derivative of characteristics I-V curve achieved by Langmuir probe in case of invasion to anode spot. As shown in **Fig. 1.3. (a)**, the electrons inside anode spot can be divided into two group: drifted electron from ambient plasma and trapped electron inside anode spot

by double layer structure. The density fraction of trapped electron is even higher than that of accelerated electron in the anode spot. The current passing through the biased electrode represents the plasma density of anode spot that it is proportional to the bias current as shown in **Fig. 1.3. (b)**.

Furthermore, the dynamics of anode spot including oscillation ('A' – 'B' regime of **Fig.1.2. (a)**) and instabilities has been researched by analyzing current flown into electrode and light intensity of anode spot in both continuous and pulsed operating mode [13, 18-19, 21,26, 28].

1.2. Application of Anode Spot : High Brightness Ion Source

The main applications of anode spot is used as electron source [29] or ion source [15, 30-32] based on its basic characteristics with high plasma density. The active application of anode spot might be the development of high brightness ion source for Nano-applications at Seoul National University. Currently, the commercial devices for Focused Ion Beam (FIB) are mainly adopted the liquid metal ion sources (LMIS) because of their high brightness characteristics [33]. However, the LMIS has some limitations that it only supplies ion beams with limited ion species, such as Gallium ions, and Gallium ions are not suitable for Nano-applications because they cause the contamination or damages to the target material. In addition, it is reported to use Gallium ion beams that a phase-alloy has been found the limitation on aspect ratio at

Nano-scale machining in the milling or sputtering processes. Recently, the extracted ion beams with various gas species by plasma ion source (PIS) is being developed instead of LMIS for high brightness source. The PIS has lower brightness compared to LMIS since high ion beam current is extracted from plasma ion source with high angular density. The brightness, one of the indexes representing the beam quality, is a function of extracted ion beam current and emittance expressed as Eq. (1.5).

$$B = \frac{I_{beam}}{\varepsilon_x \varepsilon_y} \quad (1.5)$$

where I_{beam} is extracted ion beam current, ε_x , ε_y are emittances at $x-x'$, $y-y'$ plane in phase space, respectively [34, 35]. The brightness can be enhanced that the more ion beam current is extracted with low beam spread. In case of using plasma ion source, high brightness is obtained by reducing the beam extraction aperture to micrometer level. However, the applied electric field for beam extraction is difficult to penetrate into plasma because of its low aspect ratio: the diameter of aperture is very small compared with the thickness of aperture. In order to overcome the difficulty of beam extraction with micro-aperture, it needs to enhance the plasma density near to beam extraction aperture. It is generally increased the plasma density of entire discharge chamber by applying higher discharge power or using magnetic field to confine the plasma. However, there is an efficient way to increase the plasma density by generating the anode spot plasma near to the extraction aperture. The penetration of the electric field for ion beam extraction becomes easier since the thickness of the

electron sheath formed in front of electrode is decreased at high plasma density. Therefore, utilizing the anode spot to plasma ion source is suitable to be used as high brightness ion source.

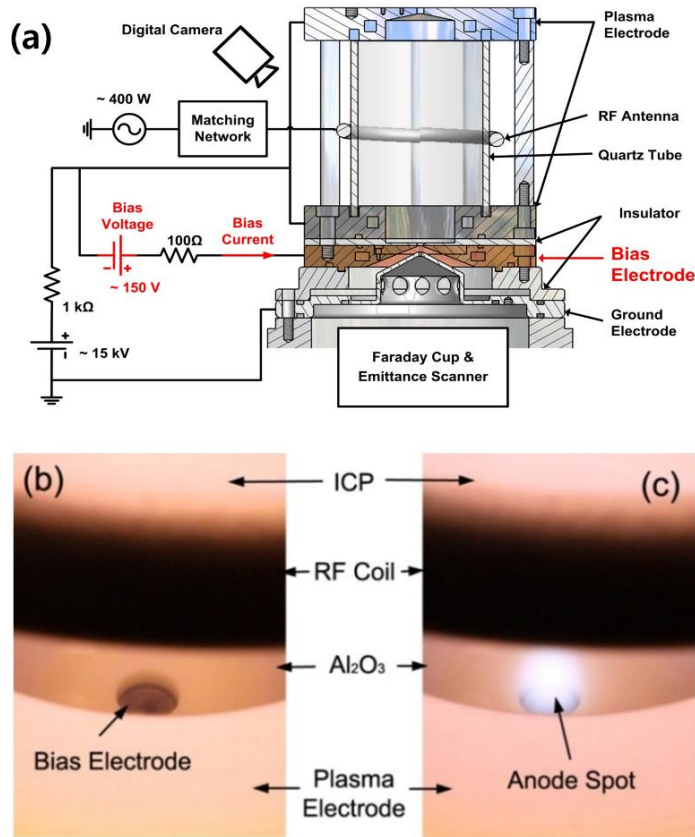


Figure 1. 4. Anode Spot plasma ion source (ASPIS) developed as high brightness ion source with micro extraction aperture: (a) Schematic diagram of ASPIS, (b) recorded configuration near to the beam extraction aperture by photograph, (c) photograph of anode spot near to extraction aperture.

Figure 1.4. (a) is schematic diagram of ICP plasma ion source with utilized anode spot near to beam extraction aperture. It is general way to extract the ion beam

current from plasma ion source by using the potential difference between plasma electrodes and grounded electrode. The additional electrode, named as Bias electrode, is located between plasma electrode and ground electrode, has an extraction aperture at the center and is isolated electrically from plasma electrode blocked by an insulator. The bias electrode, covered by insulator disk with a 3mm-diameter hole at the center, is partially exposed on the ambient plasma in order to satisfy the area criterion for generating electron sheath in front of it (**Fig. 1.4. (b)**). In case that the sufficient positive voltage is driven to the bias electrode, the anode spot is generated near to the extraction aperture as shown in **Fig. 1.4. (c)**. It is reported that the extracted ion beam currents from anode spot plasmas are 10-100 times higher than those from ambient plasmas because of its high plasma density compared to that of pre-existing plasma, generated by ICP plasma in this source.

Table 1.1. explains the comparison the beam performances among the various plasma ion sources in terms of their beam current density and power efficiency. It is found that the beam current density extracted from anode spot plasma, 204 mA/cm^2 is 43 times higher than that extracted from ambient plasma generated by ICP, 5 mA/cm^2 . It also shows directly that the applications of anode spot to plasma ion source is advantageous to enhance the extracted ion beam current with high power efficiency. The power efficiency mentioned in **Table 1.1.** is the ratio of beam current density to input power for sustaining plasma. Since high input power is required to increase the

Table. 1. 1. Comparison of ion source performances among various plasma ion source in terms of beam current density and power efficiency [15, 31-32, 41-43]

Source type	Operating gas species (pressure)	Operating power [W] (Frequency)	Beam Energy [kV]	Beam current density [mA/cm ²]	Power Efficiency [μ A/W·cm ²]
RF Helicon plasma ion source [41]	H ₂ (10 mTorr)	1500 (13.56 MHz)	30	212	141.3
TCP plasma negative ion source [42]	H ₂ (3-20 mTorr)	1000 (13.56 MHz)	12	3.32(H ⁻)	3.3
Microwave plasma ion source [43]	Ar (< 1 Torr)	200 (2.45 GHz)	6	17.8	89
ICP plasma ion source without anode spot[15,32]	He, Ne, Ar, Kr (10-150 mTorr)	200 (13.56 MHz)	10	5	25
Anode Spot plasma ion source [15,32]	He, Ne, Ar, Kr (10-150 mTorr)	300 (13.56 MHz) +30(DC)	20(He)	127	384.8
		200 (13.56 MHz) +30(DC)	12(Ar)	204	886
Muti-cusp RF plasma ion source[31]	He	1000/ (13.56 MHz)	20	5.7	5.7

plasma density of whole discharge chamber, the other types of plasma ion source has high beam current density with poor power efficiency. However, the input power for generating anode spot is required about 10% of RF power since the volume of anode spot is much smaller than that of ambient plasma, so that the anode spot plasma ion

source has high beam current density as well as high power efficiency.

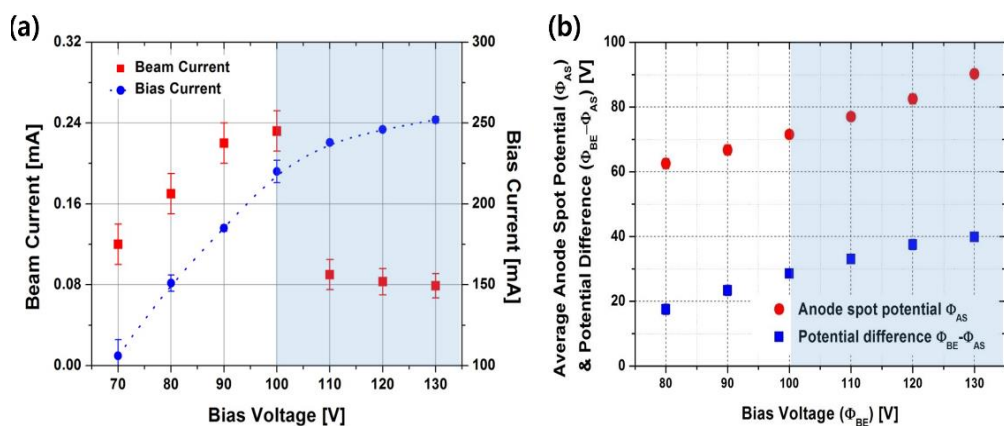


Figure 1. 5. Determination of optimum operating condition of bias current for beam extraction: (a) comparison trend of bias current and beam current changes in terms of bias voltage, (b) the variation of potential differences between anode spot and bias voltage with applying higher bias voltage to bias electrode.

It has been investigated the operational conditions of ASPIS for high current beam extraction with stable operation as shown in **Fig. 1.5** [15]. As varied the operating parameters for ambient plasma properties, such as RF power, operating pressure and gas species, The ion beam current, current flown into electrode, called as bias current, I_{bias} , are varied with respect to the voltage driven to the bias electrode(bias voltage, V_{bias}). The bias current rapidly increases with the increase of the bias voltage, the slope of increasing bias current is changed into the gentle slope that the bias current exceeds a certain value as shown in blue-dot-line of **Fig. 1.5. (a)**. Increasing bias voltage to electrode causes to enhance the bias current as well as plasma density of anode spot since the bias current is direct index of plasma density at anode spot. It is also expected

that the extracted ion beam current from anode spot would be followed the trend of bias current. However, a positive potential barrier worked as an obstacle to extract ion beam from anode spot and is found to increase in case of biased voltage higher than 100V (blue-square-dot of **Fig. 1.5. (b)**). For the reason, the maximum ion beam current can be achievable operated near to the knee point at characteristic current-voltage curves of anode spot.

1.3. Motivation of this Research

An anode spot is additional localized plasma generated in front of positively biased electrode exposed in pre-existing plasma, and it is separated into the pre-existing plasma by double layer. The anode spots have been considered only as a tool to generate the double layer in space plasma field. Recently, the anode spot has been studied itself characteristics by directly measuring the plasma properties of anode spot by Langmuir probe or Retarding Field Energy Analyzer (RFEA). Based on the experimental results, It has been figured out the correlation among the plasma properties of anode spot, those of ambient plasma and operating parameter of bias current and it has been also investigated the electron components of anode spot that consists trapped electrons and drifted electrons.

Although the researches related to anode spot are focused primarily on the electrons, the most active application of anode spot might be the development of the

plasma ion source with high power efficiency. Since the ion beam current is proportional to the plasma density near to the beam extraction aperture, it is general way to enhance the extracted ion beam current by increasing the plasma density in entire volume of discharge chamber. In this case, the increasing rate of required input power is comparably higher than that of ion beam current so that more input power is necessary to be worked as high current plasma ion source with poor power efficiency. However, an anode spot can be an answer to be efficiently enhanced the extracted ion beam by generated near to extraction aperture. Since it requires only 10% -20% of the input power for sustaining the pre-existing plasma to generate an anode spot, the plasma ion source utilized the anode spot has high power efficiency compared to the conventional plasma ion sources extracted same ion beam currents. Anode Spot Plasma Ion Source, ASPIS, has been successfully used as high-brightness ion sources in Nano-application fields, particularly FIB (Focused Ion Beam) and Nano-MEIS (Medium Energy Ion Scattering), which mainly require high beam current density with low beam spreading characteristics. When ion beam is extracted through micro-meter range of aperture, the ion beam extraction has little influence on the anode spot sustainment that the extraction beam current is under sub micro-ampere level while the electron current flown out to the electrode is about several hundreds of mA.

In recent years, it has been emphasized the necessity of high current, large-area plasma ion sources in the industrial fields for Nano-applications, such as ion implantation field. Since a plasma ion source used as a large-area ion source is

required to cover a large area of substrate that it is basically larger than other ion sources with more power required to increase the extracted ion beam current, and whole system of ion source becomes more complicated to prevent the side effects, such as cooling system or substrate damages. However, as applied the anode spot plasma to develop the high current large area plasma ion source, it is more likely to obtain a higher ion beam current with high power efficiency compared to the conventional plasma ion sources used for achieving high current with large area treatment. It is aimed to develop the anode spot plasma ion source operated as high current ion source with utilizing the enlarged extraction aperture. It is expected that the ion beam extractions with aperture size level in sub mm affect the plasma characteristics of anode spot plasma as well as its sustainment.

In this research, it is investigated ion beam current changes according to external operating parameters of ASPIS and figured out the operating conditions of anode spot sustainment considered the ion beam extraction in Chap. 2. It is also examined the correlation between plasma properties of anode spot including the size variations and the operating parameters of ASPIS in Chap. 3. Based on the experimental results, it is set up the 0-D particle balance model of anode spot with considered the additional ion loss due to ion beam extraction at Chap. 4. It is addressed to suggest a design parameters and the effective operating range of engineering parameters of ASPIS utilized as high current ion source.

2. High Current Ion Beam Extraction from ASPIS with Larger Aperture

Since the ASPIS has very small size of extraction aperture compared to that of anode spot mentioned in previous section 1.2., the anode spot can enhance the plasma density near to the extraction aperture in order to be extracted higher ion beam current at all bias current regime except the saturated bias current region shown in **Fig. 1.5. (a)** (Bias voltage > 100 V). The optimum operating bias voltage, which can be worked as the upper limit of operating regime for ASPIS, has been determined as a knee point at the discharge current-voltage curves of anode spot where the first derivative value of discharge current is maximized. However, it is expected that the anode spot size can be another important parameter to control the extracted ion beam current in case of utilizing the larger extraction aperture compared to the previous work of ASPIS. In this chapter, it is aimed to figure out the lower limit of the ASPIS's operating parameter and investigate other additional effective control parameters of ASPIS with considering the enlarged extraction aperture [32].

2.1. Experimental Details of Anode Spot Plasma Ion Source

Figure 2.1. shows the schematic diagram of a plasma ion source used in the present

study. The basic structure is the same as that used in our previous work [15], but the beam extraction aperture is enlarged to extract higher ion beam current through it. Plasma chamber is made of a Quartz tube, 75 mm high and 55 mm in inner diameter. Argon is chosen as a working gas and the operating pressure inside a plasma chamber is adjusted in the range of 10–100 mTorr, while the gas pressure in the extraction region is maintained below 1.7×10^{-4} Torr by differential pumping. The ambient plasma is generated by inductive coupling with fixed RF power of 200 W at the frequency of 13.56 MHz through double turned silver-coated copper antenna surrounding the Quartz tube. Plasma electrodes at upper and lower sides of the Quartz chamber are connected together at the same potential to provide a reference plasma potential to the ICP. An extraction hole (a_{ext}) of 2 mm in diameter is drilled at the center of a bias electrode which is located underneath the lower plasma electrode. The area of the bias electrode exposed to the ambient plasma is defined by an inner diameter (D_{bias}) of a limiting insulator made of Al_2O_3 . As depicted in **Fig. 2.1.**, three kinds of the limiting insulators with different inner diameters of 3, 4, and 5 mm are prepared to control the bias electrode area exposed to the ambient plasma. Therefore, outer diameter of the bias electrode exposed to the ambient plasma is also changed to be 3, 4, and 5 mm. It is noted that the electrode area exposed to the ambient plasma plays an important role for the formation of stable anode spot plasma [7]. A DC voltage up to +250 V is applied to the bias electrode for generating anode spot plasma and the current is measured with a current-limiting resistor of 100 Ω . Then, the

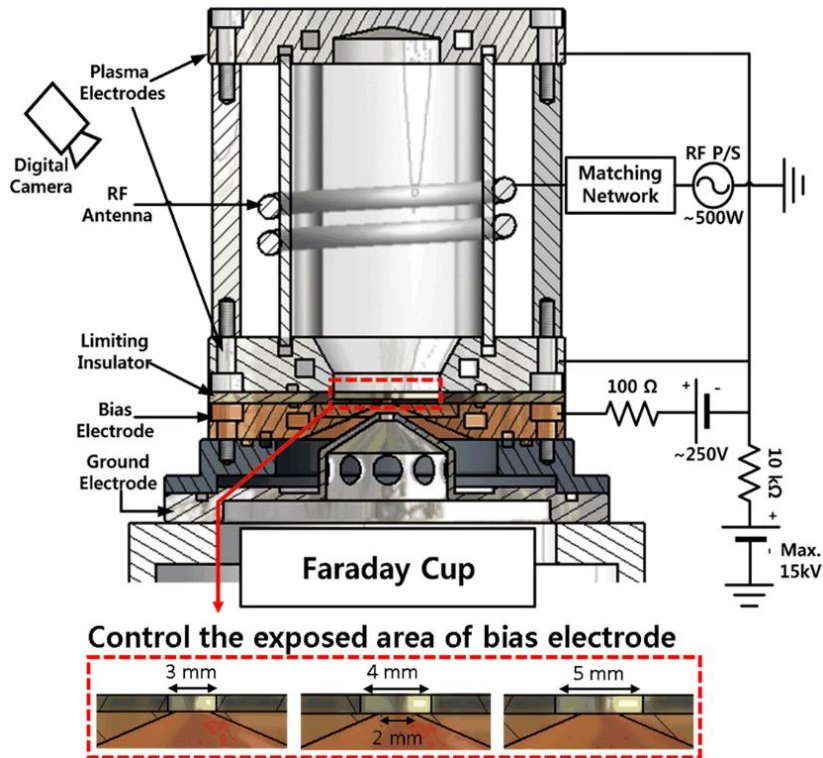


Figure 2. 1. Cross-sectional drawing of the experimental setup. The areas of bias electrode exposed to ambient plasma are controlled by covering it using a limiting insulator with inner diameter of 3, 4, and 5 mm.

current-voltage characteristics of anode spot plasma can be easily determined [15]. Ion beam extraction from the anode spot plasma has been performed by applying a high voltage to the plasma electrodes up to +15 kV with respect to the ground. The diameter of a hole located at the center of the ground electrode is 3.3 mm and the distance between the bias electrode and the ground electrode is 3.5 mm. The extracted ion beam current is collected by a Faraday cup located at 55 mm away from the ground electrode. Besides, the ion current flow to the ground electrode is also measured to

determine the optimum beam optics. Visual observations with a digital camera are also carried out to examine the changes in size and shape of the anode spot plasma.

2.2. Discharge Characteristics of Anode Spot with Aperture

Figure 2.2. shows the typical discharge current-voltage curve and pictures of the anode spot plasma generated in front of a bias electrode with beam extraction hole of 2 mm in diameter. In this case, the operating pressure is 50 mTorr and the bias electrode is covered with a limiting insulator with inner diameter of 4 mm. The bias current stays as low as ~ 100 mA until the breakdown of an electron sheath [17], or equivalently the onset of anode spot plasma, occurs at ~ 17 V. Even after the onset of anode spot plasma, the bias current is still low when the bias voltage is low, showing that the anode spot plasma is small and covers only partial region of the bias electrode (see points 'B' and 'C' in **Fig. 2.2**). However, as the bias voltage is increased, the bias current rapidly increases because the anode spot expands and covers the area of the bias electrode ('D' \rightarrow 'F'). After the anode spot plasma fills the entire area of the bias electrode, the bias current saturates and the stable anode spot plasma forms (see point 'G'). Note that the amplitude of the saturated bias current is observed not to be changed with the outer diameter of the bias electrode. Since the bias current is roughly proportional to plasma density in front of the bias electrode, it is easily recognized that the plasma density increases around 15 times than that without anode spot plasma

when the anode spot plasma operates at the saturated region.

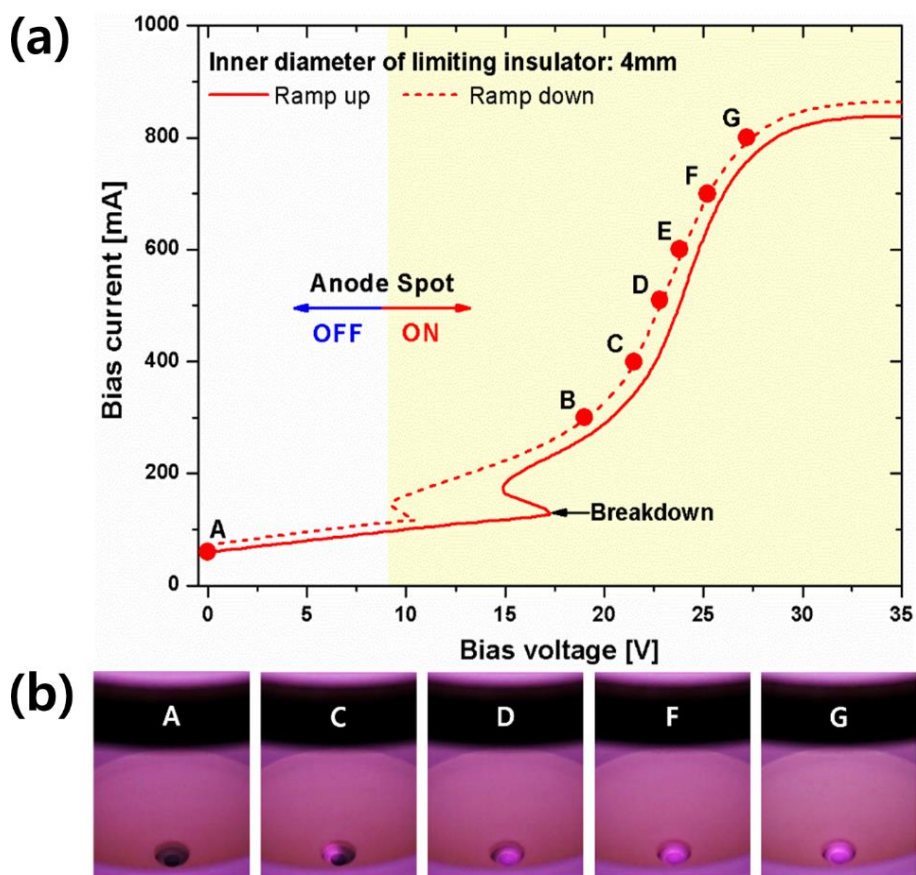


Figure 2. 2. (a) The current-voltage characteristic curve of anode spot plasma generated in front of a bias electrode with outer diameter of 4 mm at gas pressure of 50 mTorr. (b) The change in shape of anode spot plasma on the current-voltage curve.

Previously, we reported that the magnitude of the saturated bias current was not affected by the gas pressure at a given RF power for the anode spot plasma in the operating pressure range of 50–150 mTorr [15]. However, in the present experiments,

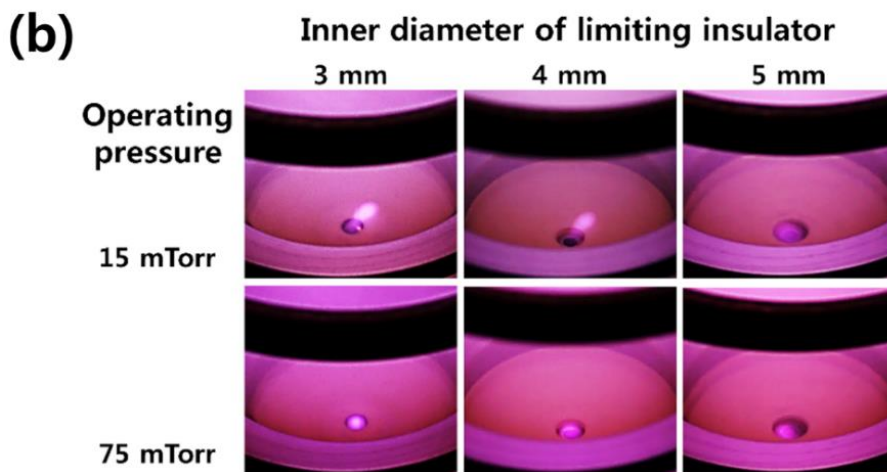
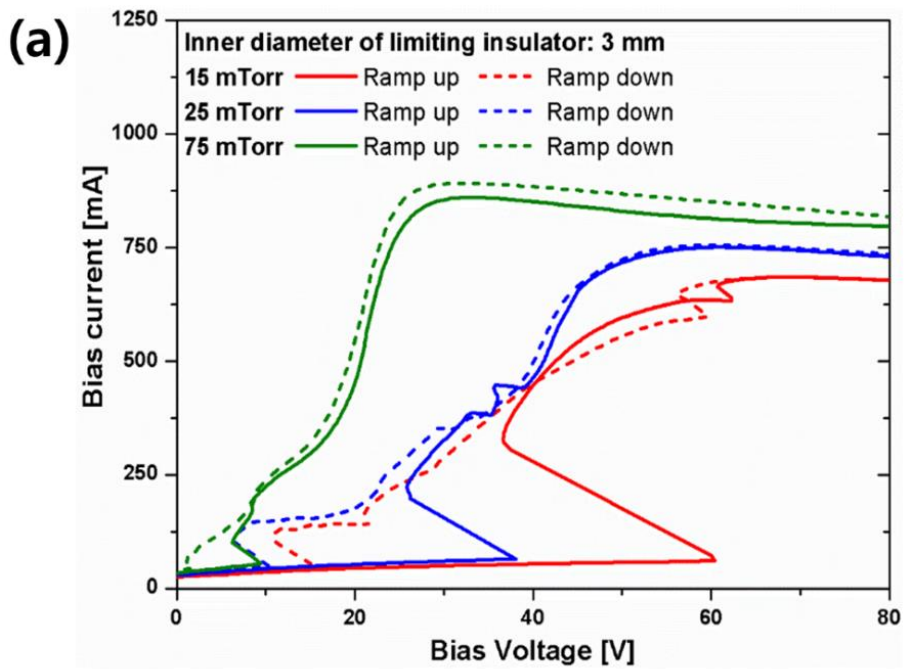


Figure 2. 3. (a) The variation of current-voltage characteristic curve of anode spot plasma with the operating pressure for a bias electrode with outer diameter of 4 mm. (b) The change in shape of anode spot plasma with the outer diameter of bias electrode and operating pressure.

it is found that the saturated bias current decreases when the gas pressure is further reduced to below ~ 25 mTorr, as shown in **Fig. 2.3. (a)**. A simple global discharge model explains that the reduction in the saturated bias current is related with the rapid increase of the electron temperature of ambient plasma at low pressure regime [24]. The increase of the electron temperature enhances the particle loss to walls across the sheath, hence lowers the plasma density at the same absorbed power. **Figure 2.3. (b)** shows the change in shape of anode spot plasma at the saturated region with the gas pressure. The anode spot plasma sustains in spherical shape at the operating pressure higher than 50 mTorr (see lower-left panel in **Fig. 2.3. (b)**), but it becomes a cylinder at the gas pressure lower than 25 mTorr as shown at the upper-left panel in **Fig. 2.3. (b)**. It is also observed that the shape of anode spot plasma is influenced by the area of bias electrode exposed to the ambient plasma. As depicted in the upper three panels of **Fig. 2.3. (b)**, the anode spot plasma becomes more spherical as the area of bias electrode increases at the gas pressure of 15 mTorr. When the gas pressure is increased to 75 mTorr, the shape of anode spot is spherical irrespective of the area of bias electrode. However, it is noted that the anode spot cannot cover the entire area exposed to ambient plasma for the bias electrode with outer diameter of 5 mm as shown at the lower-right panel in **Fig. 2.3. (b)**. The shape of anode spot plasma and its positioning on the bias electrode can be explained by the fact that the size of anode spot plasma (L_{as}) is dependent mostly on the gas pressure (p) according to the Eq. (2.1) [17]:

$$L_{as} = \frac{1}{\sigma_{ioniz} N_{gas}} \sqrt{\frac{m_e}{M_i}} \sim \frac{1}{p}, \quad (2.1)$$

where N_{gas} is the neutral density, σ_{ioniz} is the ionization cross section, m_e and M_i are the electron mass and ion mass, respectively. Therefore, when the exposed area of the bias electrode is too small to accommodate the anode spot plasma (for example, upper-left panel in **Fig. 2.3. (b)**), the anode spot plasma smears out from the area limited by the insulator so as to increase the electron-collecting area. On the contrary, if the area of bias electrode exposed to the ambient plasma is larger than the area occupied by the anode spot plasma, the anode spot plasma attaches locally to the bias electrode, as shown at the lower-right panel in **Fig. 2.3. (b)**. At specific operating condition, the anode spot plasma is not fixed at one place but wanders around the remaining area of the bias electrode.

From the experimental results shown in **Figs. 2.2** and **2.3**, the conditions necessary for the formation of stable anode spot in the presence of an extraction hole are expressed as Eqs. (2.2) and (2.3).

$$L_{as} > a_{ext} \quad (2.2)$$

$$w < L_{as} \quad (2.3)$$

where $w = (D_{bias} - a_{ext})/2$ is the annular width of the bias electrode exposed to ambient plasma. For given size of an extraction aperture, the maximum operating pressure for the formation of anode spot plasma is limited by Eq. (2.2). Unless Eq.

(2.2) is satisfied, the anode spot plasma is too small to cover the extraction hole. Once the operating pressure is determined, the maximum outer diameter of the bias electrode is restricted from Eq. (2.3). If Eq. (2.3) is not satisfied, the anode spot plasma attaches locally to the bias electrode, as depicted at the lower-right panel in **Fig. 2.3. (b)**. It should be noted that Eqs. (2.2) and (2.3) together with Eq. (2.1) are just necessary conditions for the formation of stable anode spot plasma in the presence of an extraction hole, without consideration on ion beam extraction.

2.3. Ion Beam Extraction from Anode Spot Plasma

2.3.1. Optimum Operating Pressure Variations by Diameter of Bias Electrode

Figure 2.4. (a) shows the typical dependency of the amount of ion beam currents extracted from the anode spot plasma on the operating pressure at various bias currents. In this experimental setup, a limiting insulator with 4 mm in inner diameter is utilized to limit the electrode area exposed to the ambient plasma. Besides the amount of ion beam currents extracted from anode spot plasma increases with increasing the bias current as the bias current is proportional to the plasma density in the anode spot [15], it is clearly observed that there is an optimum operating pressure of ~ 50 mTorr for the maximum ion beam extraction from the anode spot plasma. The existence of the optimum operating pressure for ion beam extraction is deeply associated with the

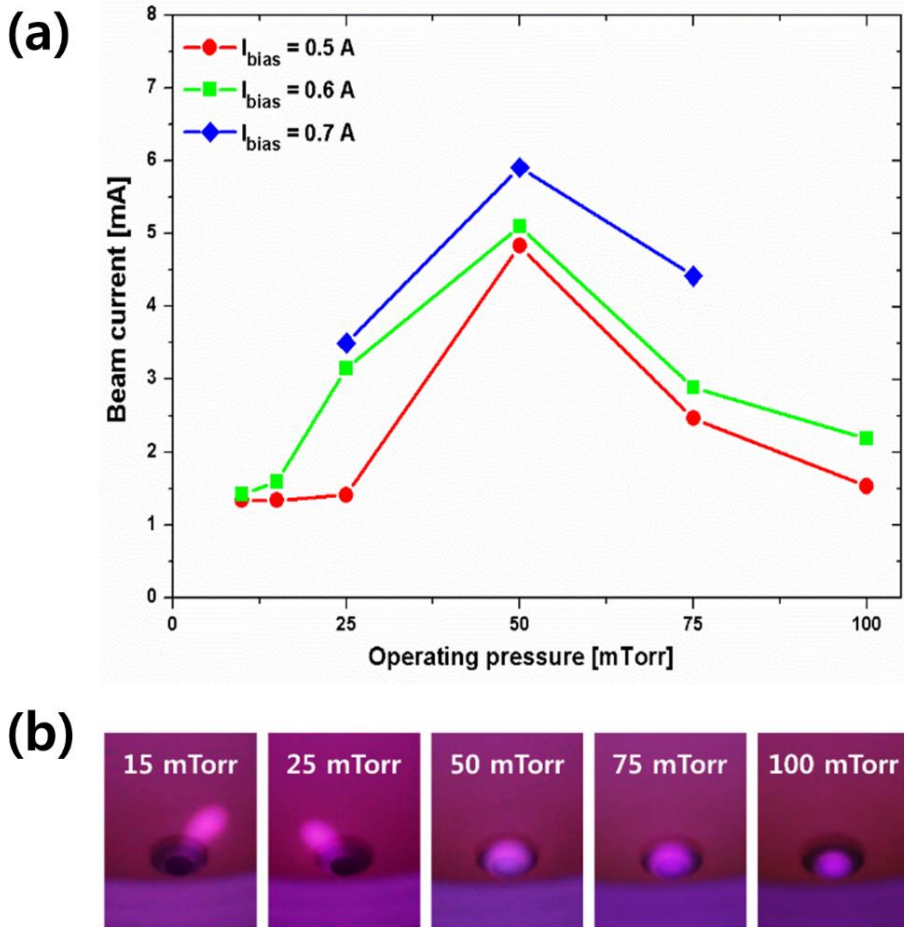


Figure 2. 4. (a) The variation of ion beam current extracted from anode spot plasma with the operating pressure for a bias electrode with outer diameter of 4 mm.
 (b) The change in shape of anode spot plasma with the operating pressure.

formation of the anode spot plasma in front of the bias electrode, as discussed in Sec. 2.2. Indeed, at the operating pressure lower than ~ 50 mTorr, the size of bias electrode exposed to ambient plasma is too small to fill the anode spot plasma whose size is

determined by the operating pressure according to Eq. (2.1). In this case, the plasma density near the extraction hole is low because the anode spot plasma smears out as shown at the left two panels in **Fig. 2.4. (b)**, so that the amount of ion beam current extracted from the hole is also low. On the contrary, for the operating pressure higher than ~ 50 mTorr, the anode spot plasma is too small to cover the entire electrode area so that the extraction current decreases with partial spot coverage of the extraction hole. At the optimum operating pressure of ~ 50 mTorr, it is obvious that the anode spot plasma covers the entire area of bias electrode exposed to ambient plasma as shown in the middle of **Fig. 2.4. (b)**.

Figure 2.5. shows the relationship between the amount of ion beam current extracted from anode spot plasma and the operating pressure for three kinds of bias electrodes with different outer diameters of 3, 4, and 5 mm at a fixed bias current of 600 mA. Note that the beam current data denoted as dashed line for the exposed bias electrode of 3 mm are estimated from the data obtained from the experiments carried out at the bias current of 500 mA. Because the extraction voltage exceeds the allowable value of the extraction system for the bias current of 600 mA in the present experimental setup. It is clearly observed that the optimum operating pressure for the maximum ion beam extraction varies with the outer diameter of the bias electrode. The optimum operating pressures for each case are determined to be ~ 75 mTorr, ~ 50 mTorr, and ~ 15 mTorr, respectively. This is because the optimum shape of anode spot plasma is influenced by the area of bias electrode exposed to ambient plasma. For the

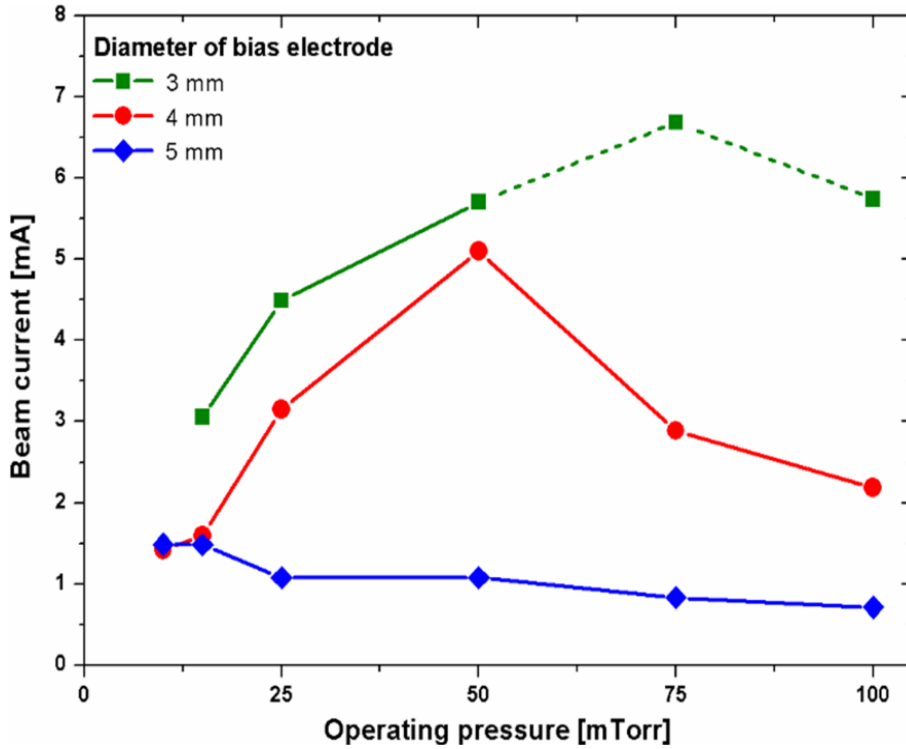


Figure 2. 5. The variation of ion beam current extracted anode spot plasma with the operating pressure: for bias electrodes with different outer diameters (3, 4 and 5 mm) at fixed bias current of 600mA.

bias electrode with large outer diameter, the optimum size of anode spot plasma is also large and thus the optimum operating pressure for the maximum ion beam extraction is reduced.

From a series of experiments on ion beam extraction from anode spot plasma, it is found that the maximum ion beam current can be extracted when the following condition is satisfied:

$$L_{as} \geq D_{bias} \quad (2.4)$$

For example, L_{as} is calculated to be ~ 3.8 mm for the gas pressure of 50 mTorr from Eq. (2.1) with assumptions of $\sigma_{ioniz} \sim 1.7 \times 10^{-18}$ cm² at $V_{DL} = 17$ eV and $T_{e,am} = 2$ eV [7]. This value coincides roughly with $D_{bias} \sim 4$ mm at the optimum operating pressure of 50 mTorr, as shown in **Fig. 2.5**. When Eq. (2.4) is satisfied, we observed that the stable anode spot plasma with a spherical shape fills the entire exposed area of bias electrode and its shape is not changed by ion beam extraction.

In **Fig. 2.5.**, it is found that the ion beam currents obtained from the bias electrode with the smallest outer diameter of 3 mm overwhelms data obtained from other sizes of bias electrode in all pressure ranges. This is due to the bias current density is inversely proportional to the area of bias electrode exposed to ambient plasma at a given value of bias current. Since the plasma density in the anode spot is roughly proportional to the bias current density for well-established anode spot plasma, the higher ion beam current can be extracted from the high-density anode spot plasma forms on the small bias electrode. Besides, it is observed that the anode spot plasma with cylindrical shape appears at low pressure (for example, see the upper-left panel in **Fig. 2.3. (b)**) changes into a spherical anode spot plasma during the beam extraction so as to enhance the plasma density near the extraction hole. The reason is not clear, but it seems that the electric field for ion beam extraction penetrates into the anode spot plasma and it perturbs the particle motion in the anode spot plasma. Also, the loss of ions through the extraction hole might perturb the particle balance in the anode spot

plasma so that the structure of anode spot plasma reorganized.

In summary, the stable sustainment condition of anode spot is suggested experimentally with considering the ion beam extraction that the anode spot should have a comparable size to the diameter of bias electrode. Moreover, the anode spot size determines the optimum operating pressure, which maximized the extracted ion beam current, at fixed the diameter of bias electrode with same bias current.

2.3.2. Nonlinearity between Bias current and Beam Current

Figure. 2.6. shows the variation of ion beam current extracted from anode spot plasma operates at optimum operating pressures for each case (75, 50, and 15 mTorr for D_{bias} of 3, 4, and 5 mm, respectively) with controlling the bias power. The bias power is a multiple of bias current and bias voltage, so that it is an effective power delivered to the anode spot plasma. Therefore, it is obvious that the bias power is directly associated with the plasma density in the anode spot, with the consideration of the nonlinear current-voltage characteristics of anode spot plasma as shown in **Fig. 2.2. (a)**. Owing to the nonlinearity of the plasma density in the anode spot with the bias power, the ion beam current extracted from the anode spot plasma also shows the nonlinear characteristics with the bias power, as clearly seen in **Fig. 2.6**. In the case of the bias electrode with outer diameter of 4 mm, the ion beam current is measured to be as small as 0.15 mA (see point ‘A’ in **Figs. 2.2. (a)** and **2.6.**) or current density

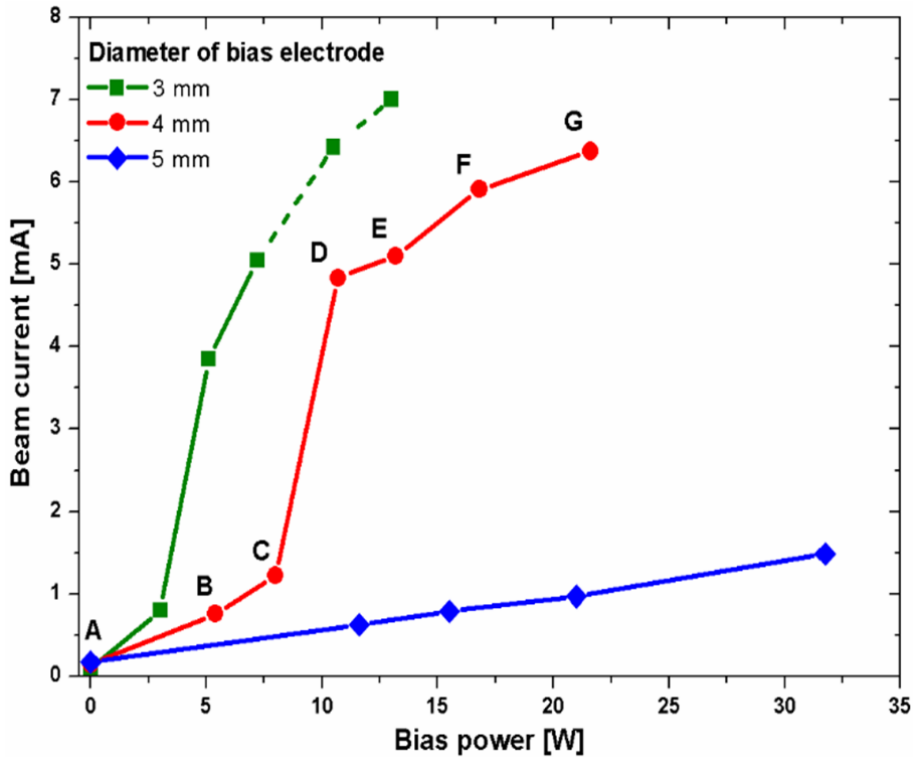


Figure 2. 6. The variation of the extracted ion beam current with the bias power operating at the optimum pressure for each case: 75 mTorr for 3 mm of bias electrode, 50 mTorr and 15 mTorr for 4 mm and 5 mm, respectively.

of 4.8 mA/cm^2 due to low plasma density near the extraction hole, when the bias power is zero, i.e. the anode spot plasma is turned off. Note that the operating points denoted as ‘A’ ~ ‘G’ in **Fig. 2.6.** is the same as the points denoted as ‘A’ ~ ‘G’ on the current-voltage curve shown in **Fig. 2.2. (a).** When the anode spot plasma is turned on, the ion beam is extracted from the anode spot plasma, not from the ambient plasma. The ion beam current extracted from the anode spot plasma increases with higher bias

power, reaching ~ 6.4 mA (204 mA/cm²) at the bias power of 22 W (see point ‘G’ in **Figs. 2.2. (a) and 2.6.**), which is 43 times larger than that extracted from the ambient plasma. It is worth noting that the huge amount of increase in the ion beam current is achieved by applying an additional DC power of just $\sim 10\%$ of the RF power to the anode spot plasma. In terms of power efficiency of the anode spot plasma (the increase of ion beam current divided by the bias power), operation at the point ‘D’ in **Figs. 2.2 (a) and 2.6.** seems to be the best for the ion beam extraction. The abrupt jump in the ion beam current (‘C’ \rightarrow ‘D’ in **Fig. 2.6.**) is caused by the change of anode spot plasma with the bias voltage or bias power. As shown in **Fig. 2.2. (b)**, the anode spot plasma is too small to cover the extraction aperture, until the bias power is increased to the operation point ‘D’ in **Figs. 2.2 (a) and 2.6.** After that, the ion beam current increases with a gentle slope (‘D’ \rightarrow ‘G’ in **Fig. 2.6.**) due to the increase in the plasma density of anode spot with the bias power.

In the case of the bias electrode with outer diameter of 3 mm, the abrupt increase in the ion beam current occurs at the bias power lower than that of 4 mm case, as the annular width of bias electrode exposed to ambient plasma (w) is too narrow for the anode spot plasma to stay on it. On the contrary, the abrupt increase in the ion beam current is not observed until the bias power up to 32 W in the case of the limiting insulator with 5 mm in inner diameter. In this case, the size of anode spot plasma is larger than that of the extraction hole at the beginning of the onset of anode spot plasma due to the operation at sufficiently low pressure of 15 mTorr. However, as

shown in **Fig. 2.2. (a)**, the bias current is low and increases gently with the bias voltage for the anode spot plasma operating at low pressure so that the ion beam current extracted from the anode spot plasma is low and increases with bias power with a gentle slope.

Therefore, the anode spot size is possible to be assumed as other effective control parameter of ASPIS that the extracted ion beam currents are varied according to the relationship among the anode spot size, the diameter of bias electrode and the extraction aperture size.

2.4. Summary: Effective Factors for Sustainment of Anode Spot with Ion Beam Extraction

To utilize the ASPIS as high current ion source, it is investigated the discharge characteristics of anode spot in presence of the beam extraction aperture of 2 mm at bias electrode, and the ion beam current is measured with various experimental conditions by controlled the diameter of bias electrode, operating pressure and bias current. It is successfully adopted the larger extraction aperture to ASPIS for high current beam extraction that the extracted ion beam current, 6.4 mA is about 43 times enhanced than that without anode spot (0.12 mA).

Figure 2.7. shows the operating parameters and design variables of the

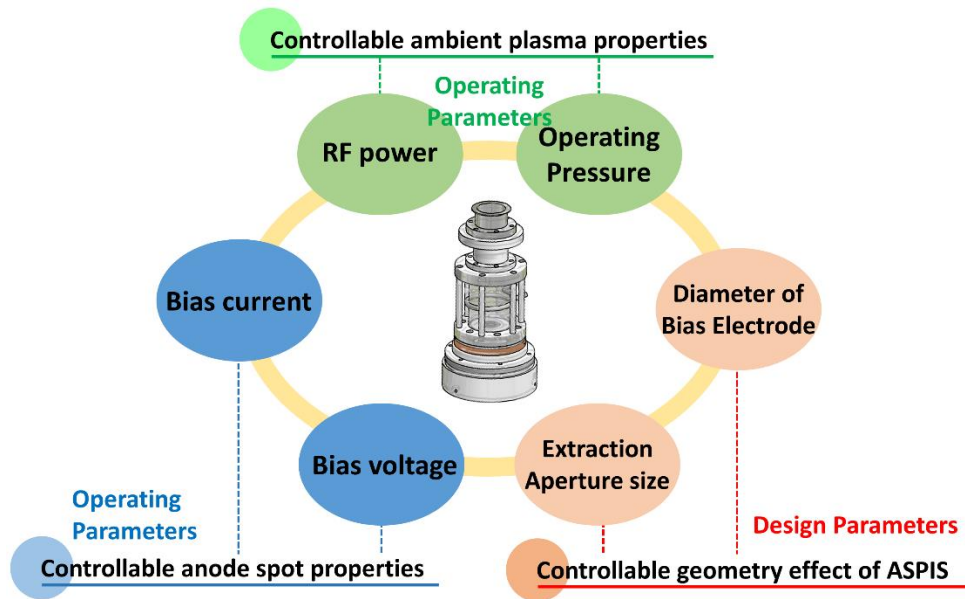


Figure 2. 7. The control parameters of ASPIS including the design parameter for high ion current extraction from ASPIS.

ASPIS: the operating parameters are RF power, operating pressure, bias voltage and current, the design variables are the diameter of bias electrode and extraction aperture. The operating parameters of RF power and operating pressure have been considered to only control the plasma properties of ambient plasma and the bias current and voltage to control the plasma properties of anode spot. In previous work, the operating parameter, especially the bias current has been considered as the dominant parameter to control the extracted ion beam current and the design parameters are not considered since the anode spot size is not much varied in this pressure range of ASPIS (50 - 150 mTorr) compared to the bias electrode's diameter.

In order to apply ASPIS as a high current ion source, it is found that the extracted ion beam currents are influenced by the anode spot size determined by the operating parameters and they are constrained the operating conditions of ASPIS by comparison between the design parameters and the anode spot size. Therefore, the design variables of ASPIS, such as the diameter of bias electrode (D_{bias}) and extraction aperture (a_{ext}) should be treated as operating parameters of ASPIS to sustain the anode spot during the ion beam extraction from it.

3. Plasma Properties and Size of Anode Spot with Operating Parameters

To figure out the optimum operating pressure and bias current range for high ion beam current extraction with stable operation, it is important to characterize the anode spot size compared to design parameters of ASPIS, such as diameter of bias electrode (D_{bias}), diameter of extraction aperture (a_{ext}) and the anode width (w) with considered the plasma properties of anode spot. It is reported by Song that the length of anode spot plasma is varied with operating pressure [13]. Theoretical approaches about anode spot size, L_{as} , have been tried that it is determined by the ion balancing between generated ions inside anode spot by electron-neutral collisions and ions escaped through the double layer potential structure and is expressed as Eq. (1.4). According to the Eq. (1.4), since the mass ratio of electron to ion and the ionization cross section determined by ionization potential of working gas are constant value in case of using single operating gas species, the anode spot size is only proportional to the reciprocal of operating pressure. The solid lines in **Fig. 3.1.** are denoted that the anode spot sizes are varied depending on the operating pressure with assumed the double layer potential as 17 eV – 20 eV. However, the sizes of anode spots change depending on the operating conditions such as operating pressure as well as bias voltage as shown in **Fig. 3.1.**, which the colored dots are represented the measured anode spot sizes with

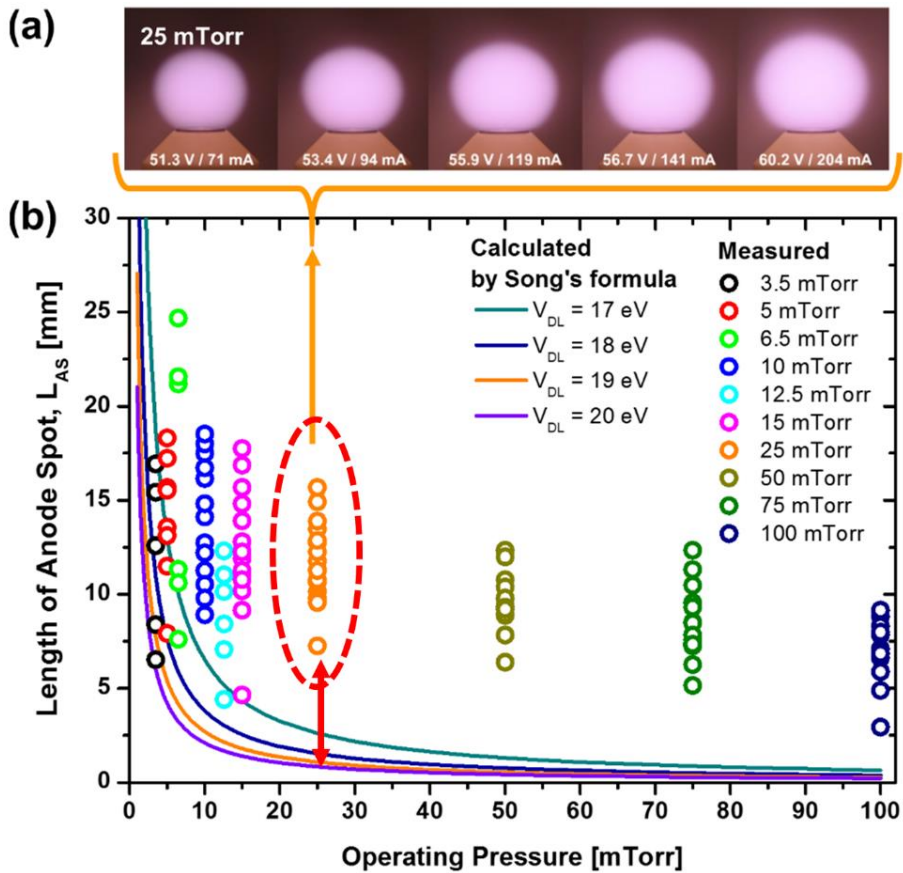


Figure 3. 1. The comparison between the estimation of anode spot size variations with different double layer potentials and the measured anode spot sizes expressed as varied the operating pressure and bias voltage.

varied the bias voltage at fixed operating pressure. For example, the anode spot size followed Eq. (1.4) is about 3 mm at 25 mTorr with the double layer potential as 17 eV, but the measured anode spot sizes are varied from 7 mm to 16 mm at same operating pressure as 25 mTorr.

Although the sustainment of anode spot in presence of ion beam extraction are essential conditions to operate the ASPIS as high current plasma ion source, there is poor research about the relationships between the operating parameters of ASPIS and plasma properties of anode spot including anode spot's size. Therefore, in this chapter, it is investigated the anode spot size variation in terms of operating parameters of ASPIS and measured the plasma properties of anode spot as well as ambient plasma in order to figure out the relationship between the operating parameters and the changes of plasma properties of two plasmas. It is modified the formulae related to the anode spot size expressed with the operating parameter of ASPIS and the plasma properties of ambient plasmas.

3.1. Experimental Details of Plasma Source and Diagnostics

3.1.1. Plasma Source and Bias probe

The whole system of vacuum chamber represents as **Fig. 3.2**. It is mostly made of stainless steel and fused silica (Quartz). Its basic structure of vacuum chamber is same as that used in previous work [25]. It consists of the plasma source for producing ambient plasma, bias probe for generating anode spot and diagnostics. In this research, the beam extraction module is additionally installed in front of vacuum duct, which is close to the Turbo Molecular Pump (TMP). By beam extraction module, the vacuum

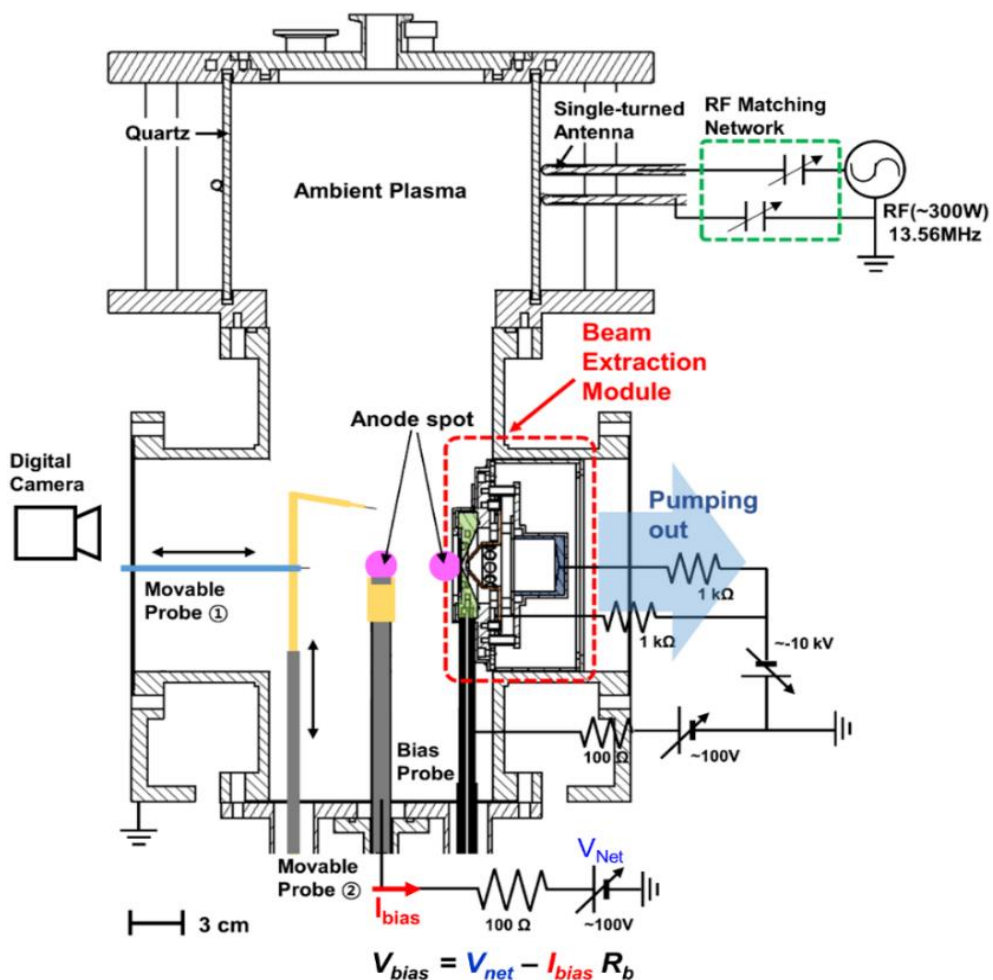


Figure 3. 2. Schematic diagram of plasma source, bias probe and diagnostics: the plasma properties are measured by Langmuir probes and the shapes of sizes change of anode spots are recorded by Digital camera.

chamber is divided into discharge chamber where is filled by plasma and extraction chamber where is maintained low operating pressure for beam extraction by differential pumped. The ultimate base pressure of vacuum chamber is sustained at

2.5×10^{-6} Torr without gas injection. Argon is chosen as operating gas, flown into discharge chamber controlled through mass flow controller (MFC). The operating pressure at discharge chamber is sustained in range of 10- 100 mTorr while working pressure at extraction chamber is maintained below 5×10^{-4} Torr. The ambient plasma is ignited at the upper part of discharge chamber enclosed by fused silica tube of 148 mm in height and 200 mm in diameter. The 150W- 250 W of RF power with 13.56 MHz is transmitted to silver plated, single-turned copper antenna which is surrounding the fused silica (Quartz) tube. The RF matching network (Alternative L-type [36]), which is installed between copper antenna and RF power supply, manually controlled to make the reflected power be minimized within 1 % of forward RF power. The inductive coupled plasma (ICP) generates inside the Quartz tube, and it diffused into discharge chamber made of stainless steel. All series of experiments in this research are performed at diffused plasma, which is operated as ambient plasma to anode spot, in order to be minimized the RF fluctuation from ICP plasma for measurement accuracy. Measured diffused plasma properties are kept in $10^9 - 10^{10} \text{ cm}^{-3}$ of plasma density, 1- 3 eV of electron temperature, respectively.

The auxiliary electrode, named as “bias probe”, is installed inside the discharge chamber to generate the anode spot plasma [16]. The bias probe is 200 - 300 mm away from the center of plasma source to be minimized the RF noise for measurement of plasma properties. The top, flat surface of bias probe is 6 mm in diameter. And lateral side of bias probe is covered by a ceramic insulator made of

Al_2O_3 that the top surface of bias probe is only exposed on ambient plasma. To generate the anode spot plasma in front of bias probe, it is positively biased on bias probe with respect to ground potential, its value is higher than plasma potential of ambient plasma. The DC Power supply connected to bias probe supplied up to 200 V. The voltage driven from DC power supply, V_{net} , and the voltage applied to bias probe named as “Bias voltage, V_{bias} ”, are measured by voltage probe via Oscilloscope. Between DC power supply and bias probe, the limiting resistance of $100\ \Omega$ (R_b) is set up to acquire the current flown from anode spot plasma to bias probe, named as “Bias current, I_{bias} ”, by measuring the voltage drop across the limiting resistance. The stable operating voltage- current region of anode spot plasma is also defined as limiting resistance so that the bias voltage and current are varied in range of 30 – 100V, 40 – 220 mA, respectively. The cooling system on bias probe is essential because 10~20 % of RF power is applied on bias probe to sustain the anode spot plasma stably. The cooling line is installed below exposed surface of bias probe to be chilled by distilled water. It is explained briefly about measurements that plasma properties are measured by cylindrical Langmuir probes with different dimension of probe tips. A series of experiments are conducted to measure the plasma properties variations by ion beam extraction from anode spot. And the shape or size changes of anode spot are recorded by Digital camera. At every experiments of measuring anode spot plasma, it is recorded the shape and size changes of anode spot plasma by commercial digital camera (Nikon D750 mounted with 105 mm lens). Its operating parameters such as F

number, ISO number and shutter speed are manually controlled, F number, ISO number and shutter speeds are varied as F 4- 5.6, ISO- 100- 250 and 1/60'' – 1/80'', respectively.

3.1.2. Langmuir Probes for Measurement of Plasma Properties

As mentioned in previous section about installation of bias probe inside discharge chamber, a series of experiments for measuring plasma properties with probes are conducted at lower part of discharge chamber to be less affected by RF noise. And it is found that RF fluctuation is ignorable and all Langmuir probes used in this experiments is also utilized with 50 - 100 k Ω of RF choke filter [37-38]. The single Langmuir probe with RF choke filter is measured the ambient plasma properties at 65 mm vertically away from the top surface of bias probe. The probe tip made of tungsten is 0.3 mm of diameter and 4 mm in length. In order to measure the plasma properties inside the anode spot, it is made as thin as possible in order to make less distortion on anode spot by probe invasion that dimensions of probe tip are 0.1 mm in diameter, 2.5 mm in length, respectively. The probe body, impinged into anode spot plasma, is less than 0.6 mm of diameter of ceramic rod. Since the anode spot is relatively very small volume compared to that of ambient plasma, the Langmuir probe for measuring anode spot plasma needs high spatial resolution that it moves in 0.5 mm step accuracy with range of 0 – 100 mm vertically away from bias probe

It is expected that the ambient plasma and anode spot plasma have different

plasma characteristics by double layer potential structure, so that it should be considered different analyzing method for current-voltage curves by Langmuir probe. The working principles of Langmuir probes are addressed in below by divided into general analysis and in case of existence of electron beam component in plasma

· **Basic Analysis I-V Curves Achieved at Ambient Plasma [38-41]**

The Langmuir probe is one of the most commonly used plasma diagnostics since it is easy to operate for achieving a various information about plasma properties by measured current through the conductor tip immersed in plasma. Generally used way of Langmuir probe is a single- tip probe method that obtains various information related to charged particles such as electron and ion density, electron temperature, plasma potential, floating potential, ion flux and electron energy distribution function. The maximum temporal resolution of this method is the time of the inverse of the ion plasma frequency and that of the maximum spatial resolution is limited to Debye length. It is important to design the proper size of probe tip since the plasma is disturbed in case of collecting large amount of current by probe. It is required that the area ratio between exposed area of probe tip and discharged chamber wall area contacted to plasma should be satisfied the conditions described as Eq. (3.1):

$$A_{probe} < \frac{n_0}{n_s} \sqrt{\frac{m_e}{M_i}} A_{wall} \quad (3.1)$$

where A_{probe} and A_{wall} are area of probe tip and wall area of discharge chamber, respectively, and n_0 , n_s represent the central plasma density and plasma density at sheath boundary. The radius of probe tip, radius of probe support and Debye length need to be very small compared to the mean free path of electron that analyzing the collected current by probe is dealt with collisionless sheath and plasma perturbation by probe is ignored.

Moreover, in case of RF plasma, the space potential normally fluctuates with RF frequency. Langmuir probes used in RF plasma source are subject to RF pickup which can greatly distort the I-V characteristics and give erroneous error. The problem is occurred because of collected current nonlinearity with voltage. The voltage is actually the potential difference $V_{LP} - V_s$, where V_s is a potential that can fluctuate at the RF frequency and its harmonics. And the current measurement takes longer time than oscillated period of RF power, the average of oscillating current is measured so that the I-V curve with higher electron temperature. Without RF compensation circuit, the plasma diagnosis becomes inaccurate since plasma properties such as electron temperature, electron saturation current, plasma potential are overestimated than those with RF compensation. Therefore, it needs RF compensation choke filter, which has sufficient high impedance to RF frequency, between probe tip and power supply in order to prevent the distortion by space potential oscillation with RF frequency.

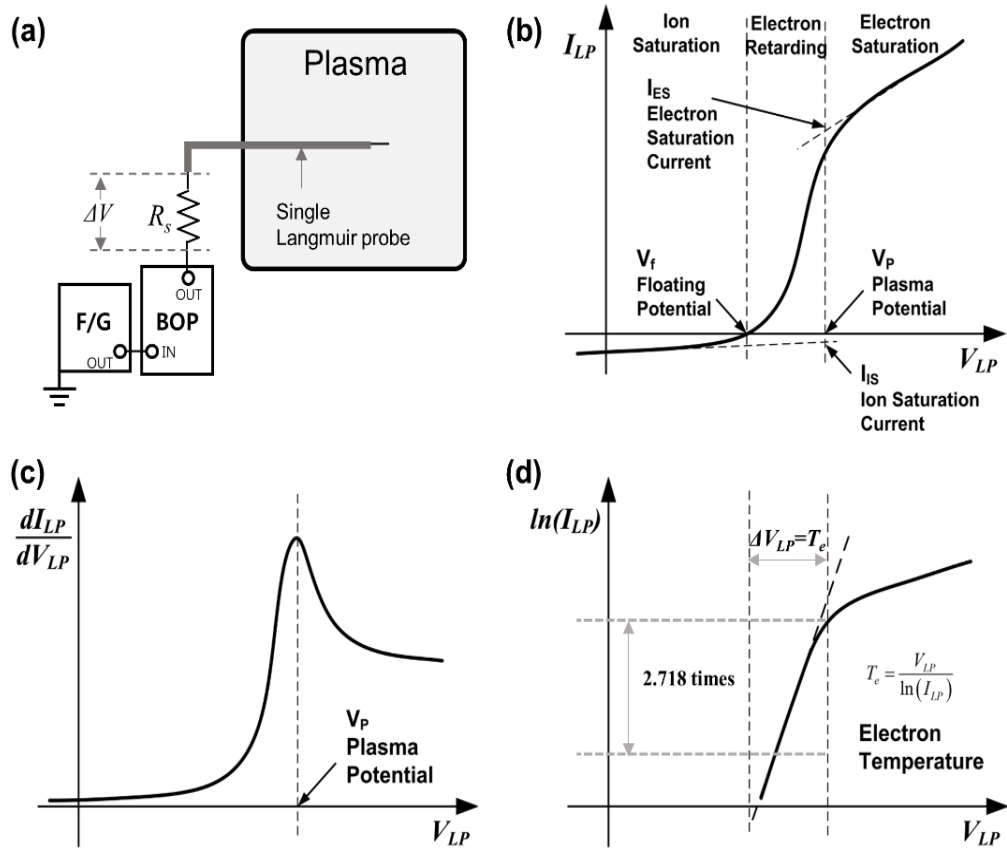


Figure 3. (a) Schematic diagram of single Langmuir probe and related circuitry configuration. (b) A typical voltage-current curve achieved by single probe with cylinder tip. (c) 1st derivative of the I - V curve and determination of plasma potential. (d) Semi-log plot of the I - V curve near to plasma potential and it shows the way to find electron temperature with linear fit.

Figure 3.3 (a) shows the simplified diagram of single Langmuir probe system and its circuitry. To obtain the net current by probe, the triangular waveform voltage signals, generated by Function generator, amplified through BOP are biased to probe tip. The

induced current flow from plasma to probe, I_{LP} , is monitored by oscilloscope as measured voltage drop across the measuring resistance R_s , which is located between the power supply and the probe. The typical current-voltage ($I-V$) curve achieved by single Langmuir probe is represented as **Fig. 3.3 (b)**. It is classified as five characteristic regimes: ion saturation region, floating potential, electron retardation region (ion-electron transition region), plasma potential and electron saturation region. The region obtained at the lowest potential is called the “ion saturation region”, where the pure ion current is collected that the electron is not travelled to the probe. The ion current increased slowly due to an increase in the sheath size. In case that the direction from probe is defined as the positive direction, as the voltage biased on probe is increased from negative to positive, the probe net current becomes more positive since the electron begins reaching the probe. At the floating potential, the same number of electrons and ions are being collected from plasma and net current collected by probe is reaching to zero. The plasma potential indicates the voltage at the knee of the $I-V$ curve (**Fig. 3.3 (b)**), and it is also figured out at the first derivative of the $I-V$ curve, where dI_{LP}/dV_{LP} is maximized (**Fig. 3.3 (c)**). The region between floating potential and the plasma potential is called the electron retardation region. Here, the most energetic electrons reach the probe, but the lower-energy electrons are still repelled. Since the number of electron being collected depends on the electron energy distribution of the plasma this region can be used to obtain that electron energy distribution function. If the electron energy distribution is a Maxwellian, the electron

temperature is also determined from this region as shown in **Fig. 3.3 (d)**. When the probe voltage is same as the plasma potential, electron can stream freely to the probe with no potential drop to retard them. The region beyond plasma potential is named as “electron saturation region”, where no ion reaches the probe, the number of electrons are collected depends on the distance that the electron field extends into the plasma and the density of electron.

It is assumed that the energy distribution of electron follows Maxwellian distribution, the electron temperature is described as a function of the current and voltage of probe. There are generally two ways to determine the electron temperature from electron retardation region of $I-V$ curve: to use the slope of $I-V$ curve in electron retardation region or the relationship between the plasma potential and floating potential. The electron current in electron retardation region is expressed as Eq. (3.2).

$$I_e = I_{esat} \exp\left(\frac{e(V_{LP} - V_p)}{kT_e}\right) \quad (3.2)$$

where A_p is exposed area of probe tip and I_{esat} is electron saturation current or random thermal current to the probe's surface at the plasma potential. Under the assumption that electron energy distribution is Maxwellian, the slope of $I-V$ curve becomes linear in plotted $I-V$ curve as semi-logarithmically current vs. probe voltage as depicted in **Fig. 3.3. (d)**. Eq. (3.3) shows that the inversed value of the slope of the $(\ln I_e) - V_{LP}$ curve is indicated the electron temperature.

$$\ln\left(\frac{I_e}{I_{esat}}\right) = \frac{e}{kT_e}(V_{LP} - V_p) \quad (3.3)$$

The electron temperature is also deduced from relationship between the plasma potential and floating potential. Floating potential refers to the voltage value when the net current flown into the probe is zero ($I_e = I_i$). It is assumed that the ion current flown into probe is described as Bohm current and electron current is one-directional thermal current with Maxwellian distribution (Eq. (3.2)), the potential difference between plasma potential and floating potentials expressed as a function of the electron temperature and mass ratio between ion and electron of operating gas (Eq.(3.4)).

$$V_p - V_f = kT_e \ln \frac{1}{\mu} \quad (3.4)$$

where

$$\mu = \sqrt{2.3 \frac{m_e}{M_i}} \quad (3.5).$$

Finally, it is estimated the electron temperature by plasma potential and floating potential, in case of using Argon as operating gas, the difference between plasma potential and floating potential is about $5.4 T_e$.

The plasma density can be obtained by the electron saturation current of ion saturation current since it has a correlation with both the electron saturation current and ion saturation current. The electron saturation current, I_{esat} , expressed as Eq. (3.6).

$$I_{esat} = \frac{1}{4} e n_e v_{th} A_{LP} \quad (3.6)$$

where n_e , is plasma density, v_{th} and A_{LP} are electron thermal velocity, the exposed area

of probe tip, respectively. The electron saturation current is determined from the linear extrapolated the electron current of electron saturation regime at plasma potential. From the characteristic current-voltage curve achieved by probe measurement, the electron saturation current, I_{esat} , refers to the electron current that linearly extrapolated in the electron current when the probe voltage is same as the plasma potential. When the electron energy distribution are followed the Maxwellian distribution, the thermal velocity of electron, v_{th} , expressed as Eq. (3.7) is a function of electron temperature, T_e .

$$v_{th} = \sqrt{\frac{3kT_e}{\pi m_e}} \quad (3.7)$$

The plasma density can be obtained from the electron saturation current with electron temperature estimated by methods mentioned above. But it is difficult to define the electron saturation current precisely since the electron saturation current is greatly affected by probe contamination, existence of magnetic field and electron sheath expansion by applied voltage to probe.

Compared to electron saturation current, the ion saturation current is less affected by external influences as mentioned above. Since the ion current is much smaller value than electron current, it is preferable to measure the ion current for avoid the signal noise by plasma perturbation. The ion saturation current, I_{isat} , expressed as Eq. (3.8), is a function of plasma density at sheath edge, n_s , probe tip area (A_{LP}), and ion Bohm velocity, u_B .

$$I_{isat} = en_s u_B A_{LP} \quad (3.8)$$

By similar process for electron saturation current, the ion saturation current is obtained from linear extrapolated value of ion current in ion saturation regime of **Fig. 1.2. (b)** at plasma potential. In case that the sheath formed between the probe tip surface and plasma is assumed as Bohm sheath, the plasma density at sheath edge and Bohm velocity are expressed as Eqs.(3.9) and (3.10), respectively.

$$n_s = n_e \exp(-0.5) \approx 0.61n_e \quad (3.9)$$

$$u_B = \sqrt{\frac{kT_e}{M_i}} \quad (3.10)$$

The plasma density, n_e , is also obtained from the ion saturation current, expressed as Eq.(3.8) with considered Eq.(3.9) and Eq.(3.10) in case of the existence of thin-collisionless sheath. In analyzing the probe current, especially ion current, since the effective area of collecting particles affects to the thickness of sheath surrounding the probe tip, the charged particle motions within sheath should be taken into account in determination of the electron and ion current. In addition, the analysis method for obtaining plasma density from ion saturation current is determined on based the comparison of the length scales among the sheath thickness(s), radius of probe tip, r_{LP} , and electron's mean free path, λ_0 .

The type of sheath distinguishes whether the collisions between particles are considerable in the sheath and the thickness of the sheath is thin enough to ignore the

orbit motions of incident particles. Assumption that the sheath thickness is about 4 times higher than the plasma characteristic length, Debye length ($s \sim 4\lambda_D$, $\lambda_D = (\epsilon_0 k T_e / n e^2)^{1/2}$). If the thickness of sheath is less than the mean free path of electron (Collisionless sheath, $s < \lambda_0$), it is assumed that the collision between particles does not occur in the sheath. And in the opposite case, the collision should be considered for probe analysis (Collisional sheath, $s > \lambda_0$). Moreover, the thickness of sheath is thinner than the radius of probe's tip (Thin sheath, $s < r_{LP}$), it can be considered that all incident particles toward the sheath are collected by the probe's surface. On the contrary to that condition (Thick sheath, $s > r_{LP}$), since some of incident particles are only collected because of different incident orbits between the particles, the probe analysis is limited to incident particle's orbit motion.

In this study, a series of plasma measurement experiments are conducted at operating pressure in range of 10- 75 mTorr, that the mean free path is maintained in range from 0.8 mm to 6.1 mm. The dimensions of probe used in those experiments is 0.05 mm in radius and 2.5 mm in length. It has been measured two types of plasma: ambient plasma and anode spot plasma. The ambient plasma is maintained 5×10^{15} - $1 \times 10^{16} \text{ m}^{-3}$ of plasma density and 1.5 eV - 3 eV of electron temperature, respectively so that the sheath thickness is estimated about 0.5 mm. The sheath formed between ambient plasma and probe tip is treated as collisionless-thick sheath that orbital-motion-limited (OML) theory considering the angular and radial momentum of

particle is generally applied to analysis for cylindrical single Langmuir probe. In OML theory, the ion saturation current is expressed as Eq. (3.11).

$$I_{isat} = 2en_s(r_{LP}l_{LP})\sqrt{\frac{2e|V_p-V_{LP}|}{M_i}} \quad (3.11)$$

where r_{LP} and l_{LP} are the radius and length of probe tip, respectively. Unlike Eq. (3.8) in case for collisionless-thin sheath, Ion saturation current expressed as Eq. (3.11) is a function of the potential difference between applied voltage to probe an plasma potential. The plasma density can be estimated the linearly slope of $(I_{isat} - V_{LP}^{1/2})$ plot.

To compare the length scale measured at anode spot plasma, the anode spot is varied in range of $5 \times 10^{16} - 1 \times 10^{17} \text{ m}^{-3}$ of plasma density and 5 eV - 7 eV of electron temperature, respectively. In this case, the Debye length of anode spot is about 0.06 mm, it is comparable value with the radius of the probe tip that the effect of sheath thickness should be considered in plasmas if sheath scale is in transition region from thick to thin. The effective area for probe is modified in Eq. (3.11) that the effective area for collecting is expressed as the multiples the exposed area of probe tip (A_{LP}) and current density (J_i) for the Bohm acceleration in the pre-sheath. The numerical solution for the ratio of probe radius to the Debye length has been given by Laframboise, who solved Poisson's equation numerically assuming a Maxwellian distribution of ions and electrons.

In addition, the electron energy distribution is not followed a Maxwellian distribution, electron temperature error may occur depending on a designated region

for calculating slope of $\ln(I_{LP})-V$ curve. It is also deduced the effective electron temperature, T_e^* and plasma density, n_e , by analyzing Electron Energy Distribution Function, EEDF. It is well-known that the EEDF is easily derived from the second derivative $I-V$ curve expressed as Eq. (3.12).

$$f_e(E) = \frac{2m_e}{e^2 A_{LP}} \sqrt{\frac{2e}{m_e}} \sqrt{E} \frac{d^2 I_{LP}}{dV_{LP}^2} \quad (3.12)$$

$$n_e = \int_0^\infty f(E) dE \quad (3.13)$$

$$\langle E \rangle = \frac{1}{n_e} \int_0^\infty E f_e(E) dE = \frac{3}{2} k T_e^* \quad (3.14)$$

The Equation of (3.13) is represented that the electron density, n_e , is about the integration value of EEDF for energy and the effective electron temperature, T_e^* , can be obtained from the average energy value of electron, $\langle E \rangle$, and it is expressed as Eq. (3.14).

· Basic Analysis of $I-V$ Curves Achieved the Plasma with Electron Beam [36, 39-40]

In the previous section of 1.1.2, the spatial distribution of plasma potential is measured in anode spot and ambient plasma that the plasma potential is abruptly dropped within 1-2 mm in distance where double layer is existed. It is also known that the anode spot has higher plasma potential value than ambient plasma and its potential difference is higher than the first ionization potential of operating gas species. Since the electrons

from ambient plasma are accelerated as much as double layer potential and entered into anode spot, it is easily predicted that the electrons inside anode spot will be existed two different groups: new electron group generated by ionization process in anode spot and other electron group with beam energy. Thus, it essentially needs to know how to interpret the characteristic current-voltage curves obtained by probe in case that the electron beam component is existed in the plasma.

When more than one electron species is present, the electron current collected by probe is often fit to the sum of two Maxwellians which are expressed as current-voltage characteristics with two ‘knees’ arise from the presence of an electron beam components in plasmas. **Figure 3.4** shows two examples of the characteristic current-voltage curve for plasma containing an electron beam without considered the ion saturation current and sheath expansion in electron saturation region (**Fig. 3.4. (a)** and **(c)**) and their first derivative current curves with respect to the voltage (**Fig. 3.4. (b)** and **(d)**).

Figure 3.4. (a) is the example $I-V$ curve of the existence of isotropic mono-energetic electrons in some of plasmas. An example which exhibits one extreme is the two electron species plasma found in low pressure devices that the plasma is produced by energetic ‘primary’ electrons by acceleration at the cathode sheath. For example, the primary electrons are existed multi-dipole device operated at very low pressure. The primary electrons are confined by the surface magnetic fields and bounce many

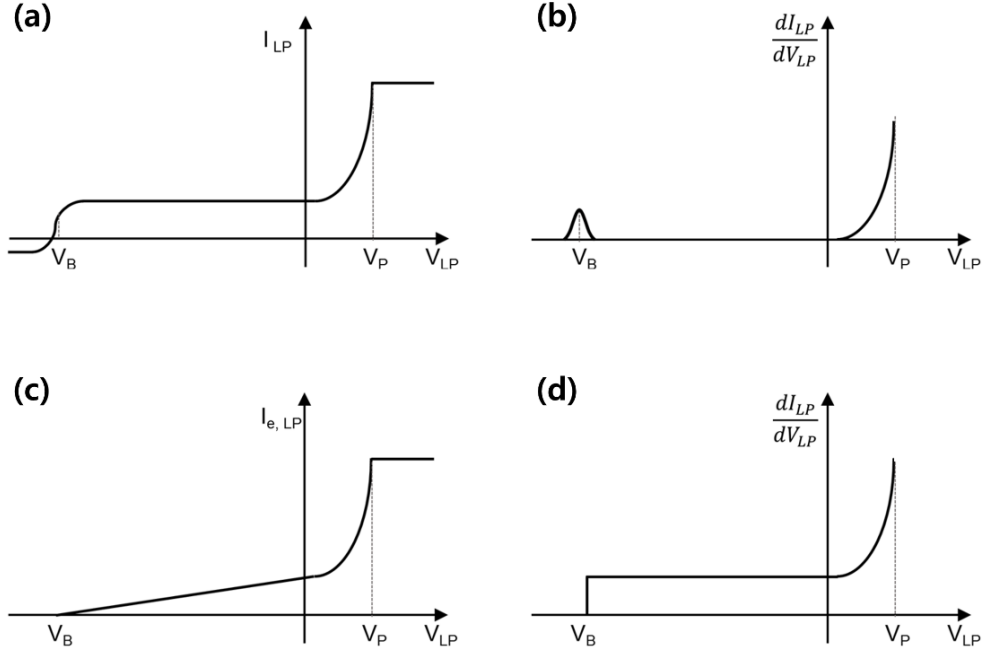


Figure 3. 4. Typical current-voltage curves and their first derivatives in case of the existence of electron beam component in plasma: drifted Maxwellian electrons represented as (a) I - V curve, (b) its 1st derivative of I - V curves and isotropic mono-energetic electrons expressed as (c) I - V curve, (d) its 1st derivative of I - V curves.

times before they ionize the neutral gas. After several bounces the primary electrons become isotropic and are still mono-energetic E_p thus the primary electrons from a shell in velocity at speed $v_p = (2E_p/m_e)^{1/2}$. It shows the results for the energetic primary electron component at E_p , which is no longer moving in one direction with respect to the probe. The electron current due to the primary electrons is given as Eq. (3.15).

$$I_e = I_p^* \left(1 - \frac{2e(V_p - V_b)}{m_e v_p^2}\right) \quad (: V_p - E_p \leq V_B \leq V_p) \quad (3.15)$$

It is difficult to estimate the tail of Maxwellian and it is not easy to guarantee the combination of only one species of primary electrons and background Maxwellian electrons.

The current which corresponds to an electron beam with a background plasma is shown in **Fig. 3.4 (c)**, described as ‘drifted Maxwellian distribution’. The pre-existing plasma, whose electron distribution is followed as Maxwellian distribution with electron temperature, T_e , is drifted by monotonic energy as E_b . Consider a drifting Maxwellian with a drift velocity, v_b , that is much greater than the velocity spread of the half width of Maxwellian, i.e., the electron drifted energy E_b is much greater than T_e . This situation could correspond to a plasma with a plasma source in the region of low potential that is followed by an increasing potential. The electron current collected by probe oriented perpendicular to the electron beam and biased to probe as V_b is given as Eq. (3.16)

$$I_e = en_b \sqrt{\frac{T_b}{2\pi m_e}} \exp(-x_m^2) + \frac{1}{2} en_b v_b (1 + \text{erf}(x_m)) \quad (3.16)$$

where

$$\text{erf}(x_m) = 2\sqrt{\pi} \int_0^{x_m} \exp(-x^2) dx \quad (3.17)$$

and

$$v_{min} = \sqrt{\frac{2e}{m_e(V_p - V_B)}}, \quad x_m = \sqrt{\frac{m_e}{2T_e}} (v_b - v_{min}) \quad (3.18).$$

The electron current corresponding to an electron beam with parallel temperature T_b . the beam I - V characteristic resemble an electron species at a plasma potential close to $V_p - E_b/e$ and one on the right corresponding to plasma potential in case that the two-knee like structure are present. The derivative $dI_{e,LP}/dV_b$ is curve shown in **Fig. 3.4. (d)**. If the bulk plasma are present as well, the derivative is expressed as Eq. (3.19).

$$\frac{dI}{dV_B} \propto \left\{ \frac{n_b \exp(-(v_{min} - v_b)^2)}{2T_{b\parallel}} + n_e \exp\left[-\left(\frac{v_{min}^2}{2T_e}\right)\right] \right\} \quad (3.19)$$

The temperatures, T_e and T_b , are chosen so that the energy spreads of the background and beam shown in **Fig. 3.4 (d)** are comparable.

3.2. Stable Operational Regime of Anode Spot

It has already been discussed the stable operational regime of anode spot in terms of bias voltage, RF power and operating pressure [13, 16, 25]. Based on the previous works, it needs to define the stable operating regime of anode spot sustainment since the instability of anode spot can be a factor to decrease the accuracy of plasma properties measurement inside the anode spot. It is known the unstable anode spot conditions that the boundary of the anode spot becomes unclear or the current spike occurs. Unstable operating region of anode spot is found that the current spikes, or anode spot oscillation, is occurred in the ‘A’-‘B’ region of **Fig. 1.2. (a)**. The current

spikes are reflected in the phenomenon that the anode spot is turned on and off periodically. The main reason for the oscillation of anode spot, i.e., bias current spikes, is the potential variation of double layer, V_{DL} . Formation of anode spot makes the potential of ambient plasma increase owing to the increased electron loss to the anode spot and the plasma potential of ambient plasma is also increased by the ion flux escaped from anode spot. As a result, the double layer potential is decreased than ionization potential of working gas and it makes the anode spot be extinguished by its low ionization rate. In order to prevent current spikes in 'A'-'B' region, the anode spot is said to be stable if the double layer potential is sustained sufficiently high even after the onset of anode spot since double layer potential can be reduced the loss of electrons in the ambient plasma. It is necessary to compensate the electron loss to anode spot that ionization rate of ambient plasma should be enhanced by increased the input RF power up to 150 W in this device.

Figure 3.5. (a) shows the discharge characteristic current-voltage curves obtained from positively biased probe as varied the operating pressure in range from 15 mTorr to 75 mTorr when the RF power for generating the ambient plasma is fixed as 150W. Before the anode spot is formed, an electron sheath is formed in front of the electrode. the bias current induced by the electron sheath increases with a gradual slope as the bias voltage increases, but the bias current level is sustained in several mA level. The current jumps in the characteristic current-voltage curves indicates that

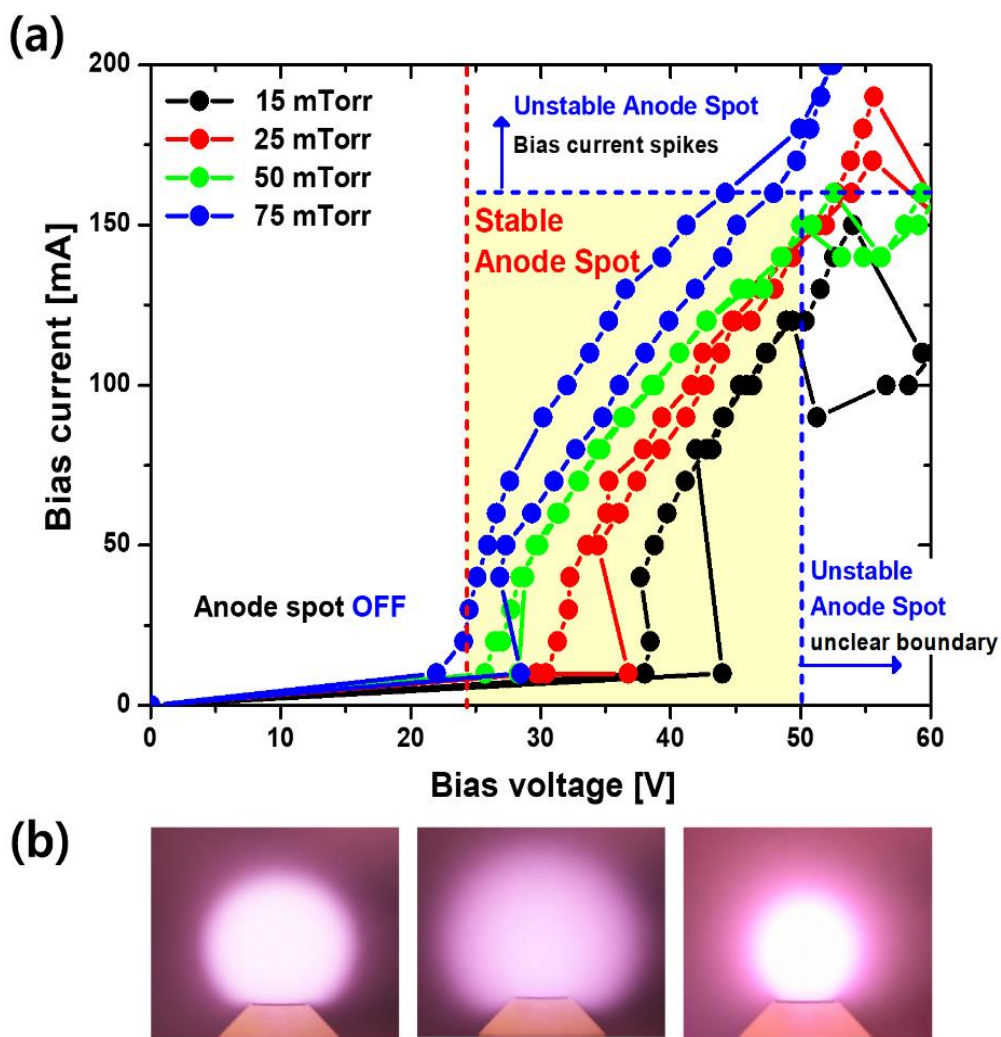


Figure 3. 5. (a) Discharge characteristic current-voltage curves obtained from positively biased electrode in pressure range from 15 mTorr to 75 mTorr with fixed RF power as 150 W. (b) Images of anode spots operated at 25 mTorr: Stable spherical anode spot(left), unstable anode spot with unclear boundary(center), unstable anode spot with current spike(right).

the anode spot is generated in front of positively biased probe. The breakdown voltage for generating anode spot is decreased with operating at high working pressure that the current jumps occur near 45 V operated at 15 mTorr and 29 V operated at 75 mTorr, respectively. After the anode spot is generated, the bias current increases linearly with the increases of the bias voltage, at this region, the anode spot is spherical shape with a clear boundary as left figure of **Fig. 3.5.(b)** so that it can be clearly distinguished from the ambient plasma.

When the bias voltage is continuously increased, there is unstable operational regions of anode spots depending on the operating pressure. At low operating pressures (<50mTorr), the unstable region where the bias current abruptly drops occurs with over-biased a certain value to bias probe and the bias current spike is taken place at high operating pressure region. In case of operating at 15 mTorr, it is observed that the bias current steeply drops when the bias voltage is 51 V. As shown in the middle image of **Fig. 3.5 (b)**, the shape of the anode spot maintains the spherical shape, though, it has about 1.5 times larger size with unclear boundary compared to stable anode spot shown in left image of **Fig. 3.5.(b)**. It is estimated that the plasma density of anode spot might be decreased because the bias current is worked as the indirect indicator of anode spot's plasma density.

It needs to be balanced between the generated electrons in the anode spot and the escaped electron as bias current in order to maintain the anode spot stably. Electrons are accumulated in the anode spot in case that the generation rate of electron

is higher than the loss rate of electron through bias probe. The space potential of anode spot is decreased, the double layer potential, the potential difference between anode spot and ambient plasma, is decreased with ionization rate in the anode spot. It is noticed that the size of anode spot also affects its stability because the electron flux from the ambient plasma to anode spot depends not only on the density of ambient plasma but also on the interfacial area between anode spot and ambient plasma. To compensate the low ionization rate, the anode spot is expanded its surface area. In order to prevent generation of unstable anode spots with operating at high bias voltage and low bias current mode, there are some methods for mitigating the accumulation of electrons in the anode spot by using wide area of bias probe or reducing the surface area of the anode spot by increasing the operating pressure.

In case of operating at high pressure, i.e., 75 mTorr, it is observed that the bias current spike is started when the bias voltage is higher than the voltage range for sustainment of spherical anode spot with clear boundary ($25 V \leq V_{bias} < 48 V$). As the bias voltage is further increased, the generation rate of current spikes is more frequent and its magnitude also increases. The current spike is an evidence that unstable anode spot plasma is additional generated that is similar characteristics of initial phenomenon where the anode spot is generated in the electron sheath explained in ‘A-B’ region of **Fig. 1.2 (a)** [13] , and the right image of **Fig. 3.5. (b)** is also shown that An anode spot with unclear boundary is additionally formed outside of existed anode spot with clear boundary [22, 44]. By decreasing the bias voltage or operated at low

pressure for increasing the breakdown voltage of additional anode spot, it is possible to prevent the additional generation of unstable anode spot in order to investigate a stable single anode spot.

Therefore, in case that input RF power is fixed as 150W and the operating pressure is varied from 15 mTorr to 75 mTorr, the proper operating range of bias voltage and current for keeping the stable anode spot, which has clear boundary without bias current fluctuations, is limited in operating range of 25V- 53V , 40 mA- 160 mA , respectively.

3.3. Analysis Probe Characteristic I - V Curves from Two Different Plasmas

In stable operating region of spherical anode spot, the operating parameter of anode spot can be operating pressure or bias current that bias current is linearly proportional to bias voltage and, unlike the operating range of bias voltage, bias current is kept in similar range regardless of operating pressure as well. As varied the operating parameters of anode spot, such as bias current and operating pressure, it is measured the characteristic current-voltage curves obtained by axially movable Langmuir probe at anode spot as well as ambient plasma. It is necessary to know how to define the plasma properties from I - V curves of anode spot plasma that I - V curves from anode spot have different trends compared to that from ambient plasma. As measured at

anode spot, it is observed the double knees at I - V curves as expected the existence of electron beam component in anode spot. In this section, we compare the measured I - V curves between anode spot and ambient plasma and define the determination of plasma properties in I - V curves with double knees. With analyzing experimental results, it is also examined the changes of the plasma properties, such as plasma density, electron temperature and plasma potential, according to the measured position variations and compared to the variations of anode spot size and shapes recorded by camera.

3.3.1. Probe I - V Curves with Varied the Operating Parameters

In this study, the Langmuir probes are mainly used to measure the plasma properties of anode spot and ambient plasma. In order to measure the plasma characteristics of anode spot without any distortion, there are two major considerations on probe fabrication: RF noise from ambient plasma and the anode spot perturbed by invasion of Langmuir probe. It may affect the probe diagnosis depending on the generation method of ambient plasma. The ambient plasma is an inductively coupled plasma that the space potential of RF plasma is normally fluctuated with its frequency. Langmuir probe in RF plasma suffers from the RF fluctuation that induces distortion on the I - V characteristics and gives tremendous errors on determination of plasma properties. In this manner, all series of experiments are performed at diffused plasma in order to be

minimized the RF fluctuation from ICP plasma by installed the bias probe 200-300 mm away from the upper part of discharge chamber where the ICP plasma is generated. We also have made an effort to minimize the RF noise to probe measurements by installing the RF choke filter whose impedance is in range of 50 k Ω -100 k Ω considered with 3rd harmonics of RF frequency.

It also should be minimized the perturbation on the plasma properties of anode spot and its sustainment by probe measurement. Since the total volume of the anode spots is very small compared to that of the ambient plasma, the anode spot is very sensitive to probe diagnosis. Especially, the probe body and tip partially exposed to anode spot should be made as thin as possible since the excessive collected current by probe can be induced the changes of anode spot plasma properties. In the series of experiments with probe diagnosis, the used Langmuir probe tip was 0.1 mm in diameter and 2 mm-2.5 mm in length, and the probe body partially exposed to the anode spot was designed as a 0.5 mm diameter ceramic tube, and the bias current is maintained within 2% variations by operated probe. It may be influenced by the anode spot measurement depending on the incident direction of the probe. It is difficult for the Langmuir probe to be entered into anode spot in a direction perpendicular to the surface of the bias probe since the anode spot tends to move in the opposite direction from the invaded probe in order to avoid the additional particle loss by probe. The probe needs to be installed a little away from the axis of the anode spot (the axis connecting the center of the anode spot and bias electrode). When the probe is

installed appropriately, the probe tip invades the anode spot although the spot seems to slightly move toward opposite direction from Langmuir probe.

Figure 3.6. (a) is an image representing the anode spot generated in front of bias probe, ambient plasma and installed movable Langmuir probe satisfied with all consideration as mentioned above. The ambient plasma is generated by 150W of RF power and 25 mTorr of operating pressure, respectively. And anode spot, whose size is kept about 11 mm, is sustained with 34 V of bias voltage, 80 mA of bias current. A series of experiments for the probe measurements is conducted with position variations of probe and the voltage variations applied to bias probe. The probe is vertically moved toward anode spot with 0.5 mm-step, its movable range is from 0 mm (at the surface of bias probe) to 30 mm. The obtained probe characteristic $I-V$ curves are varied according to the position changes of probe as shown in **Fig. 3.6. (b)**. The probe position is varied in range of 24 mm to 13 mm, that the probe is located in ambient plasma. Achieved $I-V$ curves at ambient plasmas have similar aspects with general $I-V$ curves obtained by cylindrical probe. Within this range, even if the probe approaches the anode spot, it is hard to be found the any variations at electron saturation current as well as ion saturation current obtained by probe. However, when the probe is moved closer to the anode spot, the probe position is between 11-12 mm, the electron saturation current slope begins to change further at the probe applied voltage as 30 V. When the probe is placed further inward, at a position about 9-10 mm, it is observed the existence of double knees at probe characteristic $I-V$ curves. In

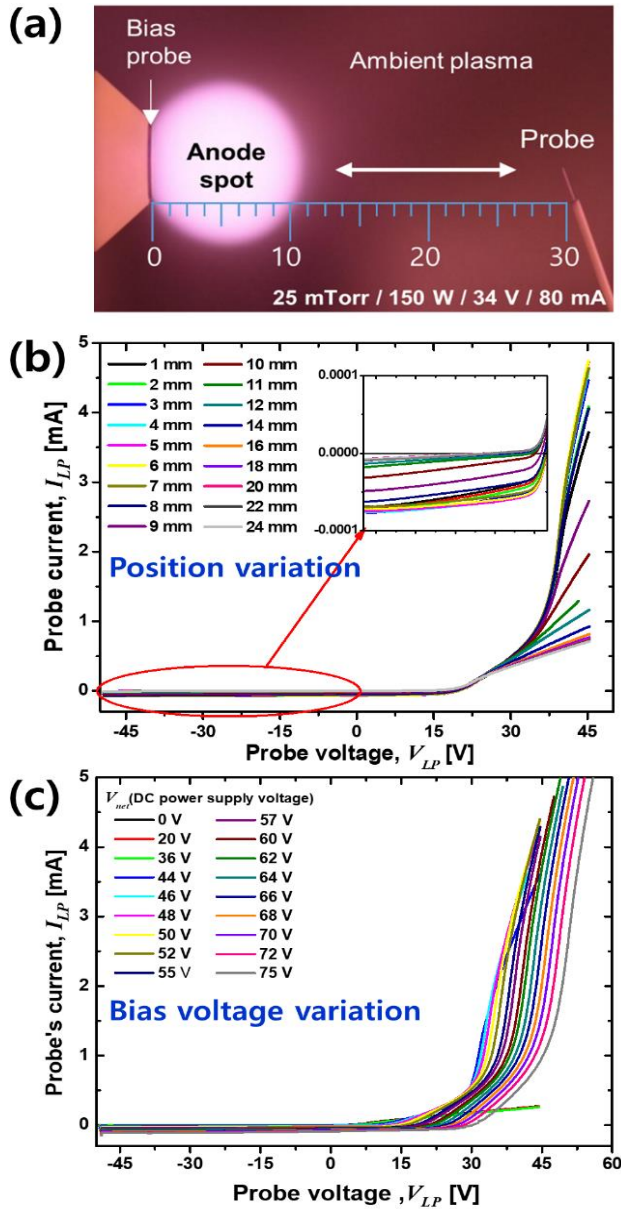


Figure 3. 6. I - V curves obtained at anode spot and ambient plasma by movable Langmuir probe: (a) the image represented the configuration of anode spot, ambient plasma and probe. (b) The typical probe I - V curves variations according to the position changes of probe, (c) changed the bias voltage with fixed position of probe.

addition, the electron saturation current achieved at second knee, is continuously increased until the probe reaches to 6 mm, where the center point of anode spot is existed, however it decreases as the probe gets closer to the surface of bias probe. In terms of ion saturation current, it shows the same tendency as the electron current does. When the probe is more than 10 mm away from the bias probe, it is kept in constant value, the ion saturation current rapidly increased where the probe reaches to 10 mm in distance, and it changes symmetrically with respect to the center of the anode spot. **Figure 3.6. (c)** shows the changes of probe characteristic current-voltage curves depending on increasing voltage applied to bias probe. The operating conditions for generating the ambient plasma were maintained as mentioned above, and the probe positions is fixed at 6 mm, which is the center of the anode spot based on the measured results obtained with position variation of probes. The voltage driven by DC power supply is changed in range from 0 V to 75 V and it is obtained I-V curves by probe in each cases. As varied the power supply voltage is 0 V to 43 V, and the probe characteristic I-V curves are obtained only from ambient plasma that it has only one knee near to plasma potential. The anode spot is generated in case that applied voltage is 44 V on bias probe. In this case, electron saturation current as well as ion saturation current is abruptly increased and it has same tendency of $I-V$ curves achieved inside the anode spot that the double knees is existed. When the applied voltage is further increased, both knees are shifted toward higher voltage, and the electron saturation current determined at the second knee and ion saturation current is continuously

increased.

The anode spot is expected as non-Maxwellian plasma that it exists the double knees at $I-V$ curves at anode spot, in this manners, it needs to different approach to analysis the plasma properties of anode spot from obtained $I-V$ curves compared to that for general plasma.

3.3.2. Plasma Properties Determinations of Anode Spot and Ambient Plasma

The electron current as well as the ion current collected by probe are varied with probe's position, especially inside and outside of anode spot. by compared each $I-V$ curved obtained at two different plasma, it is aimed to analyze the $I-V$ curves in detail to determine the plasma properties of ambient plasma and anode spot as well. Under same experimental conditions as 150W of RF power, 15 mTorr of operating pressure for ambient plasma and 42 V of bias voltage and 110 mA of bias current for anode spot, **Figure 3.7. (a)** and **(c)** represent the typical $I-V$ curves obtained from the anode spot plasma and ambient plasma and **Figure 3.6. (b)** and **(d)** also represent the current-voltage curves changed the format as a semi-log plot each cases, respectively. The characteristic $I-V$ curve achieved from ambient plasma is like general $I-V$ curves obtained by cylindrical probe. It is well-known that the probe voltage where the first derivative value is maximized is plasma potential. **Figure 3.8. (a)** and **(b)** show the first derivative of the current-voltage curve shown in **Fig. 3.7. (a)** and **(c)**, respectively.

Generally, the plasma has only one plasma potential as **Fig. 3. 8. (b)** that A single knee

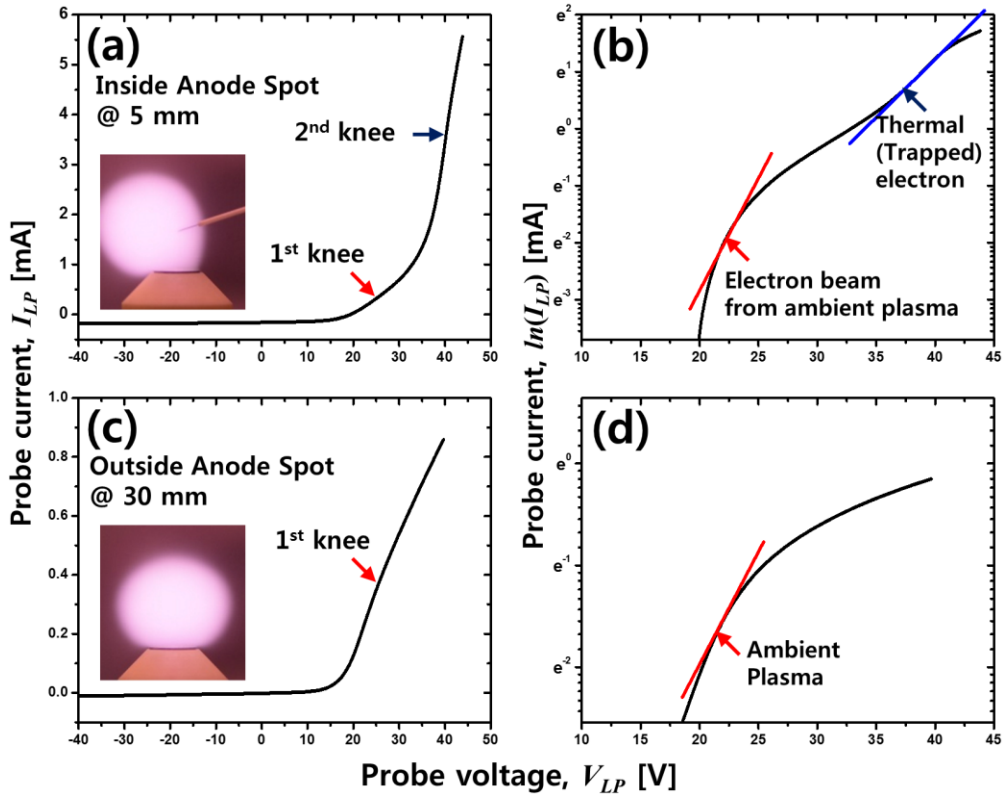


Figure. 3. 7. In case of operating at 15 mTorr of operating pressure, 42V /110mA of bias voltage and current. Inside the anode spot: (a) characteristic current voltage-curve, (b) changed the plot format as log plot for electron temperature. Outside the anode spot, ambient plasma: (c) characteristic current-voltage curve, (d) changed the plot format as semi log plot.

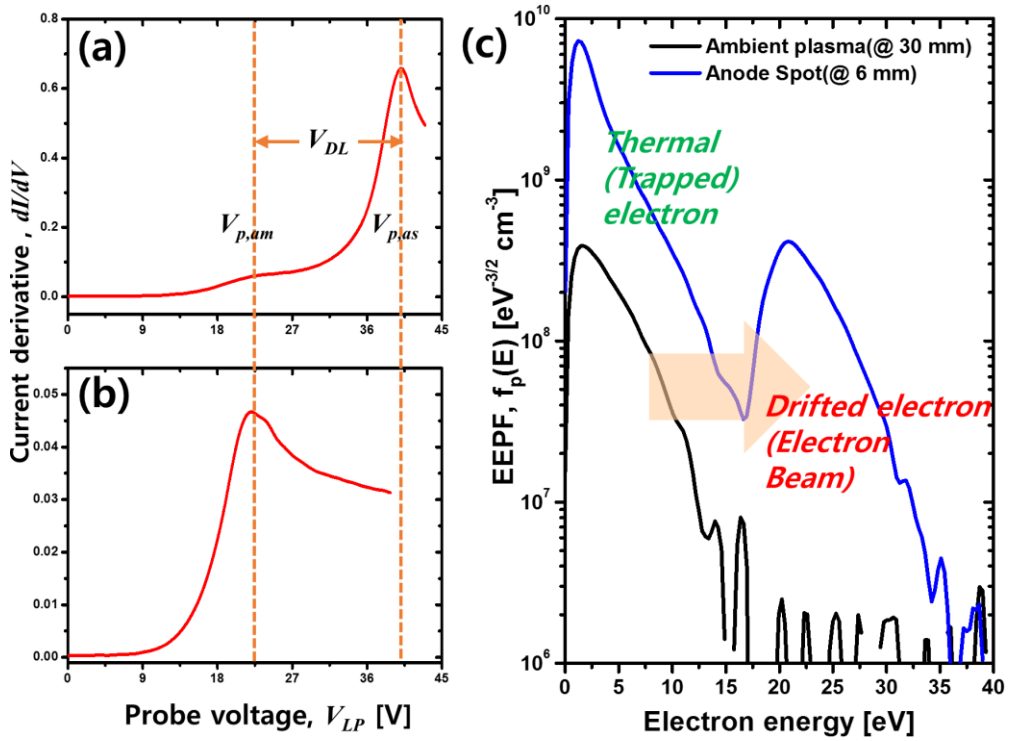


Figure 3. 8. In case of operating at 15 mTorr of operating pressure, 42V /110mA of bias voltage and current: (a) inside anode spot: probe current 1st derivative to bias voltage, (b) outside anode spot (ambient plasma): probe current 1st derivative to bias voltage and (c) comparison the EEPFs between achieved at anode spot and ambient plasma.

is found at 25 V of the probe voltage, which is indicated as the plasma potential of ambient plasma. Moreover, the electron temperature is about 3.5 eV, which is estimated from the inverse value of slope in the semi-log plot of $I-V$ curve (Fig. 3.7. (d)). Therefore, the plasma properties of ambient plasma are easily found from $I-V$

curve obtained at outside of anode spot by using the formulas explained in previous section.

On the other hand, the I - V curve achieved from anode spot is noticeably different to that from ambient plasma by the existence of double knees in electron current. Based on the conventional method for estimating the plasma properties in probe's characteristic I - V curves, the anode spot has two different plasma potentials as well as electron temperature as shown in **Fig. 3.8. (a)** and **Fig. 3.6. (b)**, respectively. With comparison between **Fig. 3.7. (a)** and **(c)**, the current increasing tendency is similar to each other that I - V curve obtained at anode spot also have a knee near to 27 V. However, the electron current achieved at anode spot is not saturated and increased more steeply and the increasing rate with respect to the probe voltage starts to decrease and make a second knee near to 41 V of probe voltage. And two different electron temperatures are existed in anode spot that one estimated near to 1st knee of I - V curve is about 3.5 eV and the other estimated near to 2nd knee is about 7 eV. It is known that the presence of electron beam component in plasmas, especially isotropic mono-energetic electron beam or drifting Maxwellian electron beam, is reflected as double knees of I - V curves, and the plasma potential at first knee is represented the plasma potential of electron beam component. Interestingly, the plasma potential and electron temperature obtained near to the first knee of I - V curve with anode spot coincide with plasma properties of the ambient plasma, and it is deduced that the one of electron component in anode spot is originally from the electrons of ambient plasma with

acceleration.

With I-V curves or 1st derivative I-V curves, it is too difficult to conclude whether the electron beam is mono-energetic or not, since the slope near to the fits knee at I-V curve of anode spot is relatively smooth compared to the 2nd knee. If the only mono-energetic electron beams exists in anode spot, the first derivative of I-V curve should have a discrete knee and steep slope depicted as **Fig. 3.4. (d)**. In order to figure out how to electrons be accelerated and inspect the characteristics of the electron beam in more detail, it needs to investigate the electron energy distribution in anode spot to achieve the plasma properties of electron beam as well as anode spot precisely. The electron energy distribution function, EEDF, is derived from the 2nd derivatives of the *I-V* curves expressed as Eq. (3.12). Electron energy probability function, EEPF, which excludes the electron energy to identify the degree of electron distribution at a specific energy, can be derived from EEDF divided by the electron energy related term of \sqrt{E} and it is expressed as Eq. (3.20).

$$f_p(E) = \frac{1}{\sqrt{E}} f_e(E) = \frac{2m_e}{e^2 A_{LP}} \sqrt{\frac{2e}{m_e}} \frac{d^2 I_{LP}}{dV_{LP}^2} \quad (3.20)$$

where A_{LP} is probe's surface area, m_e is electron mass and $d^2 I_{LP}/dV_{LP}^2$ is second derivatives of I-V curve. **Figure 3.8. (c)** is represented the EEPFs obtained at anode spot and ambient plasma, the blue line of **Fig. 3.8.(c)** is acquired in ambient plasma and black lines is represented for anode spot plasma. Electrons originated from ambient plasma are distributed in electron energy range within 15 eV. Within the

operating pressure range from 15 mTorr to 75 mTorr, the measured energy distribution of ambient plasma's electrons consist of the intermediate form of Maxwellian and Druyvestyn distribution since the electron mean free path becomes shorten and the electrons who have high energy are rapidly depleted as they easily lost their energies by collisions. The energy distribution for ambient plasma is expressed as Eq. (3.21).

$$f_{e,am}(E) = \frac{2}{\sqrt{\pi}} \left(\frac{1}{kT_{e,am}} \right)^{3/2} \sqrt{E} \exp \left(-c \left(\frac{E^a}{kT_{e,am}} \right) \right) \quad (3.21)$$

where $T_{e,am}$ is electron temperature of ambient plasma, c is constant for Druyvestyn distribution, 0.243, and a is multiple factor varied in range of 1-2: 1 for Maxwellian, 2 for Druyvestyn, in a series of experiments, the constant a is about 1.5. Nevertheless, it is clear that the ambient plasma has a single energy distribution of electrons and the electron beam component is not existed in it.

On the other hand, the EEPF achieved from anode spot covers the wider electron energy range of 0 - 35 eV compared to that from ambient plasma's energy range as 0 - 15 eV. It is inferred that the electron distribution of the anode spot do not follow a single Maxwellian distribution. In electron energy range of 0 - 15 eV, there is thermal electron inside anode spot. In addition, it is observed another electron peak in EEPF of anode spot, never seen at that of ambient plasmas, at 21 eV of electron energy, that is an evidence of electron beam component existed in anode spot plasma. The anode spot is believed to have two electron components with different electron energies: thermal electrons and accelerated electron beam components. Interestingly,

it is confirmed that the electron energy distribution of the beam component corresponds to that measured from ambient plasma. Comparing between the EEDF of electron beam component in anode spot and that of ambient plasma, the tendency of the electron energy distributions are consistent each other, but distributed electron energy level is shifted with a constant value, 19 eV. It is confirmed that the accelerated electron beam component is followed the drifted Maxwellian distribution since it maintains the electron energy distribution of ambient plasma, that is, its thermal energy represented by electron temperature of ambient plasma, $T_{e,am}$, with drifted energy. The drifted energy of electron beam is estimated from the potential difference between 1st and 2nd knee of probe voltage as shown in **Fig. 3.8. (a)**. The second knee is regarded as the potential of anode spot and the potential at the first knee of the $I-V$ curves for anode spot is same as that of ambient plasma. Consequently, the potential difference between two knees is found to be a potential difference between two different plasma, since the double layer is exists between them, the drifted electron energy inside anode spot may come from the potential difference, about 19 eV, across the double layer.

With typical probe characteristic $I-V$ curves, it is generally way to estimate the plasma density from the ion saturation current by using derived the electron temperature from the inverse slope value near to knee at $I-V$ curve. However, the compositions of electron components in anode spot are classified as thermal electrons and electron beam accelerated from ambient plasma, as well as the electron

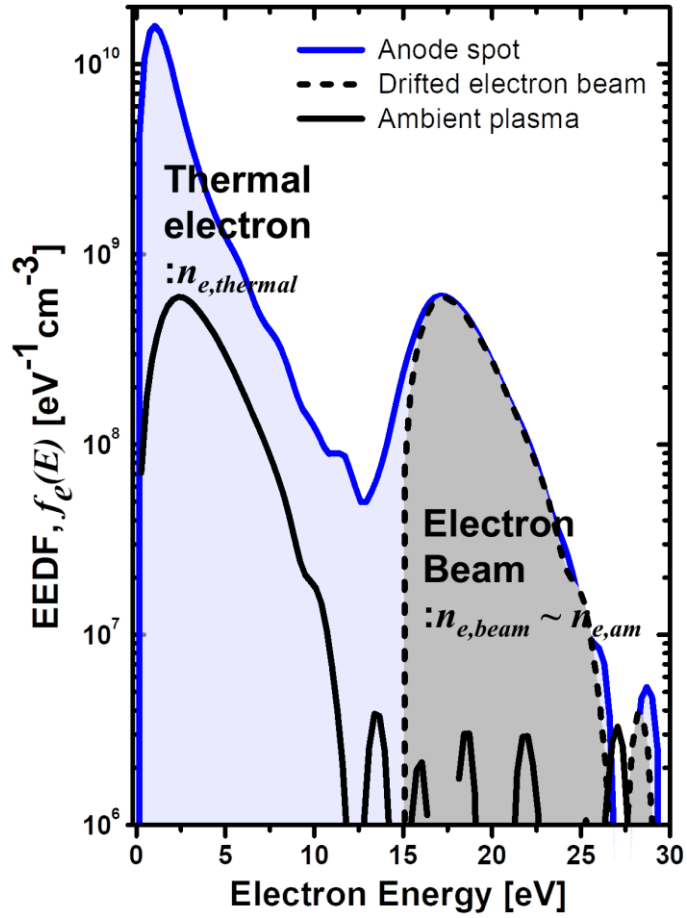


Figure 3. 9. How to achieve the electron density fraction of trapped electron to accelerated electron from ambient plasma at EEDF of anode spot.

temperature and plasma potential also exist in two different values by the type of electron components. So that it might make tremendous error to estimate the plasma density from ion saturation current depending on which electron temperature is used. In this manner, it is necessary to figure out which electron group, such as electron

beam or thermal electrons, is more dominantly existed in anode spot. **Figure 3.9.** shows the electron energy distribution function of anode spot expressed as blue line, that of ambient plasma depicted as black line and that for electron beam component expressed as black- dotted line. The probe measurement as shown in **Fig. 3.9.** is performed in experimental conditions at 150 W of RF power, 50 mTorr of operating pressure, 36V of bias voltage and 100 mA of bias current, respectively. It is known that the integrated area value of the EEDF indicates the electron density expressed as Eq. (3.13), in this manner, With EEDF analysis, the density of the thermal electron and that for the electron beam are easily deduced from the integrate values with different electron energy range. The regime where the thermal electron is distributed is approximately defined in electron energy range from 0 to 12 eV. As the electron energy distribution of ambient plasma electron is drifted with the drifting energy expressed as black dotted line, the electron energy range for electron beam component is estimated from 12 eV to 27 eV where finds the additional energy peak at 17 eV. With Calculated result of the integrated areas according the each electron energy range, it is confirmed that the thermal electron density, $n_{e,thermal}$, and that for electron beam, $n_{e,beam}$, are about $3.67 \times 10^{10} \text{ cm}^{-3}$ and $3.1 \times 10^9 \text{ cm}^{-3}$, respectively. The thermal electron has 10 times higher electron density than electron beam component, moreover, it is also figured out that the thermal electron density is at least 6 times higher than the electron beam density based on experimental results with various operational conditions so that most of the electrons inside the anode spot are thermal electrons. In

this manner, the plasma potential and electron temperature of anode spot are determined by the plasma properties of thermal electron. The plasma potential of anode spot can be defined as the probe voltage at second knee and the electron temperature as the reciprocal of the slope of the linearly increasing region near the second knee.

The anode spot has been known to satisfy quasi-neutrality independently from the ambient plasma that the electron density in the anode spot should be approximately same as the ion density. The total plasma density in the anode spot can be estimated from the sum of thermal electron density and electron beam density, which are obtained from EEDF, or from the ion saturation current. The plasma density is estimated from the ion saturation current with electron temperature. It is known that the cooler electron temperature is decided the Bohm velocity in case that two temperature plasmas are existed in same volume. For anode spot, the thermal electrons generated in anode spot have lower electron energy than electron beam, therefore, the total plasma density can be derived from the ion saturation current with electron temperature of thermal electrons.

In summary, plasma characteristics of ambient plasma can be figured out by using a conventional method for analyzing the I - V curve obtained from plasma. On the contrary, it needs to approach in different way to analyze the probe characteristic I - V curves in order to obtain properly the plasma properties depending on the existence of electron beam components in plasmas. The double knees are observed at

the I - V curves achieved from anode spot plasma. Since the plasma density of anode spot is dominantly composed by thermal electron, electron temperature and plasma potential estimated near to 2nd knee of I - V curves should be understood as representative value of anode spot properties. The distribution of electrons with different energies in the anode spot can be estimated according to the area ratio of EEDF, and the total plasma density can be derived from the ion saturation current based on the electron temperature of the thermal electron. As following **Table 3.1**, it is summarized how to obtain the plasma properties of anode spot as well as the ambient plasma from measured I - V curves.

Table 3. 1. Determination of Plasma properties for ambient plasma as well as anode spot from probe characteristic I - V curves.

Plasma properties	Ambient plasma	Anode spot	
		Drifted electrons	Thermal electrons
Plasma potential, V_p	Knee at I - V curves of electron current	Probe voltage at 1 st knee	Probe voltage at 2 nd knee
Electron temperature, T_e	Inverse slope value near to plasma potential	Inverse slope value near to 1 st knee	Inverse slope value near to 2 nd knee
Plasma density, n_e	From ion saturation current	From ion saturation current	
Double layer potential, V_{DL} (Drifted energy of electrons)		Potential Difference between 1 st and 2 nd knees	
Density fraction between electron components		Achieved area ratio at EEDF.	

3.3.3. Spatial Distribution of Plasma Properties

The plasma properties of the anode spot as well as the ambient plasma are investigated by using Langmuir probe diagnostics that moves in range from 0.5 mm to 30 mm by 0.5 mm-step. **Figure 3. 10.** shows the plasma properties variations by distance changes from the bias probe's surface, kept with a certain experimental conditions: anode spot sustains with 36 V and 100 mA of the bias voltage and bias current, respectively, and the ambient plasma is sustained with 150 W of RF power and 50 mTorr of the operating pressure. The spatial distributions of plasma properties such as the plasma potential, electron temperature and electron density are explained briefly since they are similar trends compared to the previous work by Park [25].

Figure 3.10. (b) shows the space potentials as a function of the distance from bias electrode. Before generating the anode spot, the space potential of the ambient plasma is about 10 V. As the anode spot is turned on, the ambient plasma potentials are increased to 21.5 V since the plasma chamber wall is grounded, not at floating potential. It is observed that the plasma potential of anode spot (36.6 V) is 15.1 V higher than that of the ambient plasma (21.5 V). It is noticeable that the plasma potentials are almost constant, regardless of the displacement in the anode spot. From the measured potentials, the size of the anode spot is about 10 mm as shown in **Fig. 3.10. (a)**, corresponds to the position where the potential drops occurred, that it is reliable results are not achieved due to the perturbation by the Langmuir probe.

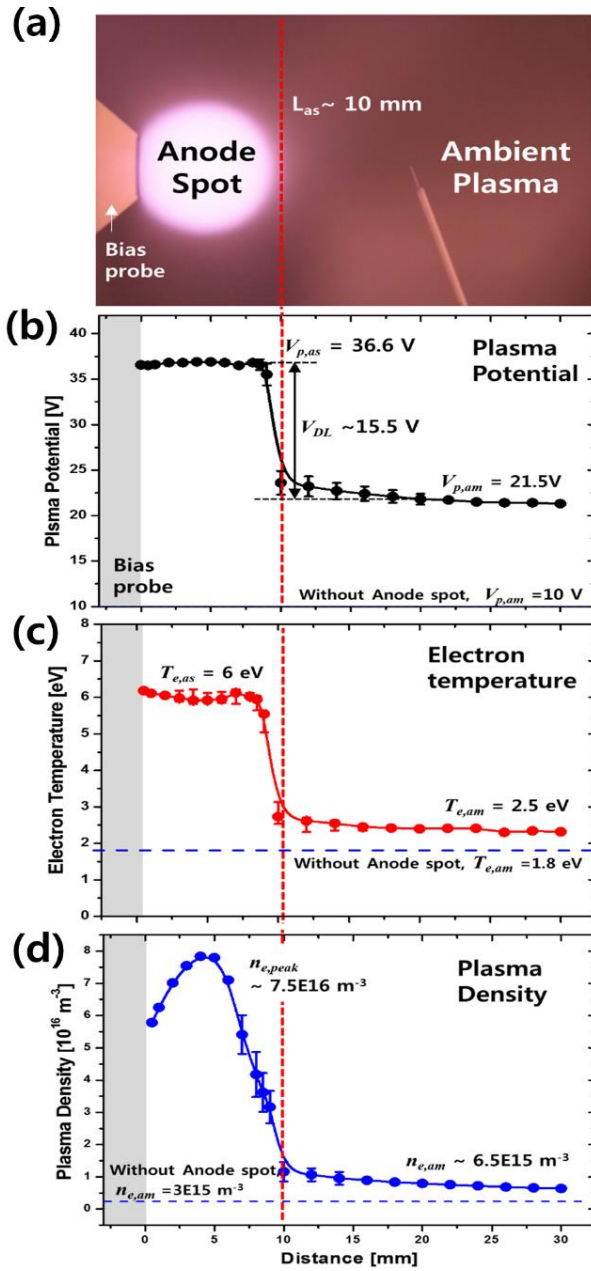


Figure 3. 10. (a) The image of anode spot and ambient plasma and spatial distribution of (b) plasma potential, (c) electron temperature, (d) plasma density with experimental conditions: 36 V/ 100 mA with sustained pressure as 50 mTorr.

The spatial distribution for the electron temperatures is shown in **Fig. 3.10. (c)**. Without the anode spot, the electron temperatures of the ambient plasma are about 1.8 eV. When the anode spot is onset at the surface of bias probe, the electron temperature of ambient plasma is abruptly increased as 2.5 eV. The electron temperature of the anode spot is measured to be about 6 eV, almost 3.5 eV higher than the electron temperature of the ambient plasma. Similar to the plasma potential profile, the electron temperature is almost constant with respect to the position inside the anode spot but is slightly increased (10-20 % of anode spot's electron temperature) near the double layer of the anode spot and close to the bias probe's surface.

Plasma density of the ambient plasma without anode spot is of $3 \times 10^{15} \text{ cm}^{-3}$. After generation of the anode spot, the plasma density of the ambient plasma increases, compared to without anode spot as shown in **Fig. 3.10. (d)**. Because of the increase of the plasma potential of the ambient plasma, enhancement of the electron confinement in the ambient plasma is probably the reason of the density increment. Different from the plasma potential and electron temperature, the plasma density inside the anode spot has a variation with respect to the position. The plasma density shows the maximum value over $7.5 \times 10^{16} \text{ cm}^{-3}$ at the center of the anode spot, which is 5 mm away from the bias electrode. But, the plasma density is steeply decreased to $3 \times 10^{16} \text{ cm}^{-3}$ near the edge of the anode spot at 10 mm. The parabolic shape of the density profile in the anode spot corresponds to the distribution of the plasma density acquired by solving a diffusion equation in spherical geometry [24]. Although there is

reduction of the plasma density at the edge of the anode spot, the density of anode spot is higher than that of the ambient plasma.

3.4. Determination of Anode Spot Size by Operating Parameters

The researches related to anode spot have approached experimentally to figure out the potential structure surround the anode spot, the relationship between the anode spot plasma density and bias current and the generation mechanism of two electron groups in anode spot as well. Though the anode spot size varies with various experimental conditions, the changes of anode spot size were not taken into the consideration of anode spot researches. However, it expects that the anode spot size influences on the determination of anode spot plasma properties since the total number of accelerated electron entered into anode spot is important to generate and sustain the anode spot.

In this section, it is observed the size variations of anode spot with varied experimental conditions and investigated the effective factors to determine the anode spot size. It is modified the formulae related to anode spot size with considered the correlation among the plasma properties of anode spot and operating parameters as well as anode spot size.

3.4.1. Anode Spot Size Variations by Operating Parameters

It is known that the RF power for generating the ambient plasma does not affect the saturated bias current value, but it does affect the anode spot size. With fixed RF power as 150 W for generating the ambient plasmas, the anode spot size, L_{as} , and bias current, I_{bias} , are measured with varied the operating parameters, such as operating pressure and the applied voltage to bias probe, V_{bias} . **Figure 3.11.** shows the size variation of anode spot and bias current as increasing the operating pressure with fixed bias voltage. The operating pressure is controlled in range in 15 – 75 mTorr. The black, red and green solid line indicate the spot size changes with applied the voltage of 40 V, 42 V and 44.5 V to bias probe, respectively. When the applied voltage to bias electrode is fixed as 40 V, the anode spot shrinks from 14 mm to 10.5 mm and the bias current is increased from 100 mA to 165 mA as increasing the operating pressure in range of 15 -75 mTorr. The anode spot size is proportional to the reciprocal of the operating pressure at constant bias voltage, which is the expectation result by Eq. (1.4). However, the estimated value from Eq. (1.4) is underestimated that it is smaller than the measured value. Assumed that the experimental conditions are kept in 15 mTorr of operating pressure and 44.5 V of bias voltage, the anode spot size is measured as 14.8 mm, while it is estimated as 2 mm in case of using the double layer potential measured as 18 eV (from blue solid line of **Fig. 3.1**). In this manner, it is expected that other factors except the operating pressure affects to the determination of anode spot size.

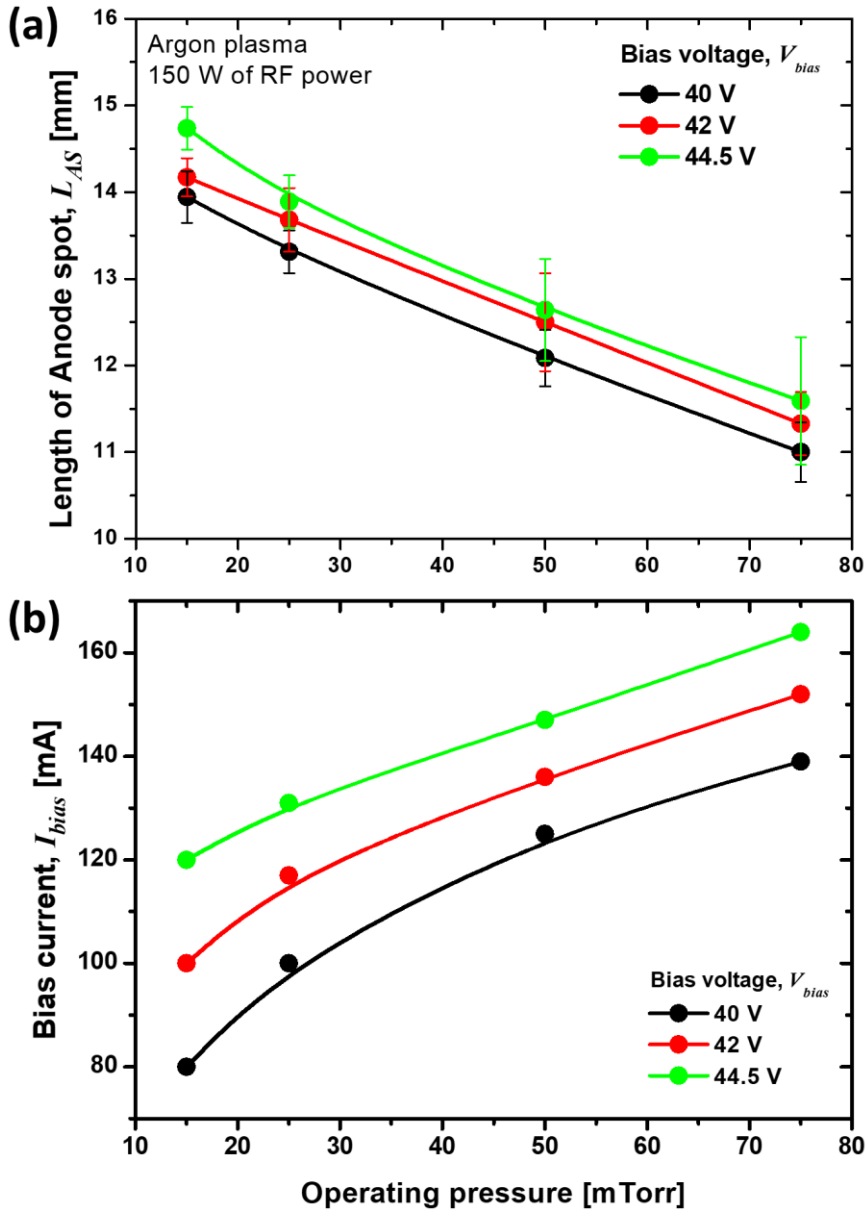


Figure 3. 11. (a) The anode spot size variations and (b) the bias current variations as increasing the operating pressure from 15 mTorr to 75 mTorr with fixed bias voltage and RF power of 150 W.

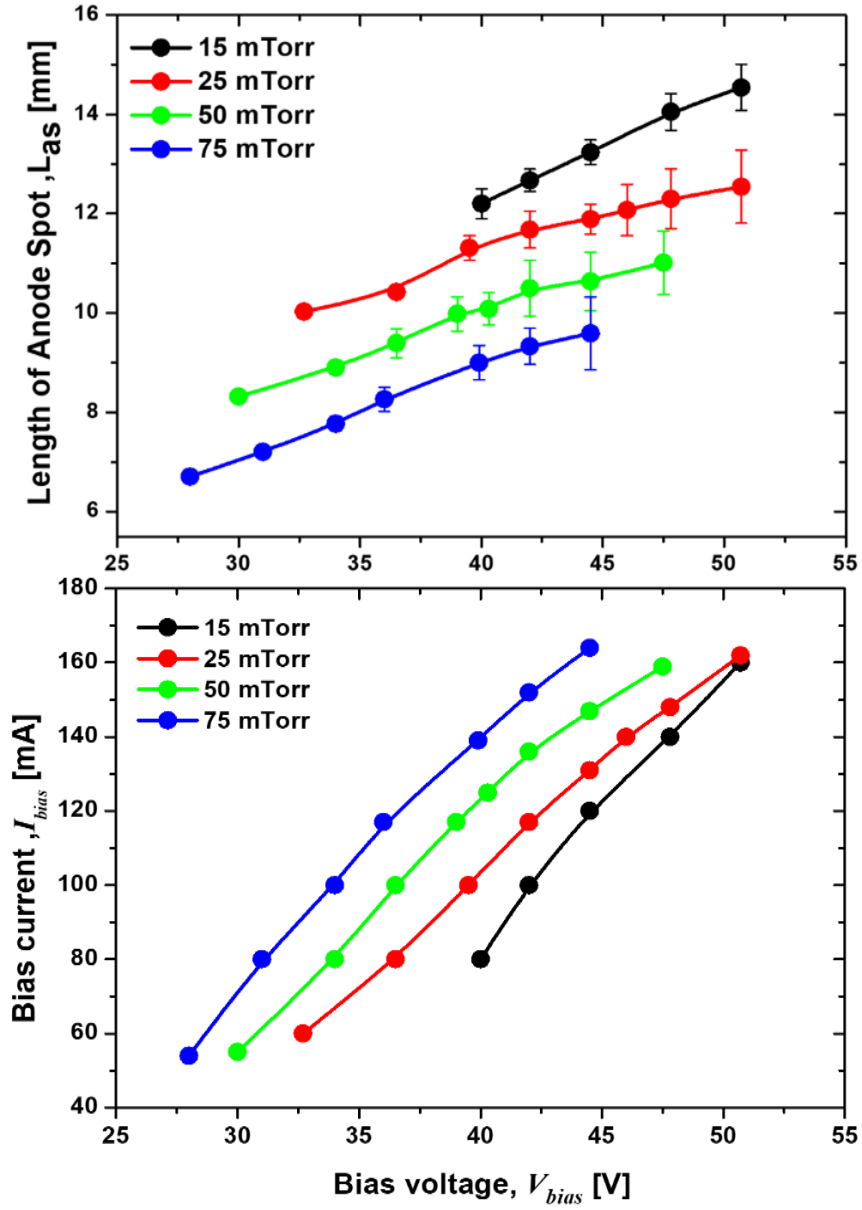


Figure 3.12. (a) The anode spot size variations and (b) the bias current variations as increasing the bias voltage from 25 V to 53 V with fixed RF power of 150 W and the operating pressure range as 15 -75 mTorr.

It is observed that the varied bias voltage also affects to determine the anode spot size.

Figure 3. 12 shows the bias voltage effect on the size variations of anode spots and bias current with the operating pressure range from 15 mTorr to 75 mTorr. The operational bias voltage range is changed according to the operating pressure that it is kept in the limited operating conditions, 25 V- 53 V of bias voltage, given in previous section 3.2 in order to sustain stable spherical anode spot. The anode spot size as well as bias current is proportional to bias voltage at fixed operating pressure. The size of anode spot is increased from 8.3 mm to 11 mm and the bias current is also increased

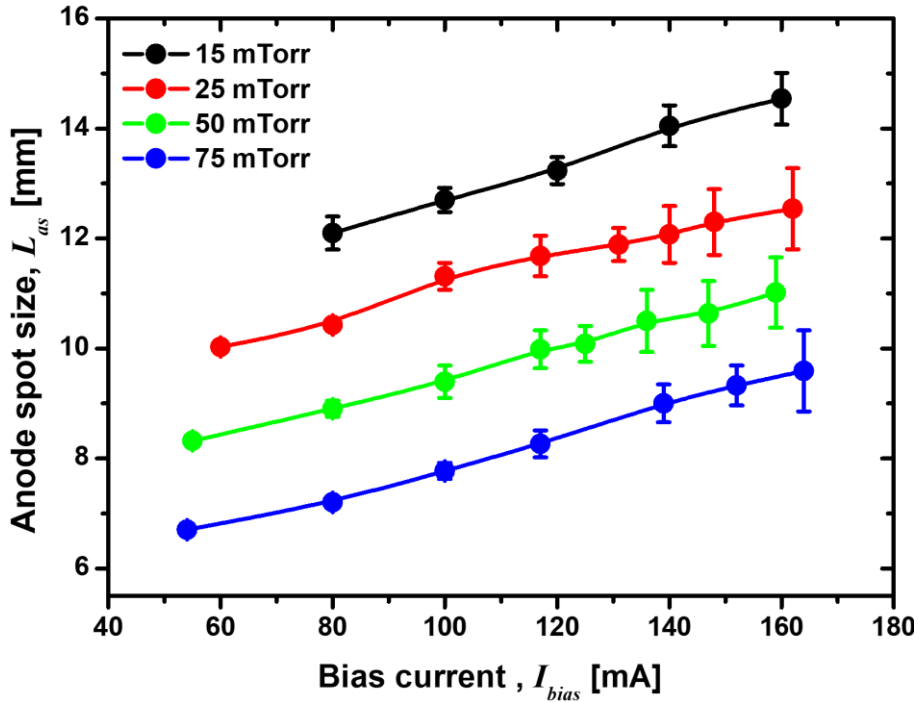


Figure 3. 13. The anode spot size, L_{as} , is expressed as a function of bias current by combined the relationship among the bias current, bias voltage and the anode spot size as shown in **Fig. 3.12**.

from 60 mA to 160 mA as well in case of operating pressure as 25 mTorr. In **Fig. 3.12. (a)** and **(b)**, each slopes has a constant value regardless of the operating pressure that the anode spot size and bias current increase linearly with respect to the bias voltage, it can be shown that the size of anode spot increased linearly with bias current as shown in **Fig. 3.13.**

In summary, the anode spot size is expressed as a function of the operating pressure and bias current and it is proportional to the bias current and the reciprocal of operating pressure. In **Fig. 3.12**, although the bias current is proportional to the operating pressure with fixed bias voltage, the size of anode spot is decreased since the increasing rate of bias current is lower than that of operating pressure at the same bias voltage. As the bias voltage fixed at 40 V, the operating pressure is increased 5 times higher than the starting pressure of 15 mTorr, whereas the bias current operated at 75 mTorr is 136 mA that is only 2.3 times increased from 60 mA with operating at 15 mTorr. Even if the size of anode spot has proportional relationship with bias current as mentioned, the anode spot size is decreased at experimental conditions with high operating pressure. Therefore, the operating pressure has the greatest influence on the size range of the anode spot, but the size of the anode spot can be controlled by the bias current, at fixed operating pressure.

3.4.2. Correlation between Anode Spot Plasma Properties and Operating Parameters

As increasing the operating pressure or increasing the applied bias voltage, the bias current is generally increased as shown in **Figs. 3.11. (b)** and **3.12. (b)**. On the other hand, the size variations of the anode spot tends to be different from the tendency of bias current according to the variation of the operating parameters that it decreases operated at higher pressure, but it expands its surface area as increasing the bias voltage. And it is also observed that the measured sizes of anode spot generated in front of bias probe is different from that of anode spot generated at ASPIS even at same operating pressure and bias current. In this section, it is identified the effective factor to determine the anode spot size and the existence of anode spots with different size at same operating conditions by clarifying the correlations between the plasma parameters and the operating parameters.

· **The electron temperature of anode spot is determined by double layer potential.**

The double layer is a boundary between the ambient plasma and anode spot, and its value, V_{DL} , is defined as the potential difference between the plasma potential of the anode spot and ambient plasma ($V_{p,as} - V_{p,am}$). The double layer potential plays two important roles in maintaining the anode spot. One provides the energy as much as

double layer potential to drifted electron from ambient plasma to anode spot by acceleration and the other is worked as a potential barrier to electron existed in anode spot not to be returned to the ambient plasma.

In the previous work, the electron groups in the anode spot are divided into two groups with different electron temperatures. It is known that the electron temperature of the anode spot is followed the electron temperature of thermalized electron since the number of thermalized electrons dominates in anode spot. The accelerated electrons are trapped in double layer potential barrier by the elastic collisions with neutral particles and they are thermalized in anode spot by the inelastic collisions such as ionization and excitation. It is expected that the electron temperature of thermal electron in anode spot is related to the electron temperature of ambient plasma as well as the accelerated electron energy by double layer potential.

The **Figure 3.14** shows the variation of double layer potential with various experimental conditions that operating pressure is varied from 15 mTorr to 75 mTorr and bias voltage is varied within the range of 25 - 51 V as well. The potential of double layer, V_{DL} can be achieved by two methods: one estimates the drifted energy from EEDF measured at anode spot with assumption that the accelerated electrons are followed the drifted Maxwellian distribution (expressed in **Fig. 3.14.** by dotted lines). The other estimates the potential difference between the ambient plasma and anode spot from the spatial distribution of plasma potential (described in **Fig. 3.14.** by solid lines). The potential variations of double layer obtained by different methods are well-

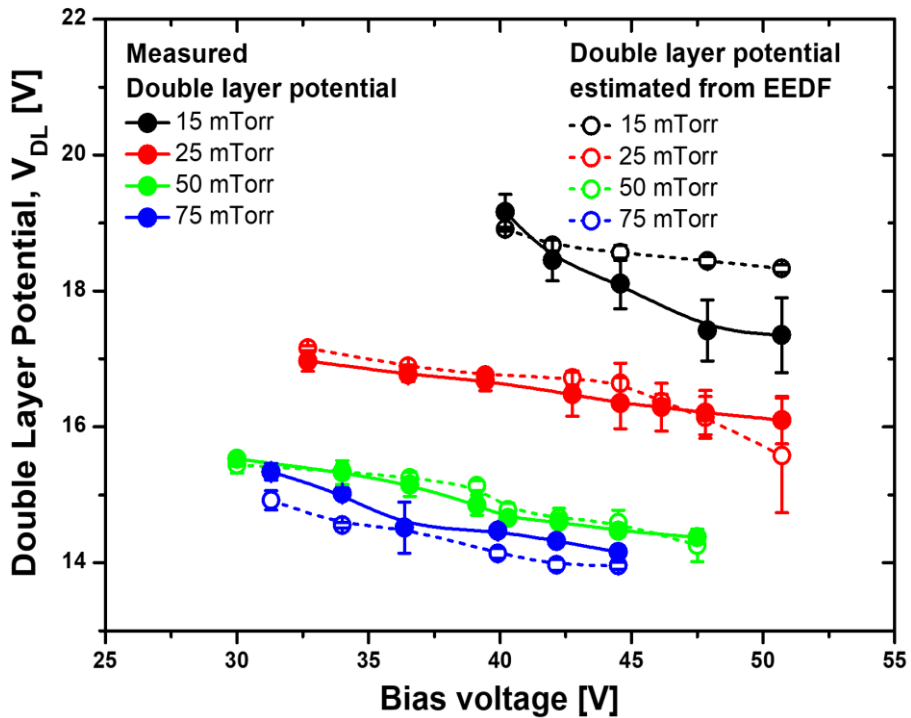


Figure 3.14. The double layer potential is decreased with operated at high pressure or high bias voltage as the RF power is fixed as 150 W.

matched each other and The difference between the two double layer potential obtained in different methods is within 1 eV, and becomes smaller as the operating pressure increases. As bias voltage fixed as 40 V, the double layer potentials are varied from 19 eV to 14.5 eV as increasing the operating pressure from 15 mTorr to 75 mTorr, respectively. At fixed operating pressure as 25 mTorr expressed as red lines of **Fig. 3.14**, the double layer potential is also decreased from 17 eV to 16.1 eV as applied higher positive voltage to bias electrode in range of 33 V - 50.7 V. The double layer potential decreases as increasing the bias voltage and operating pressure, but is more

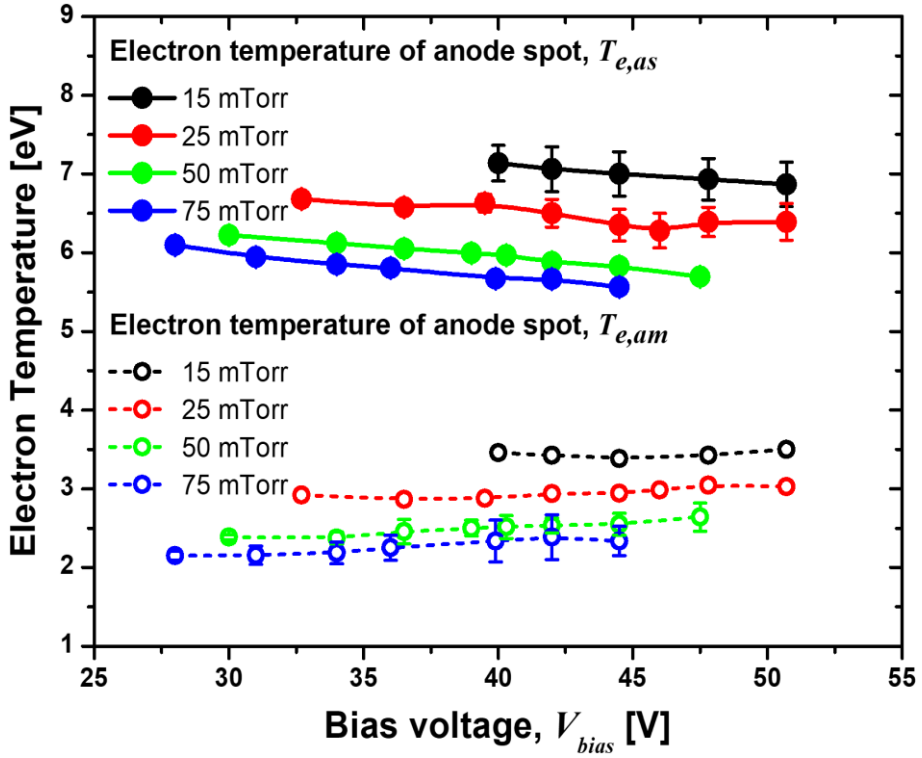


Figure 3.15. The electron temperatures of ambient plasma as well as those of anode spot are varied with bias voltage and operating pressure.

affected to the operating pressure varied than the control of bias voltage.

Figure 3.15 shows that the electron temperature of the ambient plasma, $T_{e,am}$, and anode spot, $T_{e,as}$, are varied by the operating pressure and bias voltage under the same experimental conditions at **Fig. 3.14**. The electron temperature variations of anode spot and ambient plasma are expressed as solid and dotted lines, respectively. As varied the operating pressure from 15 mTorr to 75 mTorr, the electron temperature of ambient plasma is decreased from 3.5 eV to 2.1 eV with fixed bias voltage as 40 V.

On the contrary, it is almost kept in constant value as 3 eV and its variation is within 2 % though the bias voltage is varied from 32.5 V to 50 V with fixed operating pressure as 25 mTorr. In this manner, the electron temperature of ambient plasma is proportional to the reciprocal of operating pressure, but it is hardly affected to the variation of bias voltage to anode spot since the anode spot is too small to influence on the electron temperature of entire ambient plasma volume.

The electron temperature of the anode spot, $T_{e,as}$, also decreases with the operating pressure. As varied the operating pressure in range from 15 mTorr to 75 mTorr, it is decreased from 7.1 eV to 5.6 eV at fixed bias voltage as 40 V. The electron temperature variations of anode spot are in agreement with the degree to which the electron temperature of the ambient plasma varies with the operating pressure. However, the electron temperature of anode spot decreases with increasing bias voltage, unlike the electron temperature of ambient plasma. At fixed operating pressure as 25 mTorr expressed as red solid line of **Fig. 3.15**, the electron temperature of anode spot is decreased slightly from 7 eV to 6.4 eV as applied higher positive voltage to bias electrode in range of 33V - 50.7 V which is same tendency of the double layer potential depending on the bias voltage variations. **Figure 3.16** shows that the electron temperature of anode spot is linearly proportional to the double layer potential even though the operating conditions are different each other. Why is the electron temperature of anode spot proportional to double layer potential? As mentioned above, the double layer potential supplies the acceleration energy to the electrode drifted

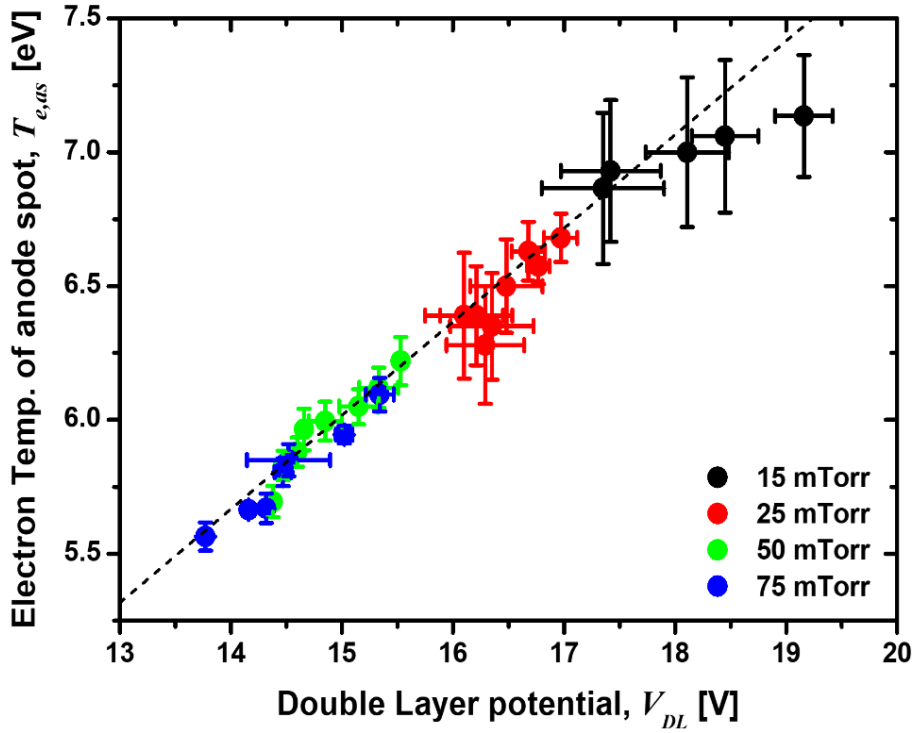


Figure 3. 16. The electron temperature of anode spot is proportional to double layer potential regardless of the operating parameters such as the operating pressure and bias voltage.

toward the anode spot. It is expected that the accelerated energy of electrons injected into the anode spot is decreased since the total energy of the electrons incident on the anode spot is expressed as the sum of the thermal energy and the acceleration energy of the ambient plasma ($T_{e,am} + V_{DL}$). Inside the anode spot, the energetic electrons, trapped in double layer potential barrier by elastic collisions, are lost their energies by inelastic collisions, such as ionization and excitation, and thermalized with electron temperature of anode spot, $T_{e,as}$. The electron energy loss by inelastic collisions are

expressed as the averaged energy for ionization and excitation that the energy loss by inelastic collisions with Ar neutrals are expressed as 15.76 eV of ionization (E_{ioniz}) and 12.14 eV of excitation (E_{ex}), respectively. It also needs to consider the effective plasma density of ambient plasma, which has higher electron energy than ionization potential or excitation threshold energy. Therefore, the electron temperature of anode spot can be estimated by Eq. (3.22) and the averaged loss electron energy, E_{avg} , is expressed as (3.23)

$$T_{e,as} = T_{e,am} + V_{DL} - E_{avg} \quad (3.22)$$

$$E_{avg} = \frac{n_{e,am}^*}{n_{e,am} (K_{ioniz} + K_{ex})} (K_{ioniz} E_{ioniz} + K_{ex} E_{ex}) \quad (3.23)$$

where E_{avg} is the averaged energy loss by ionization and excitation and K_{ioniz} and K_{ex} are expressed the rate constant of ionization and excitation, respectively. If the double layer potential is higher than the ionization potential of argon (15.76 eV), the averaged electron energy loss is approximately as 13.4 eV that the averaged value of ionization and excitation energy. Whereas the double layer potential is lower than the ionization potential, it needs to consider the effective plasma density for inelastic collisions and rate constant calculated with EEDF assumed with drifted Maxwellian distribution.

· **Bias current is affected to the plasma properties of thermal electrons.**

The bias current is commonly increased as increasing the operating pressure with

fixed bias voltage or by applied more voltage to bias probe at constant operating pressure. The bias current model explains the originality of the electrons of anode spot which the anode spot has two electron groups with different electron energies: One is accelerated electron group drifted from the ambient plasma to anode spot and the other is trapped and thermalized electrons including the generated electrons by ionization. The total electron density of anode spot is the sum of accelerated electron density and thermal electron density, which is same value as the ion density of anode spot by the quasi-neutrality condition. The bias current is the summation of accelerated electron current and thermal electron current lost through the bias electrode so that the bias current has been used as an indicator for the plasma density of anode spot [25]. Unlike the previous work related to bias current, it is observed the electron density of anode spot is proportional to bias current with density spread occurred by operating pressure. **Figure 3.17.** shows the electron density variation of accelerated electron and thermal electron in anode spot as increasing the operating pressure in range from 15 mTorr to 75 mTorr and the bias current in range of 80 – 160 mA. The drifted electrons entered into the anode spot with drifted energy, V_{DL} , is linearly increased with operating pressure as well as bias current as described in **Fig. 3.17. (a)** and the slope density of the drifted electrons becomes steeper as the operating pressure increases. It is generally known that the electron temperature is decreased as increasing operating pressure, and the plasma density is slightly increased despite of operating at fixed absorbed power [24]. However, with existence of anode spot with increasing its

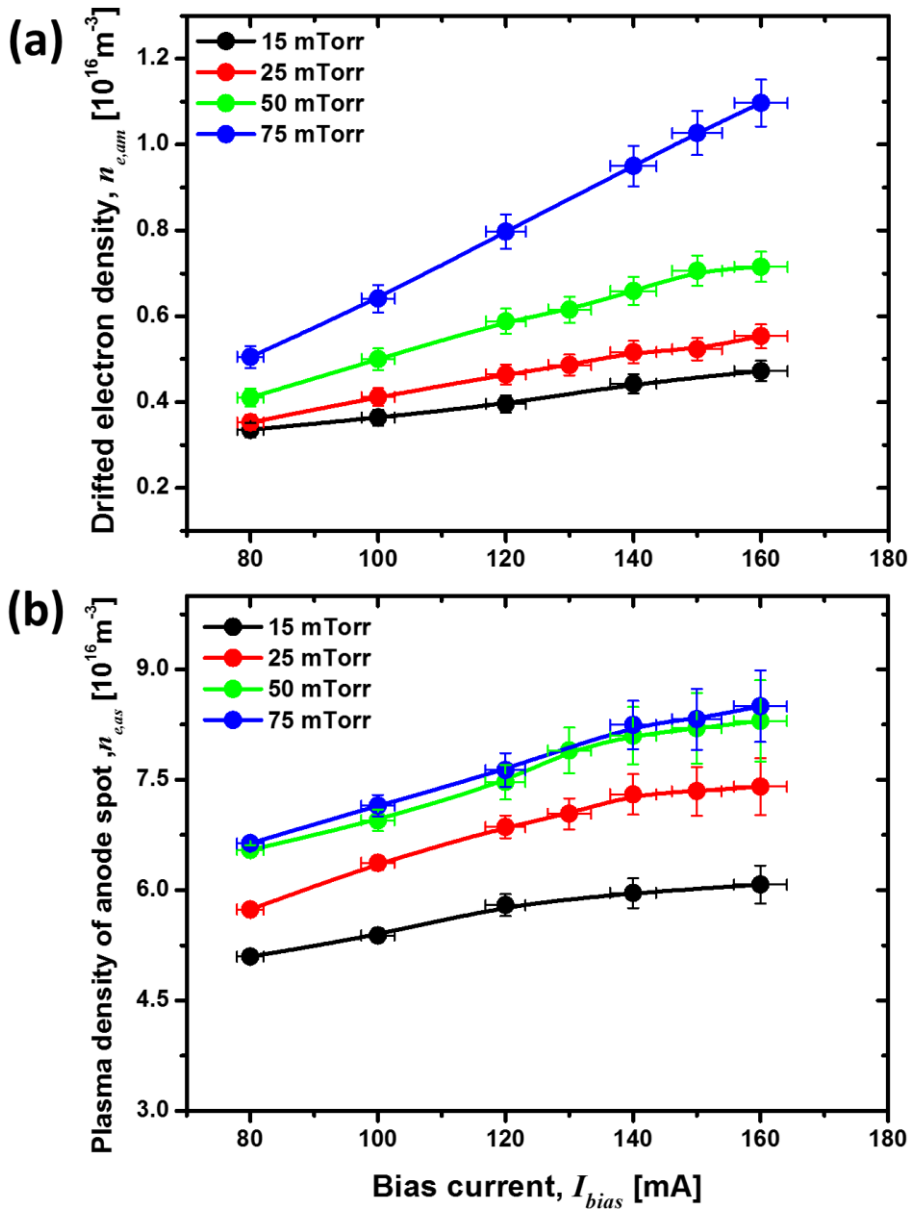


Figure 3. 17. (a) The electron density variations of accelerated electron entered into anode spot and (b) the electron density variations of thermal electron in anode spot.

driving power, the loss current flow through the boundaries is changed into global non-ambipolar mode that it help to increase the ionization rate in ambient plasma by enhancing the confinement of the energetic electrons with increasing the plasma potential of ambient plasma. Moreover, the accelerated ion current, passing through the double layer, injected into ambient plasma is worked as an additional ion production to ambient plasma. In particular, it can be inferred that the increase in the density slope of ambient plasma with operation at high pressure is due to increasing the neutral particle density with high collisional frequency.

Plasma densities of thermal electrons are also enhanced, whereas, the increasing slope of plasma density is decreased with respect to the bias current as shown in **Fig. 3.17. (b)**. The electron density ratio, β , of thermal electron ($n_{e,th}$) to drifted electron ($n_{e,am}$) also decreases as described in **Fig. 3.18**. At fixed operating pressure as 25 mTorr, the density ratio of thermal electrons decreases from 13 to 10, while the bias current increases. The factor of reducing trapped rate and ionization rate of accelerated electron can be found in the role of the double layer to anode spot. As mentioned in previous section, the double layer supplies the sufficient energy to drifted electron entered into anode spot, and it confines the energetic electrons in anode spot by its potential structure. **Figure 3.14** shows that the double layer potential drops about 1 V as the bias voltage increases at constant pressure. it is less than 10% of double layer potential value, but it can acts largely in terms of ionization in anode spot since the ionization cross section calculated with drifted energy, V_{DL} , is decreased

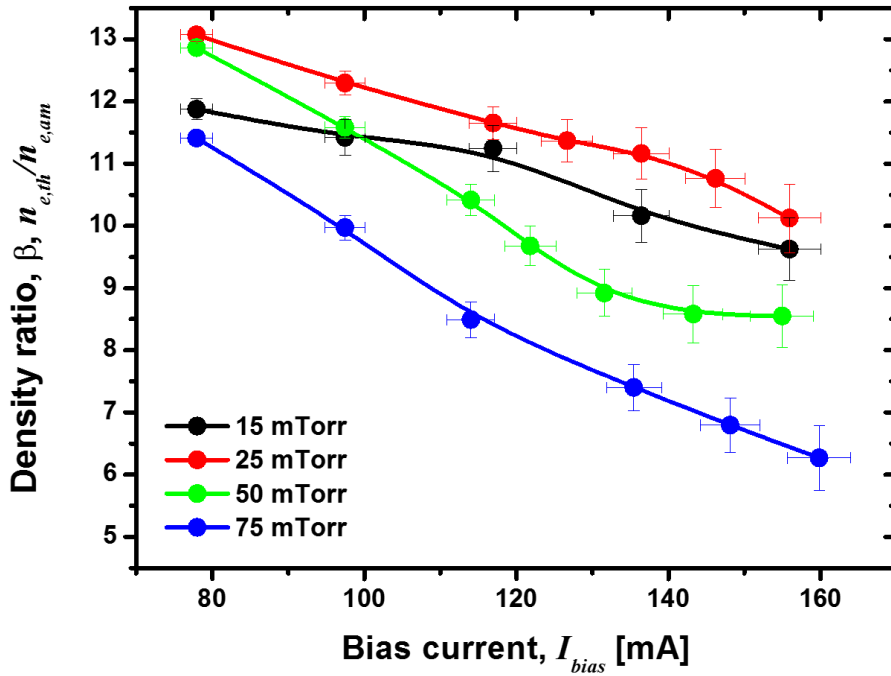


Figure 3. 18. The density ratio of thermal electron to drifted electron into anode spot is decreased as increasing the bias current.

in twice by 1 V decreasing of double layer. In addition, the effective electron density which can participate in ionization process is relatively reduced with considered its energy distribution and it is easy for energetic electrons to escape the double layer potential barrier and return to the ambient plasma.

Though the trapped rate and ionization rate of drifted electron is decreased, the bias current is composed of more than 90% thermal electrons. Therefore, the bias current can be used not only as an indirect indicator of the density of the anode spot but also as a direct indicator of the characteristics of the thermal electron that the

thermal electron flux is linearly proportional to bias current as shown in Fig. 3.19.

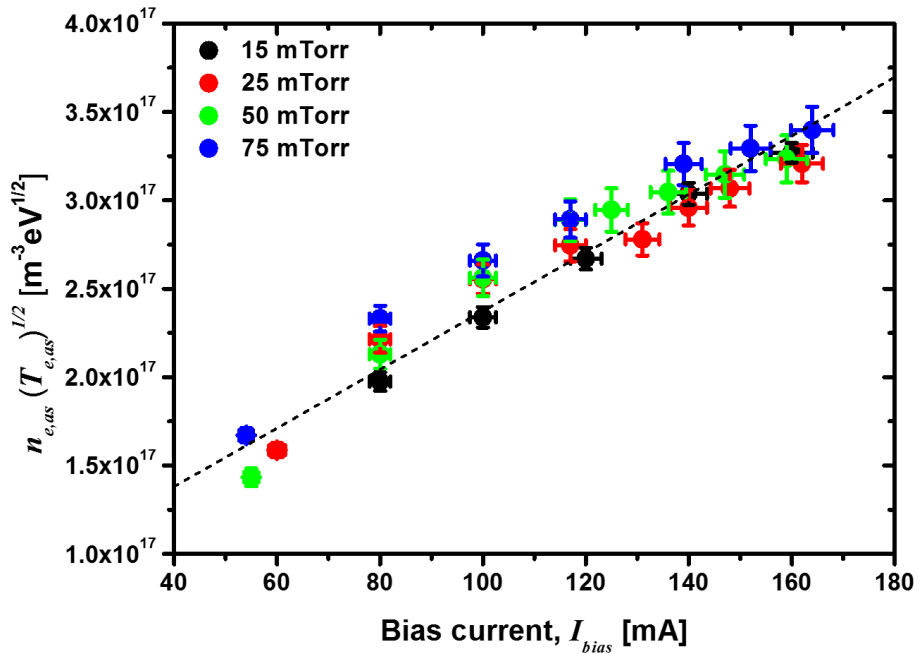


Figure 3. 19. The product of thermal electron density and the electron temperature of anode spot is linearly proportional to the bias current.

· **Anode spot size compensates the variations of operating parameters to keep the constant value of ionization rate in anode spot.**

The bias current is commonly increased and the double layer potential is decreased as increasing the operating pressure with fixed bias voltage or by applied more voltage to bias probe at constant operating pressure. However, the size of anode spot has opposite tendencies as shown in experimental results that the anode spot size becomes

smaller as increasing the operating pressure, whereas it becomes larger as increasing the bias voltage. What does the size of anode spot plays in terms of maintaining the anode spot at various experimental conditions? The ionization reaction rate in anode spot is expressed as the product of the electron density of ambient plasma, the neutral density of gas species and ionization rate constant described as Eq. (3.24).

$$\text{Ionization reaction rate} = n_{e,am} N_{gas} < \sigma_{ioniz} v_{th,am} >_{drift} \quad (3.24)$$

Increasing the bias current means that the electron density of drifted electron into anode spot as well as that of trapped and ionized electron in anode spot are enhanced. That is, the ionization reaction rate in anode spot should be increased by varied the operating parameters to increase the plasma density of ambient plasma or neutral particle density. With fixed RF power as constant value, it is effective way to increase both factors, the plasma density of ambient plasma and neutral particle density by operated at higher pressure. **Figure 3.20. (a)** shows the variations of ionization reaction rate with respect to the bias current and operating pressure. It is observed that the ionization reaction rate is increased according to the operating pressure in case of bias current kept in 120 mA. It also increases with varied the bias current and the slope of ionization reaction rate is enhanced as operated at higher pressure. It varies as much as 2.5 times, up to 26 times depending on the working pressure with operated at same bias current so that the operating pressure influences dominantly to determine the ionization reaction rate.

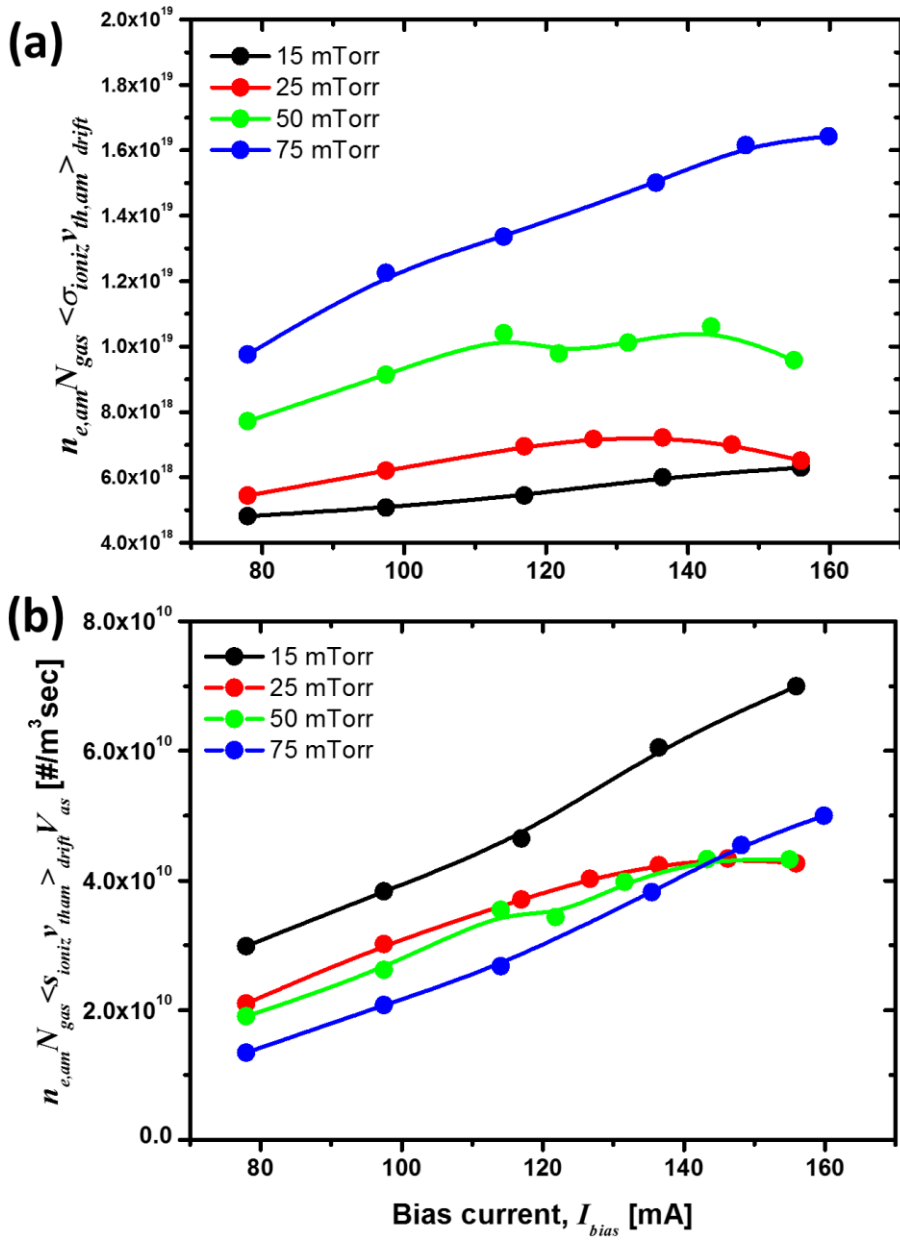


Figure 3.20. (a) The calculated ionization reaction rate in anode spot and (b) the product of ionization reaction rate and the volume of anode spot.

With considered the anode spot volume, the ionization rate is almost linearly proportional to bias current as shown in **Fig. 3.20. (b)** and the ionization rate in anode spot is determined by the bias current that the anode spot control the ionization rate in anode spot by the variation of anode spot size. It is assumed that production and loss of ions are balanced in anode spot, and it can be estimated the plasma density from the value as the ionization rate divided by the root of the electron temperature that is expressed in **Fig.3. 21.** with respect to bias current. The estimated plasma density is

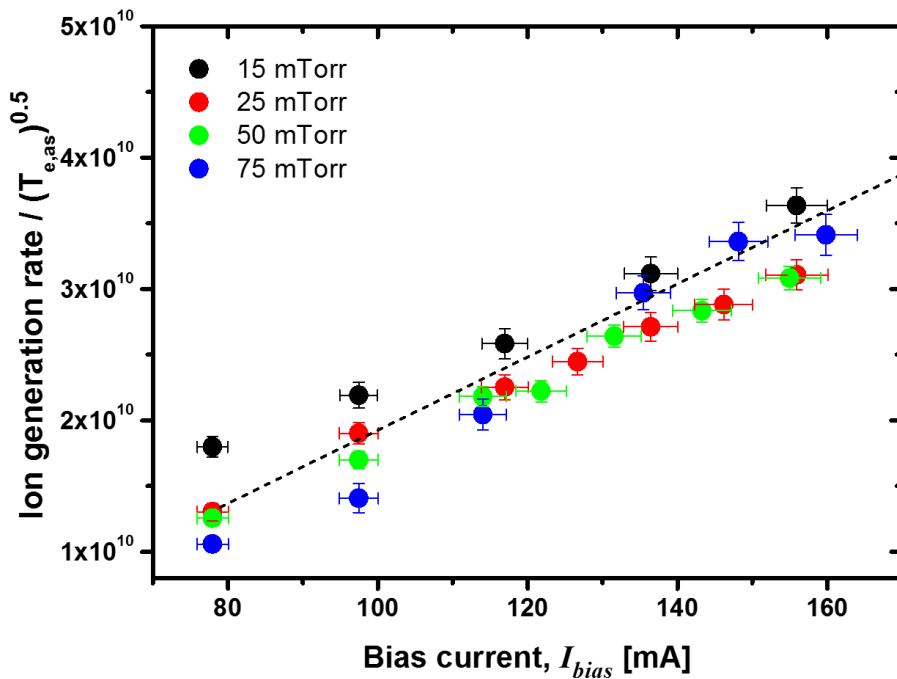


Figure 3. 21. The value as the ionization rate divided by the root of the electron temperature estimated as the plasma density of anode spot is proportional to bias current regardless of the variation of operating pressure.

linearly proportional to the bias current, which corresponds with the correlation between bias current and plasma density as shown in **Fig.3.19**.

In this manner, In order to maintain the ionization rate in anode spot as constant, the anode spot is varied its size to compensate the variation of external circumstance, such as plasma density of ambient plasma and neutral particle density.

3.4.3. Modification of Anode Spot Size Estimation

The anode spot size is varied to keep the ionization rate as constant from the variation of operating pressure or the plasma properties of ambient plasmas. The determination of anode spot size is derived from the ion balancing between ion volume production in anode spot and ion loss through the surface of anode spot expressed as Eq. (3.24).

$$n_{e,am} N_{gas} \langle \sigma_{ioniz} v_{th,am} \rangle_{drift} V_{as} - n_{s,as} u_{B,as} A_{as} = 0 \quad (3.24)$$

where $n_{e,am}$, N_{gas} and $n_{s,as}$ represent the plasma density of ambient plasma and neutral particle density and ion density at anode spot's edge, respectively. σ_{ioniz} is the ionization cross section and V_{as} and A_{as} are the volume and surface area of anode spot. The ions in anode spot is escaped with Bohm velocity, the ion density at the edge of anode spot is assumed as $0.61 n_{i,as}$ since the ions in anode spot are escape with Bohm velocity [17]. Based on the correlation between the plasma density of anode spot and bias current, the product of Bohm velocity and ion density of anode spot is expressed

as the bias current, I_{bias} . Assumed that the electron loss current through the bias electrode consists most of trapped electron, the ion loss flux through double layer is estimated by the multiple product of μ and bias current density J_{bias} ($=I_{bias}/A_{bias}$). The ionization rate constant, $\langle\sigma_{ioniz} v_{th,am}\rangle$ is calculated with EEDF analysis. With experimental results, In some cases of anode spot, the double layer potential is lower than ionization potential of working gas at high pressure ($V_{DL} < E_i$). The ionization rate constant is calculated by approaching the electron kinetics of ambient plasma and double layer potential as Drifted Maxwellian distribution expressed as Eq. (3.25).

$$\langle\sigma_{ioniz} v_{th,am}\rangle_{drift} = \frac{1}{n_{e,am}} \int_{15.76}^{\infty} \sigma_{ioniz}(E) \sqrt{E} f_{drift}(E) dE \quad (3.25)$$

In this manner, the anode spot size, L_{as} is a function of bias current, the plasma properties of ambient plasma, double layer potential and operating pressure and expressed as Eq. (3.26).

$$L_{as} \cong \frac{\mu I_{bias}}{e A_{bias} n_{e,am} N_{gas} \langle\sigma_{ioniz} v_{th,am}\rangle_{drift}} \quad (3.26)$$

The **Figure. 3.22** shows that the measured anode spot sizes are compared with the calculated values estimated with measured plasma properties of anode spot as well as ambient plasma kept the experimental conditions within 15-75 mTorr of the operating pressure range and the 60 -160 mA of the bias current range. And the anode spot size variation of measured and calculated results are expressed as solid and dotted lines, respectively. The variation of anode spot size corresponds with the tendency of anode

spot size with respect to varied operating pressure as well as bias current. However, it is possible to predict the anode spot size at various operating conditions since the modified formulae of anode spot size not only covers the inverse trend of the operating pressure reported at previous work, but also reflects the change in the size of the anode spot induced by the change of the plasma properties of ambient plasma.

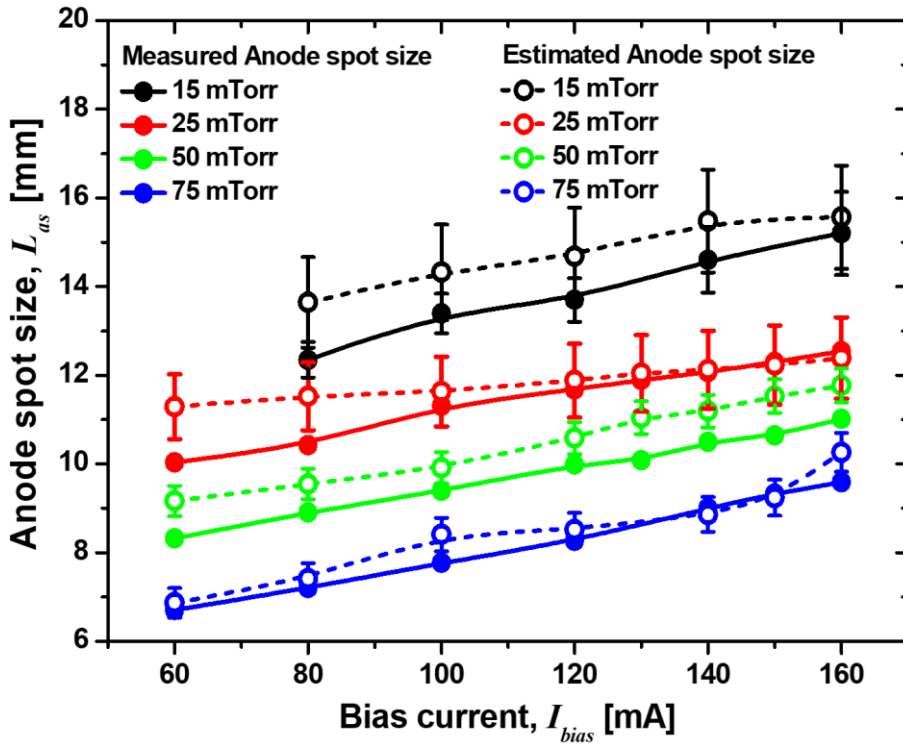


Figure 3. 22. Comparison the anode spot size between measured results and estimated value with measured plasma properties of ambient plasma and anode spot by modified formulae.

3.5. Summary: Why Is the Anode Spot Size Varied?

In order to figure out the cause of the size variation of anode spot by the operating parameters, such as the operating pressure and bias voltage, it is conducted a series of experiment to measure the plasma properties of the ambient plasma as well as anode spot with varied the operating pressure in range of 15 mTorr - 75 mTorr and the bias voltage of 25 V – 51 V. **Figure 3. 23** shows the relationship among the operating parameters of ASPIS, bias current and anode spot size variation explained in terms of

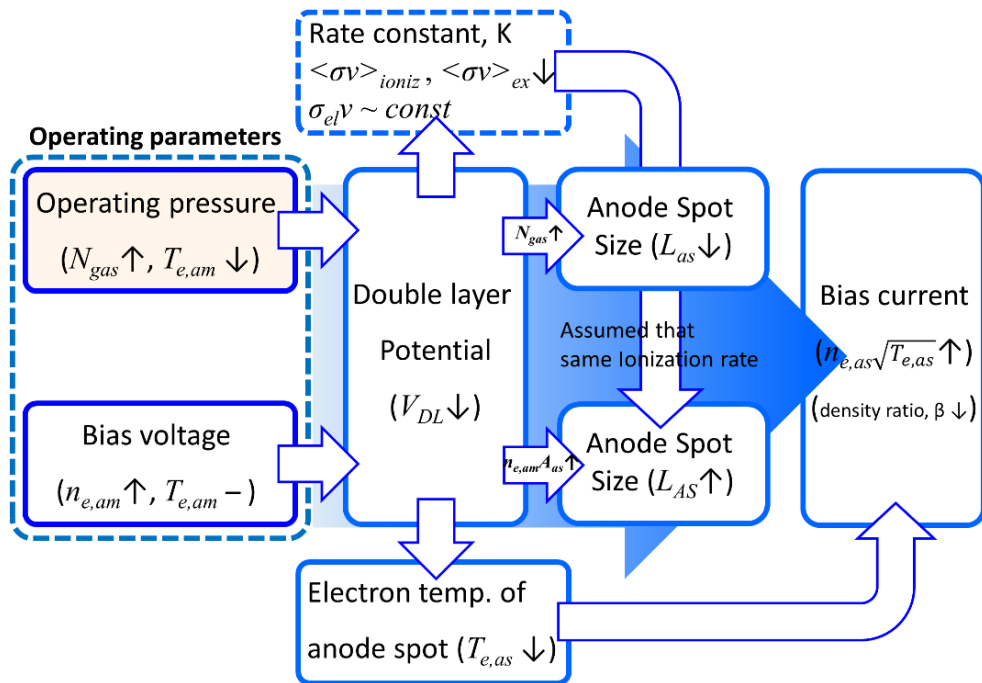


Figure 3. 23. The correlation among the operating parameters, plasma properties of anode spot and the size variation of anode spot.

the plasma properties of anode spot and double layer potential. As the operating pressure or applied voltage to bias probe is increased, in common, the bias current increases and the double layer potential decreases in each case. However, the size variation of anode spot has opposite trends according to the operating parameters of ASPIS that the size of the anode spot decreases as the operating pressure increases with fixed bias voltage, but enlarges as increasing the bias voltage at fixed operating pressure. The reason for different tendencies of anode spot size variation can be found in the relationship among total charged particle generation rate in anode spot, double layer potential and bias current. The most of bias current consists electron current that the trapped and generated electron in anode spot is lost through the bias probe by the potential difference between anode spot and bias probe. Since the anode spot satisfies the quasi-neutrality condition, the bias current indicates roughly the plasma density of anode spot. In order to keep the bias current constant despite of varied the operating conditions, the anode spot changes its size to keep the total volume ionization rate in anode spot. The higher operating pressure is caused to enhance the ionization rate in anode spot since the neutral particle density as well as the plasma density of ambient plasma are increased. However, the anode spot reduces its size to keep the bias current constant at fixed bias voltage that it works as the factor to be decreased the total number of incident electrons as well as the total volume production in anode spot. In addition, the anode spot enlarges its surface to increase the total number of electrons incident on the anode spot to increase the total ionization rate when the bias voltage

is increased at a fixed operating pressure.

As a result, it suggests the modified formulae for predicting the anode spot size based on the experimental results and previous work related to anode spot size and properties and it well explains the relationship among the operating parameters of ASPIS, the plasma properties of ambient plasma and that of anode spot including the anode spot size.

4. Prediction of Operational Conditions of ASPIS for High Beam Current Extraction

The ion beam extraction, acts as an additional ion loss to anode spot, can be an unstable factor in sustaining the anode spot in front of bias electrode. Especially, it has been confirmed experimentally that the area ratio among the bias electrode, extraction aperture and anode spot can be an effective factors to sustain the anode spot as well as estimation of extractable ion beam current operated as high current plasma ion source. However, it has a difficulty to verify experimentally all case with various aperture size and bias electrode in order to find out the appropriate area ratio between bias electrode and extraction aperture. Therefore, the main purpose of this chapter suggests the design parameters of ASPIS and controllable range of operating parameters to utilize the ASPIS as a high current ion source with understanding the plasma properties variations at anode spot in terms of operating parameters including ion beam extraction.

4.1. Necessity of 0-D Particle Balance Model of Anode Spot

The anode spot is usually used as a tool for generating the double layer so that the research related to anode spot is mainly focused on the analysis of double layer

potential structure where is generated between the anode spot and ambient plasma. The double layer analytical model depends on the classification of electrons and ions in the surrounding plasma and anode spot. Langmuir, which first proposed a double layer analysis model, considered only two kinds of particles as accelerated electrons and ions through a double layer and claimed that the current ratio, α , between electron flow in and the ion flow out though the double layer is a constant value as 1 for sustaining the double layer structure expressed as Eq. (4.1).

$$\alpha = \frac{I_i}{I_e} \sqrt{\frac{M_i}{m_e}} \quad (4.1)$$

But it has a limitation that it is only applied to strong double layer whose potential is more than 10 times higher than the electron temperature ($\frac{eV_{DL}}{kT_e} \geq 10$). Since the double layer, potential difference between the anode spot and ambient plasma, is classified as a weak double potential. The ratio of double layer potential to electron temperature of anode spot is about 3 ~ 5, it is difficult to analyze it with Langmuir's model. Park has been analyzed the double layer by using 4 kinds of particles classifications considering electrons and ions accelerated through the double layer, as well as trapped (thermalized) electrons in anode spot and trapped ions in ambient plasma [25]. By solving the 1-D Poisson equation at double layer, it shows the conditions for double layer formation between the ambient plasma and anode spot in terms of the current ratio, α that should be always higher value than that suggested by Langmuir for formation of double layer between two different plasmas. Based on the

results, it is possible to estimate the potential structure and thickness according to the surrounding plasma parameters, the anode spots, and the potential of the double layer. However, since it should need to input parameters, such as the electron temperatures of two plasmas ($T_{e,am}$ and $T_{e,as}$) and the double layer (V_{DL}), obtained from the experimental results. It is difficult to use it as a predictive model because it is not enough to explain the correlations between operating parameters and plasma parameters as well as the relationship among the plasma parameters including the spot size and double layer potential.

Recently, it has been investigated the researches about anode spot itself, especially focused on electrons in anode spot. Since the electrons accelerated by double layer potential play a key role in the generation and sustainment of anode spot as well as understanding the role of double layer, it is mainly emphasized about the originality of electrons inside anode spot performed the bias current analysis in terms of plasma density and electron temperature of accelerated and trapped electrons. Bias current is believed to mostly consist of electron current. Two kinds of the electron current are assumed to contribute to the bias current: drifted (accelerated) electron current from ambient plasma and trapped (thermal) electron current in anode spot. The electron currents collected by the bias electrode is expressed as Eq. (4.2)

$$I_{bias} = eA_{as}\Gamma_{e,am} + eA_{as}\Gamma_{e,am}N_{gas}\sigma_{ioniz}r_{as} \quad (4.2)$$

where the first terms of the right-hand side represents the electron current from ambient plasma and the second term is for the contribution of the electron generated

at anode spot, and $\Gamma_{e,am}$ and r_{as} are electron flux from ambient plasma and radius of anode spot, respectively. Since $N_{gas}\sigma_{ioniz}r_{as}$ of the second terms in Eq. (4.2) has much less value than 1, Song [13] is claimed that the bias current is dominantly consist the electron current from ambient plasma with ignoring the generated electron current from anode spot.

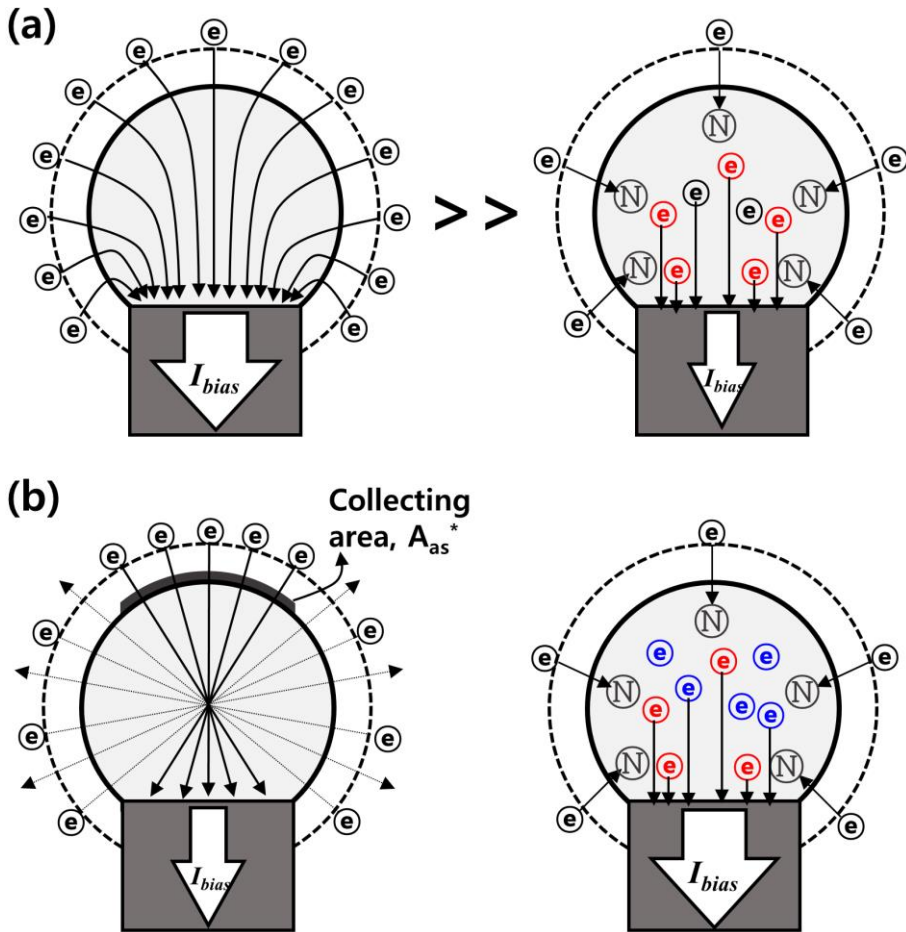


Figure 4. 1. Schematic diagrams of the originality of electrons components in anode spot to be interpreted the bias current flown into bias electrode by (a) Song, (b) Park.

However, it is confirmed that there are electron beams and thermal electrons accelerating in the anode spot by measuring the internal plasma characteristics of the anode spots. The most of thermal electrons are generated from the drifted electrons that they are trapped to double layer potential structure by elastic collisions and thermalized by inelastic collisions with neutral particles such as ionization or excitation processes [25]. And it is found that the thermal electrons has several times higher plasma density than that of electron beam like. The bias current model has been modified using the ratio of thermal and drifted electrons to the ratio of the anode spot size to the bias electrode area. The modified bias current model, expressed as Eq. (4.3), is considered the thermalized electron by elastic collisions, and the current ratio between thermal and drifted electrons expressed by using the area ratio of anode spot's surface and bias electrode.

$$I_{bias} = eA_{bias}\Gamma_{e,am} + eA_{as}\Gamma_{e,am}N_{gas}\sigma_{el}L_{as} \quad (4.3)$$

where the first term of the right-handed side describe the drifted electron current flown directly into bias electrode and the second term represent the thermalized trapped electron by elastic collisions. Through the modified bias model, the electron currents flown from the anode spot to bias electrode have been successfully analyzed according to the electron components in anode spot with the anode spot size. However, it is difficult to figure out the correlation between the bias current and the anode spot, and the relationship between the anode spot density variations and the bias current easily because the density of the anode spot is not directly expressed on the bias

current model. It can be only utilized as a tool to analyze the experimental results that the bias current is proportional to the plasma density.

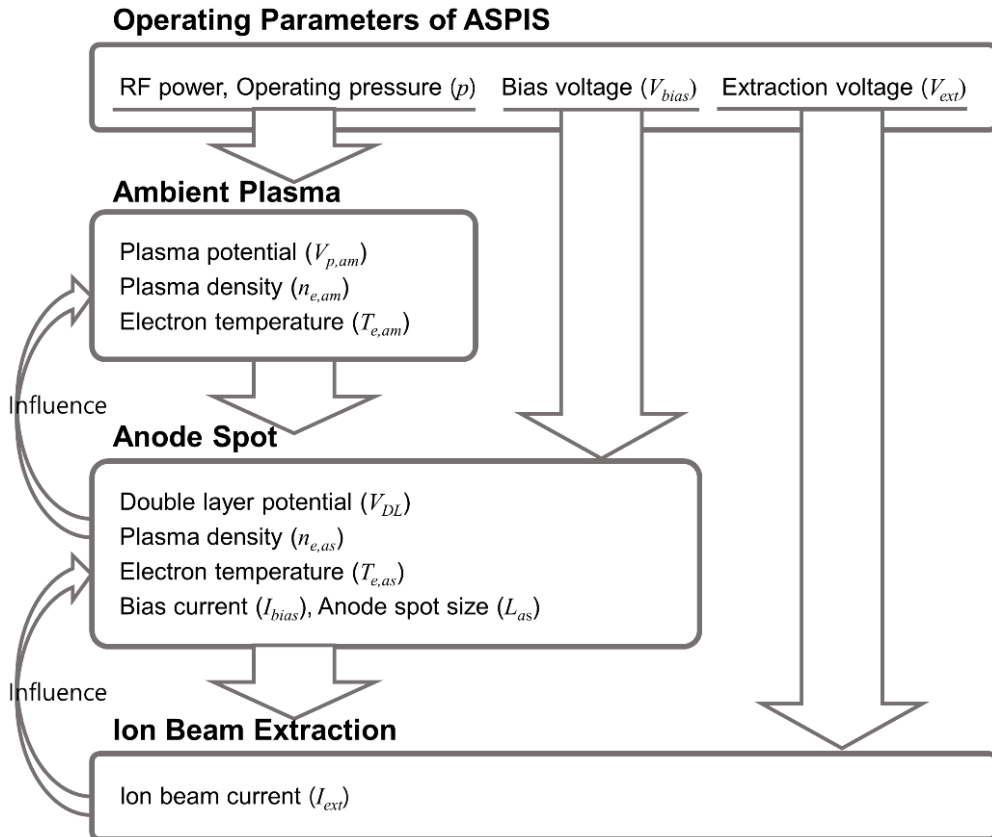


Figure 4. 2. A schematic diagram illustrating the relationship between the operating parameter and plasma properties and influence between plasma and ion beam extraction with generation and maintenance of anode spot.

Until now, the analyzing models of anode spot are developed in separately: the double layer model analyzed in terms of temperature and its potential, and the bias current in terms of the originality of the electron components in anode spot. However, it is

insufficient to analyze the ion beam extraction from anode spot, generated in front of bias electrode, with separated analyzing models of anode spot. **Figure 4.2** is a schematic diagram of the interactions among the operating parameters, the plasma properties ambient plasma and anode spot as well as ion beam extraction based on the experimental results and the previous works of anode spot plasmas [13, 25].

The relationship between the operating parameters such as operating pressure and RF power, and the plasma properties of ambient plasma is deduced from the well-known uniform discharge model [24]. Electron temperature and plasma density of ambient plasma are determined from the particle balance and energy balance, respectively. The electron temperature of ambient plasma, $T_{e,am}$ is estimated from the particle balance by satisfied between the total surface loss and total volume ionization so that it is expressed by a function of operating pressure and the dimension of discharge chamber. The plasma density, $n_{e,am}$, is determined by the total power balance by equating the total power absorbed and total power loss by inelastic and elastic collisions in the discharge chamber and is a function of the absorbed power (P_{RF}) as well as operating pressure (p) because of the dependence of electron temperature on pressure. Moreover, the plasma potential is determined from the loss current through the chamber wall that is related linearly to electron temperature. In this manner, without the anode spot, the electron temperature and plasma potential of ambient plasma is decreased, but plasma density increased as increasing the operating pressure with fixed RF power to discharge chamber.

When an anode spot is generated in an ambient plasma, the two different plasmas are affected each other. The ambient plasma affects to the generation and sustainment of anode spot because the ionization rate in anode spot is depending on the total number of incident electrons toward anode spot and their accelerated energies by double layer potential. The anode spot also affects the determination of the ambient plasma properties since the ion generated in the anode spot are accelerated into the ambient plasma by the double layer potential. The effect of anode spot to ambient plasma is figured out by Park [25] based on the comparison of the measured results of ambient plasma properties before and after the generation of anode spot. All plasma properties of ambient plasma are enhanced by the existence of anode spot that the electron temperature is increased by 1.2 times, the plasma potential by 2 times and the plasma density by 2-7 times as compared with the experiment cases in the absence of anode spot. As operated without anode spot, the plasma potential of ambient plasma is balanced ion and electron loss current through the discharge chamber wall, which is call as ambipolar flow mode. As generated anode spot, the flow mode is changed in non-ambipolar flow mode that the net current lost through the chamber wall is not zero, is balanced with the electron current lost through the bias electrode. The non-ambipolar flow mode enhance the plasma potential of ambient plasma, which is proportional increased to bias current. As the plasma potential of ambient plasma is increased, the electron current lost through the boundaries of discharge chamber decreases. So that the electron temperature can be increased by the enhanced

confinement of electrons had higher electron energies compared to the case without the anode spot. At last, the plasma density of ambient plasma can be enhanced to compensate the increasing ionization rate by raising the particle wall loss. Because the additional ion generation term of ambient plasma is supplied by the accelerated ion current toward ambient plasma through the double layer potential and the ionization rate in ambient plasma can be enhanced by the energetic electrons confinement.

The ion beam extraction at the anode spot can act as an additional ion loss in terms of the anode spot sustainment. When ASPIS is used as a high-brightness ion source, the bias current has been operated at sub Ampere level, on contrary, the extracted ion beam current is about sub micro Amperes so that the ion beam extraction was negligibly small and did not affect the plasma properties of the anode spot. However, the plasma properties of anode spot can be affected to ion beam extraction since it is observed that the bias current is decreased or the anode spot is disappeared by high current ion beam extraction from anode spot. The previous work related the anode spot have been mainly focused on the generation mechanism of accelerated and thermal electrons in anode spot, but we need to understand the particle balance between electron and ion considered the additional ion loss in order to use the ASPIS as high current ion source. Based on the experimental results of measured the plasma properties' spatial distributions, the anode spot can be regarded as a uniform plasma that density distribution is followed the Boltzmann relation in terms of plasma

potential and electron temperature variations of anode spot. Therefore, the particle balance model can be applied to understand the plasma characteristics of the anode spot varied with operating parameters of ASPIS. The particle balance model is also important for the analysis of the anode spot in order to investigate the interaction of electrons and ions with considered the additional ion loss process by ion beam extraction.

4.2. Development of 0-D Particle Balance Model of Anode Spot

Though, an anode spot plasma is generated and sustained by incident energetic electrons through double layer potential, but it can be regarded as independent plasma from the ambient plasma since it satisfy the basic characteristics of plasmas, quasi-neutrality. To analyze the anode spot by particle balance model, it need to figure out the generation and loss terms of charged particles in anode spot in details based on the experimental results and the previous works related to anode spot characteristics. As mentioned in previous section, the plasma potential is determined by net current lost through the boundaries so that the generation and loss terms in anode spot are expressed as current. In this section, it is formulated the charged particle balance equations based on the summaries about the generation and loss terms in anode spot and discuss the details of particle balance model to consider in the calculations.

4.2.1. Terminologies Used in Particle Balance Model of Anode Spot

In this section, it is aimed to define the terminologies used in the description of 0-D particle balance model of anode spot. **Figure 4.3** shows the schematic configuration of anode spot and ambient plasma expressed with the plasma properties and design

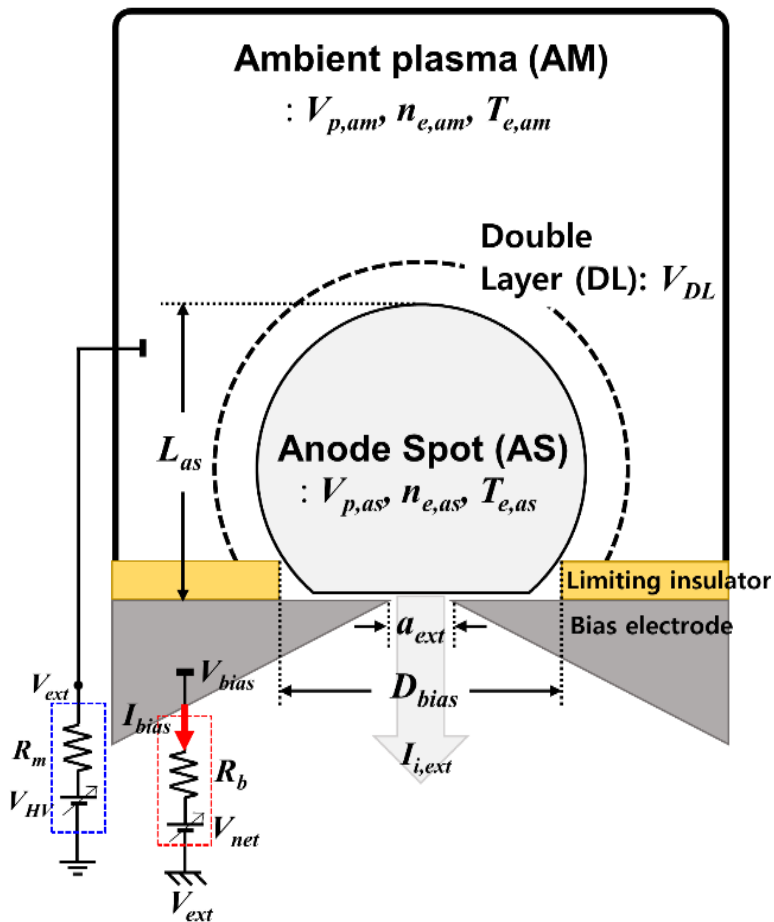


Figure 4.3. The schematic configuration of anode spot and ambient plasma expressed with the plasma properties and design parameters.

parameters. The ambient plasma and anode spot are abbreviated as AM and AS, respectively. The double layer formed between anode spot and ambient plasma is denoted as DL, and the electron sheath existed between anode spot and bias electrode is denoted as ES. $n_{e,am}$, $T_{e,am}$ and $V_{p,am}$ are defined to express the plasma density, electron temperature and plasma potential of ambient plasma, respectively. The plasma potential difference between ambient plasma and anode spot called as double layer potential is denoted as V_{DL} . The anode spot size and its plasma properties are determined by the operating pressure (p) and applied voltage to bias electrode. The anode spot is driven by the bias voltage, V_{bias} , provided by the DC power supply (V_{net}) and the electron current flowing from the anode spot to the bias electrode is called as the bias current, I_{bias} . The plasma properties of anode spot plasma are expressed as $n_{e,as}$ of plasma density, $T_{e,as}$ of electron temperature and the plasma potential as $V_{p,as}$. Its size is denoted as L_{as} and the surface area and volume of anode spot are expressed as A_{as} and V_{as} , respectively. The design parameter of ASPIS is related to the area ratio of bias electrode to the discharge chamber wall and the diameter of bias electrode and the extraction aperture. The discharge chamber area except wall made of insulators is denoted as A_{wall} . The bias electrode where the anode spot is generated is partially exposed on the ambient plasma by covered with a ceramic disk with a hole at the center called as a limiting insulator. The diameter of partially exposed bias electrode to the ambient plasma is denoted as D_{bias} and its area as A_{bias} . In order to extract ion beam from the anode spot, the bias electrode which is drilled at the center is used in

ASPIS, the diameter of extraction aperture is denoted as a_{ext} and its area is expressed as A_{ext} . Through the beam extraction aperture, the ion beam current, I_{ext} , is extracted by applied the extraction voltage, V_{ext} . The plasma properties of two different plasmas and design parameters and operating parameters of ASPIS are summarized as **Table 4.1**.

Table 4. 1. The terminologies used in 0-D particle balance model of anode spot.

D_{bias}	:Diameter of bias electrode [mm]	$n_{e,as}$: Anode spot plasma density [m^{-3}]
a_{ext}	:Diameter of extraction aperture [mm]	$T_{e,as}$: Electron temp. of anode spot [eV]
A_{ext}	:Area of extraction aperture [mm^2]	$V_{p,as}$: Plasma potential of anode spot [V]
A_{bias}	: Area of bias electrode [mm^2]	V_{DL}	: Double layer potential [V]
A_{wall}	: Area of discharge chamber wall [mm^2]	L_{as}	: Length of anode spot [mm]
N_{gas}	: Neutral density [m^{-3}]	I_{bias}	: Bias current [mA]
$n_{e,am}$: Ambient plasma density [m^{-3}]	V_{bias}	: Bias voltage [V]
$T_{e,am}$: Electron temp. of ambient plasma [eV]	V_{ext}	: Extraction voltage [kV]
$V_{p,am}$: Plasma potential of ambient plasma [V]	I_{ext}	: Extracted ion current [mA]

4.2.2. Generation and Loss Processes of Charged Particles in Anode Spot

Figure 4.4 shows the schematic diagrams about the generation of charged particle in anode spot and the losses of the charged particles in terms of current with connected circuit. The important factors for generating and sustaining the anode spot

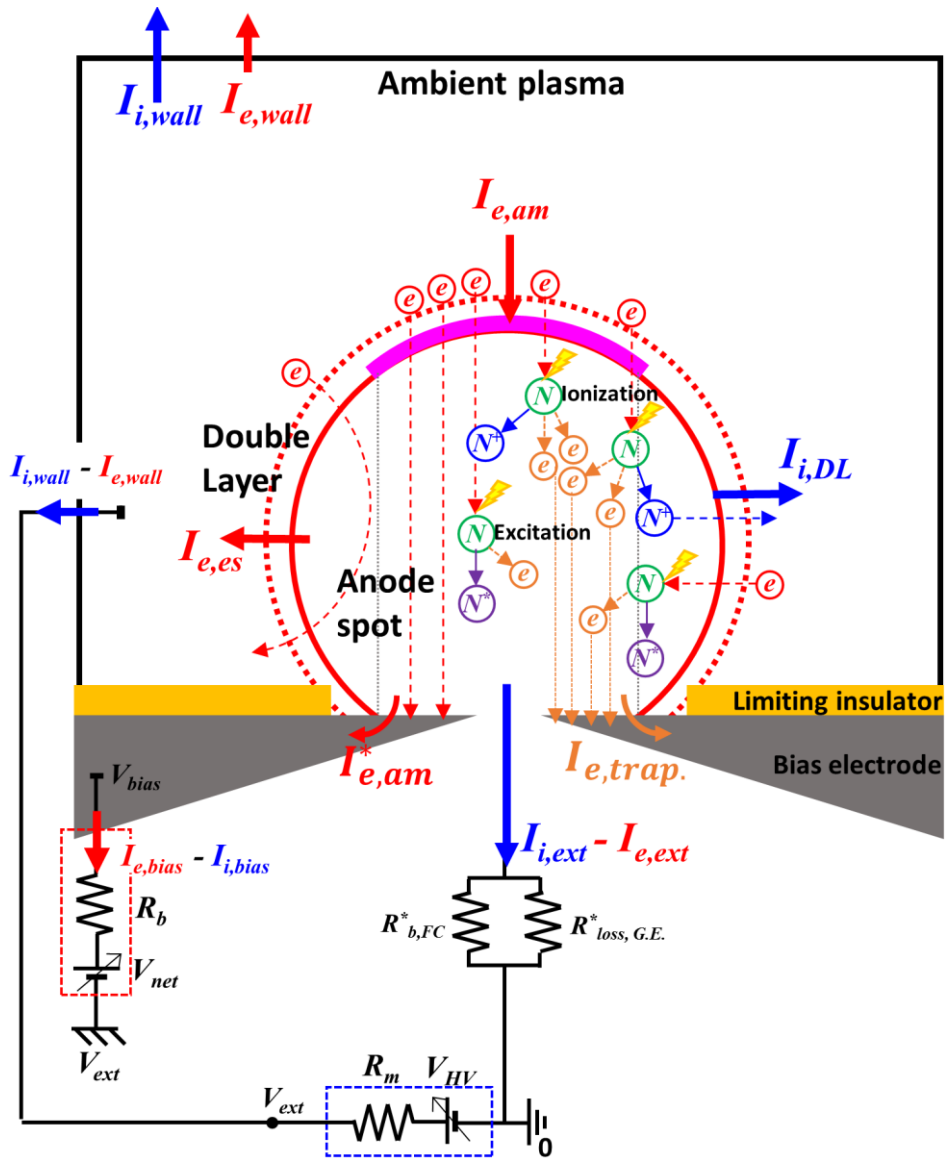


Figure 4. 4. The schematic diagram for explanation of generation and loss terms of charged particles in anode spot and the circuit schematic connected to ion source for sustaining the anode spot and extracted ion beam current from anode spot.

in front of bias electrode are the total number of incident electrons drifted by the double layer potential, toward anode spot and their accelerated energies (red marked electrons in **Fig. 4.4.**). The total number of incident electrons toward the anode spot is expressed as the multiple product of the electron density from ambient plasma, $n_{e,am}$, and the surface area of anode spot, A_{as} and their accelerated energies are same as V_{DL} based on the experimental results. The generation rate of electrons in the anode spot is dominated by the reaction that takes place when accelerated electrons are trapped and thermalized in anode spot. The incident energetic electrons are collided with neutral particles in elastic collisions. The drifted electron trapped in anode spot by elastic collisions becomes to be thermalized by inelastic collisions, captured by bias electrode and escaped from anode spot after other elastic collisions [25]. Due to the elastic collisions with the neutral particles, the energetic electrons are mainly trapped in the anode spot by the double layer potential, worked as the barrier to electrons. The trapped energetic electrons are thermalized by the inelastic collision with neutral particles (orange marked electron in **Fig. 4.4.**), which generate the additional electrons and ions through the ionization reaction or excites the neutral particle with electron energy loss. Since the elastic and inelastic reactions of the accelerated electrons occur within the anode spot, the total electron generation rate of anode spot can be expressed as Eq. (4.4).

$$n_{e,am}N_{gas}(\sigma_{el}(V_{DL})v_{th,am} + 2 \langle \sigma_{ioniz}(V_{DL})v_{th,am} \rangle + \sigma_{ex}(V_{DL})v_{th,am})V_{as} \quad (4.4)$$

where the N_{gas} is neutral particles density, $v_{th,am}$ is the electron thermal velocity which

is distributed with electron temperature of ambient plasma, $T_{e,am}$, and σ_{el} , σ_{ioniz} and σ_{ex} are cross section of elastic collisions, ionization and excitation, respectively, determined by electron accelerated energies, V_{DL} . However, based on the experimental results, It is observed that the double layer potential is decreased with increasing operating pressure and is also decreased with increasing the biased voltage to bias electrode at fixed operating pressure. It is normal to calculate the ionization rate constant as the multiple product of the electron thermal velocity and the ionization cross section. In case that the drifted electrons have lower energies than the ionization potential of Argon, 15.76 eV, then, the ionization rate constant is zero according to calculate with the conventional method. However, ionization rate constant needs to be calculated with approaching as electron kinetics since ion and electron are generated due to ionization reaction with lower electron energy in the anode spot. Assuming that the drifted electron energy distribution is followed the drifted Maxwellian distribution, the ionization rate constant in anode spot is expressed as an averaged sigma-v parameter, $\langle \sigma_{ioniz} v_{th,am} \rangle$, by considering the integrated region started from the ionization potential of gas species. The volume of anode spot (V_{as}) is estimated as the product of the anode spot size (L_{as}), and the surface area of anode spot (A_{as}). The electron generation rate in anode spot can be enhanced by operated at higher pressure to increase the neutral particle density or increasing the total number of accelerated electrons $n_{e,am} A_{as}$, and their energies, V_{DL} .

The loss of electrons from anode spot occurs through two paths. It is note

that it needs to consider the electron components in anode spot in order to estimate the electron loss through the boundaries of anode spot, such as the surface of anode spot and the exposed area of bias electrode to plasma. The two kinds of electron with different energies are existed in anode spot that the electron beam components accelerated by double layer potential and the thermalized electrons which is trapped in anode spot by the double layer potential barrier and thermalized by inelastic collisions with neutral particles. The electron beam components drifted into anode spot can be analyzed separately with thermalized electron in the EEDF curves achieved in anode spot with varied the probe's position. The electron density of beam component decreased as closed to the bias electrode, but it is maintained at a substantially constant value in anode spot because of the density reduction within 10% of incident electron beam density. The main electron loss is occurred through the bias electrode. Since an electron sheath is formed between the anode spot and the surface of the bias electrode as shown in **Fig. 4.5. (b)** , it is relatively easy to escape through the bias electrode regardless of the energy of electrons. The bias current, which is the electron loss current through the bias electrode, is also divided into an electron beam current and a thermal electron current like the electron components in anode spot. The total number of electron lost through the bias electrode are expressed as Eq. (4.5).

$$\frac{1}{4}(n_{e,am}v_{th,am} + n_{e,th}v_{th,as})A_{bias} \quad (4.5)$$

where A_{bias} is the partial area of bias electrode exposed to the plasma. As shown in the

right side of **Fig. 4.1.**, many of electrons entering the anode spot from ambient plasma pass through and leave the anode spot without being collected in the bias electrode. Only the drifted electrons almost normally facing the bias electrode after accelerated are believed to be collected by the bias electrode and contribute to electron loss in anode spot. The first term of Eq. (4.5) shows the electron accelerated from ambient plasma contributed to bias current that is calculated with 1-directional electron flux and surface if the anode spot facing the bias electrode, which is almost same value of the area of bias electrode. The second term of Eq. (4.5) shows the thermal electron in anode spot contributed to bias current with calculated with 1-directional electron flux.

The other losses of electrons is that the electrons escape from the anode spot to the ambient plasma. In order to overcome the potential barrier of the double layer, only the electrons with higher energy than double layer potential can go back to the ambient plasma as expressed in Eq.(4.6).

$$\frac{1}{4} \left(n_{e,am} v_{th,am} \exp\left(-\frac{V_{DL}}{T_{e,am}+V_{DL}}\right) (A_{as} - A_{bias}) + n_{e,trap} v_{th,as} \exp\left(-\frac{V_{DL}}{T_{e,as}}\right) A_{as} \right) \quad (4.6)$$

The accelerated electrons incident on the anode spot surface are trapped in the anode spot by elastic collision except for the electrons loss through the bias electrode. It is estimated that trapped energetic electrons are lost from anode spot by another elastic collision expressed as the first term of Eq. (4.6) since it can be increased the velocity in normal direction to the anode spot surface than the double layer potential. The second term of Eq. (4.6) is expressed the thermal electron escaped toward the ambient

plasma that the escaped electrons which have higher energy than double layer potential is easy to overcome the potential barrier. Between the two terms representing the electrons escape from anode spot to the ambient plasma, it can be expected that most of the electrons escaped from anode spot to ambient plasma is dominant composed by the thermalized electrons (second terms of Eq. (4.6)). Because the density ratio of electron beam from ambient plasma to thermal electron in anode spot is about 10 based on the experimental result, so that most of electrons are dominantly composed by the thermalized electrons.

Compared to the complexity of generation and loss rate of electrons in anode spot, the generation of ion is volume production at anode spot only considered to direct ionization by collisions with energetic electrons as expressed as Eq. (4.7).

$$n_{e,am}N_{gas} < \sigma_{ioniz}v_{th,am} > V_{as} \quad (4.7)$$

As mentioned at the explanation of electron generation rate in anode spot, the ionization reaction in the anode spot is expressed with calculated ionization rate constant considered with the electron energy distribution of electron drifted into anode spot.

In contrast, the ions generated in anode spot are lost through the double layer as well as bias electrode expressed as Eq. (4.8).

$$n_{s,as}u_{B,as}A_{as} + n_{s,as}u_{B,as}A_{bias} \exp\left(-\frac{V_{ES}}{T_{e,as}}\right) \quad (4.8)$$

where $n_{s,as}$ is ion density at the edge of anode spot, $u_{B,as}$ is the ion Bohm velocity with

electron temperature of anode spot, $T_{e,as}$, V_{ES} is the space potential on electron sheath and A_{as} , A_{bias} are represented the area of anode spot and bias electrode, respectively. The first term of Eq. (4.8) is expressed the ion lost through the surface area of anode spot with assumption that the ion flows from anode spot to ambient plasma with Bohm velocity. The plasma potential profile is shown in **Fig. 4.5. (b)**. Ions generated in the anode are not only easy to escape into the ambient plasma, but also accelerated due to their potential structure of double layer. The second term of Eq. (4.8) represents the ion lost through the bias electrode. Compared with the ion current path through the double layer, it is rarely to collect the ion current at bias electrode since the electron sheath formed between the anode spot. The bias electrode can act as a potential barrier for ions and the ions have generally low temperature than the electron temperature that it is not easy to overcome the electron sheath barrier without sufficient ion energies. In addition, the ions are extracted from anode spot that worked as an additional ion loss to anode spot expressed as Eq. (4.9) as applying the high voltage, V_{ext} , to the bias electrode of which is drilled at the center.

$$n_{s,as}u_{B,as}A_{ext} \quad (4.9)$$

where A_{ext} is the area of extraction aperture for ion beam extraction. In order to sustain the anode spot stably, the current ratio between the electron current injected into anode spot and the ion current escaped from anode spot to ambient plasma needs to be kept in a constant value. The ion beam extraction can be changed the ion current flow through double layer that makes anode spot be unstable. Therefore, the current ratio

between the ion loss through the double layer and ion beam extraction can be worked as an important factor for determining whether the anode spot sustain stably at anode spot plasma ion source. The generation and loss rate of electrons and ions in the anode spot are summarized as in **Table 4.2**, which should be taken into account on particle balance model of anode spot.

Table 4. 2. The detail explanation of generation reaction in anode spot and charged particle loss terms through the boundaries of anode spot.

Generation rate of charged particles in anode spot		
Electron	Elastic collisions	$e^- \rightarrow e^-$ (direction change) $n_{e,am} N_{gas} \sigma_{el} v_{th,am} V_{as}$
	Ionization	$e^- + N \rightarrow N^+ + 2e^-$ $n_{e,am} N_{gas} < \sigma_{ioniz} v_{th,am} > V_{as}$
	Excitation	$e^- + N \rightarrow N^* + e^-$ $n_{e,am} N_{gas} < \sigma_{ext} v_{th,am} > V_{as}$
Ion	Ionization	$e^- + N \rightarrow N^+ + 2e^-$ $n_{e,am} N_{gas} < \sigma_{ioniz} v_{th,am} > V_{as}$
Loss rate of charged particles in anode spot		
Electron	Bias electrode	$\frac{1}{4} (n_{e,am} v_{th,am} + n_{e,trap} v_{th,as}) A_{bias}$
	Double layer	$\frac{1}{4} \left(n_{e,am} v_{th,am} \exp\left(-\frac{V_{DL}}{T_{e,am} + V_{DL}}\right) + n_{e,trap} v_{th,as} \exp\left(-\frac{V_{DL}}{T_{e,as}}\right) \right) A_{as}$
Ion	Double layer	$n_{s,as} u_{B,as} A_{as}$
	Bias electrode	$n_{s,as} u_{B,as} A_{bias} \exp\left(-\frac{V_{ES}}{T_{e,as}}\right)$
	Beam extraction	$n_{s,as} u_{B,as} A_{ext}$

4.2.3. Determination of Plasma Potential Varied with Bias Current

As driven higher voltage to bias electrode, it observes that the ambient plasma potential as well as anode spot plasma potential is increased, but the double layer potential, a potential difference of two plasmas, decreases. The plasma potential generally have a positive value with respect to the grounded wall potential in order to balance between ion loss current and electron loss current through the sheath formed between plasma and chamber wall. In general, single plasma is bounded in a container whose potential are kept in single potential as reference and its plasma potential, V_p , is expressed as Eq. (4.10).

$$V_p = \frac{T_e}{2} \ln \left(\frac{M_i}{2\pi m_e} \right) \quad (4.10)$$

where T_e is electron temperature and m_e and M_i are electron mass and ion mass of gas species, respectively. In case of ASPIS, it has a complex potential structure as shown in **Fig. 4.5. (b)**. **Figure 4.5. (a)** shows the various electron and ion currents paths through each boundaries caused by its complex potential structure. Since the two different plasma, such as ambient plasma and anode spot, are in contact with each other the boundaries for each plasma have different reference potential, it is difficult to interpret the plasma potential changes in the anode spot plasma ion source. Therefore, by defined each boundaries for different plasmas and considered the electron and ion loss current covered in previous section as loss rate, we figure out

how to define the plasma potentials in ASPIS and understand the correlation between the plasma potential and experimental conditions.

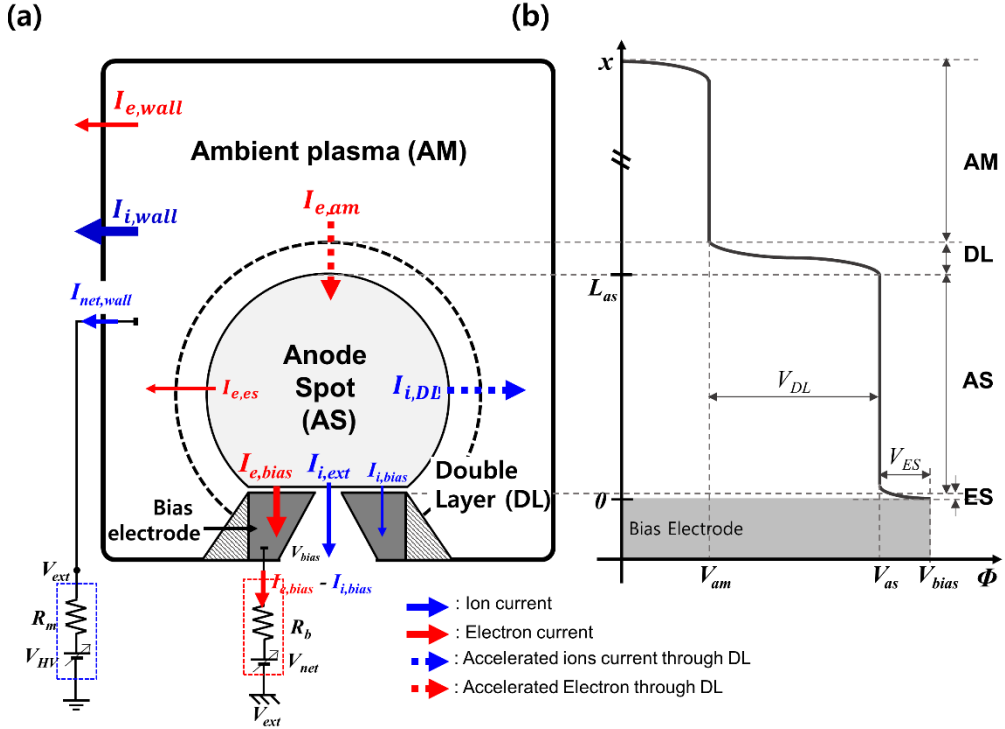


Figure 4. 5. (a) The schematic diagram of charged particle loss through the boundaries, (b) the space potential variation by the existence of ambient plasma, double layer, anode spot and bias electrode.

• **The plasma potential of ambient plasma, $V_{p,am}$**

In case of grounded discharge chamber wall, the plasma potential of ambient plasma is same as Eq. (4.10) without anode spot. The net current, the sum of the ion current and electron current ($I_{i,wall} - I_{e,wall}$), is zero by global ambipolar flow in order to satisfy

the quasi-neutrality condition. After generated the anode spot, however, the plasma boundary changes into chamber wall and bias electrode with different reference potential. The net current lost through the chamber wall is no longer zero that the all ions and some of electrons are escaped through the chamber wall and most of electrons are flown into bias electrode, which is called as global non-ambipolar flow mode. The ion current lost through the discharge chamber wall is assumed as the Bohm current expressed as Eq. (4.11).

$$I_{i,wall} = 0.61en_{e,am}\sqrt{\frac{kT_e}{M_i}}A_{wall} \quad (4.11)$$

And the electron current lost through the discharge chamber wall is assumed to follow the Boltzmann distribution near to wall and 1-dimensional flux described as Eq. (4.12).

$$I_{e,wall} = \frac{1}{4}en_{e,am}\sqrt{\frac{8kT_{e,am}}{\pi m_e}}A_{wall} \quad (4.12)$$

where $n_{e,am}$ is the plasma density of ambient plasma, $T_{e,am}$ is the electron temperature of ambient plasma, respectively.

The behavior of electron current lost through the double layer, which have drifted energy and incident on the surface of the anode spot, is figured out by the electron generation and loss rate at anode spot so that it can be determined the total electron current entered into the anode spot. Among the accelerated electron current injected into the anode spot, $I_{e,am}$, some of the electron current $I_{e,am}^*$, which is entered in normal direction to the bias electrode, are collected directly by bias electrode, but

rest of accelerated electrons are trapped in anode spot by elastic collisions. Besides, some of the trapped electrons are thermalized through inelastic collision with neutral particles, but the rest flow back to the ambient plasma due to another elastic collisions expressed as $I_{e,es}$. In this manner, the net electron current which is escaped from ambient plasma to anode spot, is approximately same as the bias current, which is the electron current flown into bias electrode, with assumption that the amount of generated electron in anode spot by ionization is negligible.

The net current is the summation value of all electron and ion currents lost through the discharge chamber wall as well as bias electrode expressed as Eqs. (4.13) and (4.14) is described the plasma potential of ambient plasma derived from Eq. (4.13).

$$I_{i,total} - I_{e,total} = I_{e,bias} \quad (4.13)$$

$$V_{p,am} = -T_{e,am} \ln \left(0.61 \sqrt{\frac{2\pi m_e}{M_i}} - \frac{1}{en_{e,am} A_{wall}} \sqrt{\frac{2\pi m_e}{kT_{e,am}}} I_{e,bias} \right) + V_{wall} \quad (4.14)$$

It is well known that the plasma potential is always higher than the wall potential and it has positive value if the wall is grounded. The value in the bracket of the natural log should be in range from 0 to 1 to have a negative value of the natural log. As the first term in the log is kept in constant value with fixed operating gas species, the ambient plasma potential can be increased with operated at higher bias current.

· **The plasma potential of anode spot, $V_{p,as}$**

In order to determine the plasma potential of anode spot, it need to figure out the net current passing through the boundaries of anode spot which are the surface of bias electrode as well as the double layer. In the case of the potential changes around the anode spot, the anode spot has a higher plasma potential than the ambient plasma and is lower than the voltage applied to the bias electrode as shown in **Fig. 4.5. (b)**. Based on the electron generation and loss rate in anode spot, the electrons incident toward the anode spot and the electrons generated in the anode spot are mainly lost through the bias electrode, else some of them, which have high energy to overcome the potential barrier of the double layer, go back to the ambient plasma. The drifted electron current, $I_{e,am}$, and the electron loss current ($I_{e,es}$) through the double layer are expressed as Eqs. (4.15) and (4.16), respectively, considered with 1-directional flux.

$$I_{e,am} = \frac{1}{4} e n_{e,am} \sqrt{\frac{8kT_{eam}}{\pi m_e}} A_{as} \quad (4.15)$$

$$I_{e,es} = \frac{1}{4} n_{e,th} \sqrt{\frac{8kT_{e,as}}{\pi m_e}} \exp\left(-\frac{V_{p,as}-V_{p,am}}{T_{e,as}}\right) A_{as} \quad (4.16)$$

It is assumed that the most of electron loss current through the double layer, $I_{e,es}$, expressed as Eq. (4.15), is described in terms of loss rate of thermal electrons and ignore the loss current composed by electron beam component because the thermal electron density is one order higher than the electron density of beam component.

In addition, the ions generated in the anode spot can escape to the ambient plasma through the double layer as well as be lost by the bias electrode. Since the electron sheath is formed between the bias electrode and the anode spot and the ion temperature is much lower than electron temperature as well, the ions in anode spot are rarely lost by the bias electrode. In this manner, the most of ions are accelerated through the double layer and escape to the ambient plasma. The ion current flow from anode spot to the ambient plasma, $I_{i,DL}$, is expressed as Eq. (4.17).

$$I_{i,DL} = en_{s,as} \sqrt{\frac{kT_{e,as}}{M_i}} A_{as} \quad (4.17)$$

where $n_{s,as}$ is edge ion density at the boundary of anode spot. The net current is the summation value of all electron and ion currents lost through the double layer as well as bias electrode expressed as Eq.(4.18) and the Eq. (4.19) is described the potential difference between anode spot and ambient plasma, called as double layer potential, V_{DL} , derived from Eq. (4.18).

$$I_{i,as,DL} = I_{e,am} - I_{e,bias} - I_{e,es} \quad (4.18)$$

$$V_{p,as} = -T_{e,as} \ln \left(\frac{n_{e,am}}{n_{e,as}} \sqrt{\frac{T_{e,am}}{T_{e,as}}} - 0.61 \sqrt{\frac{2\pi m_e}{M_i}} - \frac{1}{en_{e,as}A_{as}} \sqrt{\frac{2\pi m_e}{kT_{e,as}}} I_{e,bias} \right) + V_{p,am} \quad (4.19)$$

According to Eq. (4.19), the plasma potential of ambient plasma as well as anode spot are increased as the bias current increases, with the tendency of the experimental results. In case of considered ion beam extraction.

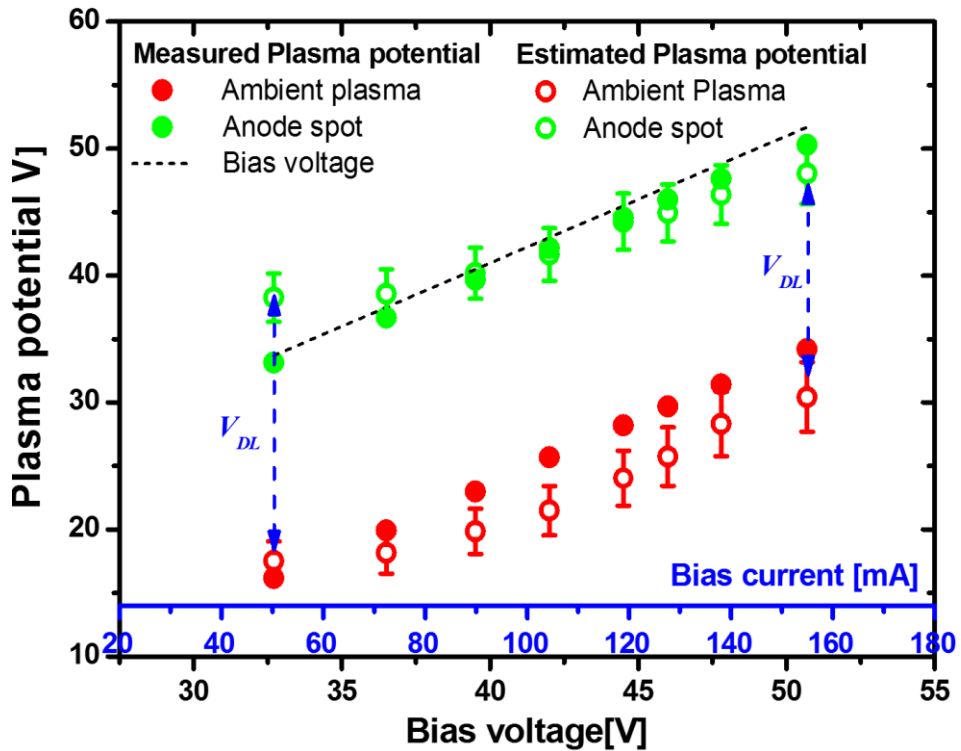


Figure 4. 6. The plasma potentials of ambient plasma and anode spot are compared between measured and estimated by Eqs. (4.14) and (4.19).

Figure 4. 6. shows the plasma potential comparison between measured and estimated by Eqs. (4.14) and (4.19) with varied the bias current from 50 mA to 160 mA at operating pressure of 25 mTorr. As the measured results, the plasma potentials of two different plasmas are increased, but the plasma potential difference between the ambient plasma and anode spot is decreased with increasing the bias current. Though the plasma potentials of ambient plasma underestimate with Eq. (4.14) because of the difficulty to define the effective chamber wall area, the estimated

results of plasma potentials are followed the trends of the measured plasma potentials with decreasing the plasma potential differences.

4.2.4. Detail Descriptions of Particle Balance Model of Anode Spot

Solving the particle balance model at anode spot expects the plasma properties of the anode spot ($n_{e,as}$, $T_{e,as}$, $V_{p,as}$) including the size of the anode spot (L_{as}) as well as the double layer potential (V_{DL}) with varied the plasma characteristics of the ambient plasma ($n_{e,am}$, $T_{e,am}$), the operating pressure (N_{gas}) and design parameters of ASPIS (D_{bias} , a_{ext}). The particle balance model has a criterion to be satisfied the quasi-neutrality condition on anode spot. In particular, the anode spot has two electron groups with different electron energies: the electron beam component with acceleration energy as double layer potential and thermal electrons trapped in anode spot and thermalized by inelastic collisions. The ion density in anode spot should be same value of the density summation of each electron groups expressed as Eq. (4.20).

$$n_{i,as} \approx n_{e,am} + n_{e,th} \quad (4.20)$$

Each continuity equations for ion and electron can be established by summarizing the generation and loss term as described in Section 4.2.2. The continuity equations of electron and ion are the govern equations of the particle balance model of anode spot expressed as Eq. (4.21) for electron and Eq. (4.22) for ions, and the particle balance model of anode spot is solve in steady state ($dn/dt = 0$).

$$\begin{aligned} \frac{dn_{e,th}}{dt} &= n_{e,am}N_{gas}(2\langle\sigma_{ioniz}v_{th,am}\rangle + \langle\sigma_{ex}v_{th,am}\rangle + \sigma_{el}v_{th,am}) \\ &+ \left(\frac{n_{e,th}}{\tau_{e,bias}} + \frac{n_{e,th}}{\tau_{e,DL}} \exp\left(-\frac{V_{DL}}{T_{e,as}}\right)\right) = 0 \end{aligned} \quad (4.21)$$

$$\frac{dn_{i,as}}{dt} = n_{e,am}N_{gas}\langle\sigma_{ioniz}v_{th,am}\rangle - \frac{n_{s,as}}{\tau_{i,DL}} - \frac{n_{s,as}}{\tau_{i,ext}} = 0 \quad (4.22)$$

where σ_{ioniz} , σ_{ex} , σ_{el} are represented the cross section for ionization, excitation and elastic collisions with neutral particles and $\tau_{e,bias}$, $\tau_{i,DL}$, $\tau_{i,ext}$ are the confinement times expressed for electron lost through bias electrode, ion lost through the double layer and ion beam extraction, respectively. The confinement times of electrons are expressed as Eq. (4.23) and the confinement times of ions are represented as Eq. (4.24).

$$\tau_{e,bias} = \frac{V_{as}/A_{bias}}{v_{th,as}}, \quad \tau_{e,DL} = \frac{V_{as}/A_{as}}{v_{th,as}} \quad (4.23)$$

$$\tau_{i,DL} = \frac{V_{as}/A_{as}}{u_{B,as}}, \quad \tau_{i,ext} = \frac{V_{as}/A_{ext}}{u_{B,as}} \quad (4.24)$$

where $v_{th,as}$ is thermal velocity of electron and $u_{B,as}$ is Bohm velocity of ions by $T_{e,as}$. Since the electron density of electron accelerated from ambient plasma is kept as almost constant value in anode spot, Eq. (4.21) deals only with the balance between the production and loss rate of thermal electrons in anode spot. The first term of Eq. (4.21) indicates that accelerated electrons are trapped by a double layer potential structure by elastic collision and are thermalized by inelastic collision such as ionization or excitation. The second term of Eq. (4.21) represents the thermal electron loss rate through the bias electrode and the double layer potential. In case of balancing

the ion generation and loss rate in anode spot, it is expressed as Eq. (4.22). The ion generation in anode spot is only considered the direct ionization by the energetic electrons accelerated by double layer. Without ion beam extraction, the ions in anode spot is mainly lost through double layer and returned into the ambient plasma, but the additional ion loss, expressed as third term of Eq. (4.22), is occurred by extracted ion beam current from anode spot.

It is normally that the double layer potential is higher than the first ionization potential of gas species, but the double layer potential sometimes decreases under the ionization potential as increasing the operating pressure as well as bias voltage. Therefore, the reaction rate, K , called as sigma-V parameter is obtained to integrate the product of the drifted Maxwellian EEDF and the cross section of the process, such as ionization, excitation. The energetic electron injected to anode spot gains the drifted energies as much as V_{DL} by passing through the double layer. The drifted Maxwellian EEDF, $f_{e,drifted}$, is expressed as Eq. (4.25) and rate constant is expressed as Eq. (4.26), respectively.

$$f_{e,drifted}(E) = 0 \quad (E < V_{DL}) \quad (4.25)$$

$$= \frac{2}{\sqrt{\pi}} \left(\frac{1}{kT_{e,am}} \right)^{1.5} \sqrt{E - V_{DL}} \exp \left(-\frac{E - V_{DL}}{kT_{e,am}} \right) (E \geq V_{DL})$$

$$K = \langle \sigma v \rangle = \int_{E_i}^{\infty} f_{e,drifted}(E) \sqrt{E} \sigma(E) dE / \int_{E_i}^{\infty} f_{e,drifted}(E) dE \quad (4.26)$$

Where E represents the electron energy, E_i is integrated low limit value in case that 15.76 eV is E_i at ionization process and 12.4 eV for excitation process. **Figure 4.7.**

shows the calculated results of the ionization rate constant according to the variations of electron temperature of ambient plasma as well as double layer potential, assuming that the electron with same plasma density is injected into anode spot. As simplified the ionization rate constant as the product of the ionization cross section and the thermal velocity of electron, the ionization rate constant is zero in case that the double layer potential is lower than the ionization potential of gas species. But it is not zero calculated with considered the electron energy distribution as drifted Maxwellian. it is followed that the ionization rate constant increases with higher electron temperature of ambient plasma at the same double layer potential.

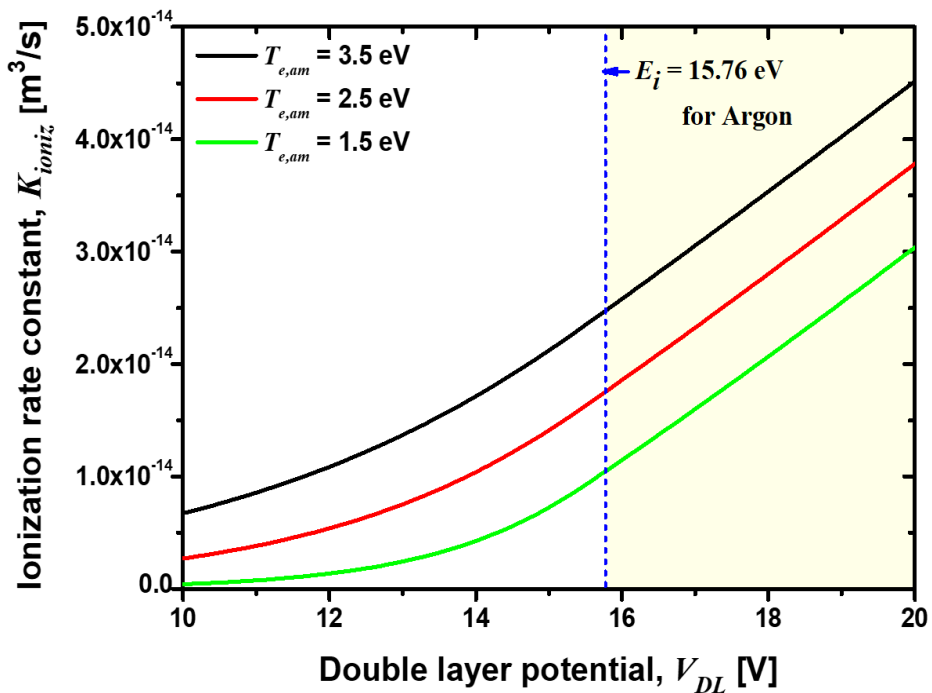


Figure 4. 7. The calculation result of ionization rate constant with varied the electron temperature of ambient plasma.

Base on the experimental results, the anode spot size, L_{as} , is estimated by Eq. (3.2 mm) and the plasma potentials of ambient plasma ($V_{p,am}$) and anode spot ($V_{p,as}$) are used the formula with Eq. (4.14) and Eq.(4.19). In addition, it is difficult to calculate the electron temperature of the anode spot, $T_{e,as}$, by numerical approach. This is because not only the particle balance and energy balance of entire discharge system, including the ambient plasma as well as anode spot, need to be approached to solve with self-consistent, but also all collisions processes by the accelerated electrons are taken into consideration to obtain the temperature of the thermalized electron in anode spot. Therefore, we assume that the electron temperature of anode spot expressed as Eq. (4.27) is followed the relationship with electron temperature of ambient plasma and double layer potential as suggested in previous work [25].

$$T_{e,as} \cong T_{e,am} + V_{DL} - E_{avg} \quad (4.27)$$

where E_{avg} is averaged loss energy by neutral-ion collision that is approximately the averaged value of the threshold energy for ionization and excitation.

4.3. Validation of 0-D Particle Balance Model with Experimental Results

4.3.1. Anode Spot Properties with Varied Bias Current

A 0-D particle balance model is established that the generation and loss rate of electrons and ions are considered in the anode spot with modified formula of anode spot size and plasma potential. Before applying to ASPIS to estimate the plasma properties variations by ion beam extraction, the 0-D particle balance model is evaluated by the comparison between measured plasma properties, including the anode spot size, and estimated values through the particle balance model of anode spot. **Figure 4.8.** shows the comparison between measured and estimated values in terms of bias current (I_{bias}), electron temperature ($T_{e,as}$) and thermal electron density($n_{e,th}$) of anode spot, double layer potential(V_{DL}) and anode spot size (L_{as}).

The experiments for measuring the plasma properties including anode spot size are conducted at fixed operating pressure and RF power as 15 mTorr and 150 W, respectively. The initial values for particle balance model are used the measured values of the ambient plasma properties and the bias current. The electron temperature of ambient plasma is fixed as 3.5 eV. The plasma density of ambient plasma is controlled from $4.5 \times 10^{15} \text{ m}^{-3}$ to $8 \times 10^{15} \text{ m}^{-3}$ and the bias current is varied in 80-160 mA as measured. It is confirmed that the changes of all the plasma parameters calculated corresponds with the variation of measured plasma parameters with respect to varied initial values of ambient plasma density and bias current. As compared with measured results, the calculated results are over-estimated within 10% of error but it can be used as predictive model of plasma properties in anode spot with respect to the variation of operating parameters. The main cause of the error comes from the overestimated

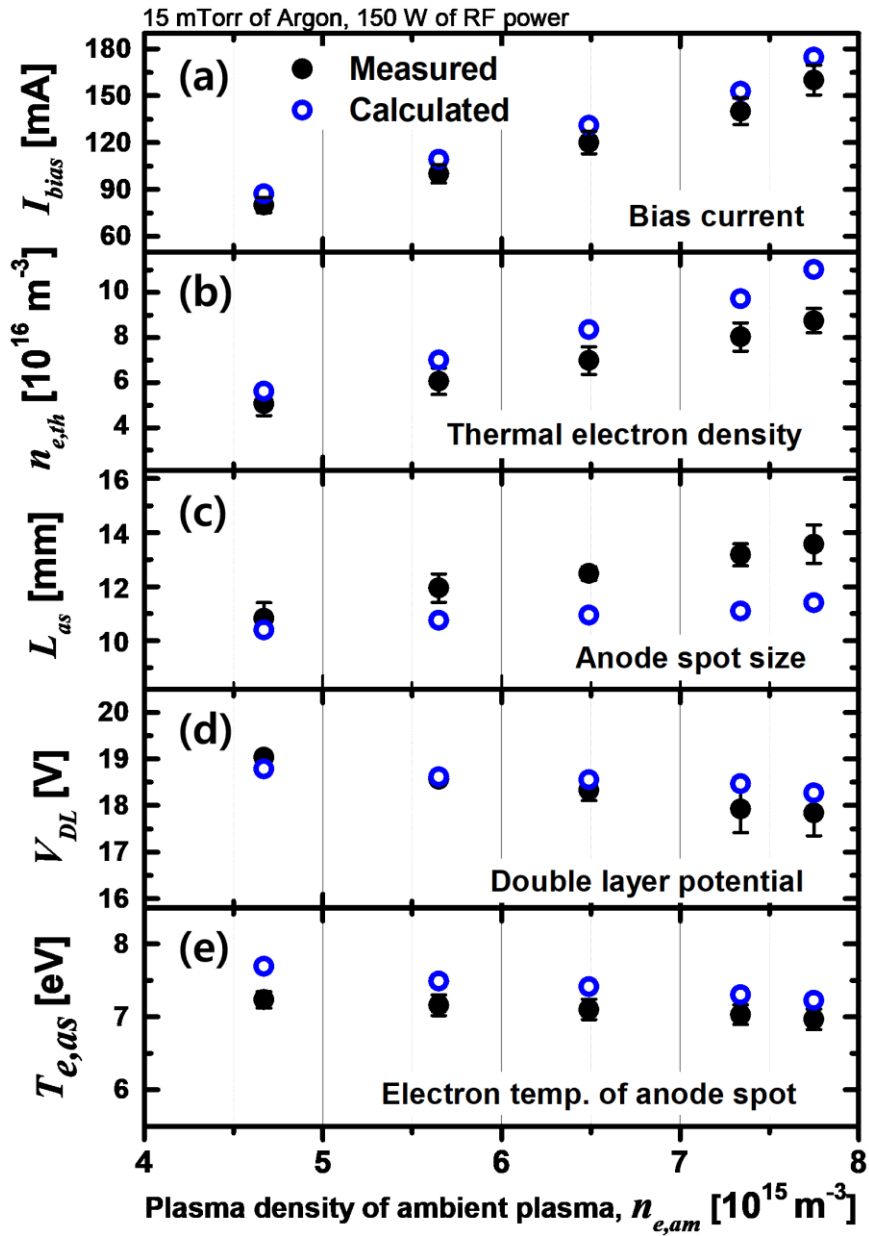


Figure 4. 8. The comparison between the calculated and measured results: (a) bias current, (b) thermal electron density, (c) anode spot size, (d) double layer potential and (e) electron temperature of anode spot.

double layer potential. Based on the experimental results, it is figured out that the ionization reaction rate is determined by the double layer potential as the operating pressure and the plasma properties of ambient plasma are fixed, and the total generation rate by ionization in anode spot is linearly proportional to bias current by the variation of anode spot. In addition, the other factor to cause the calculated error is from the modified formulae of anode spot size expressed as Eq. (3.27). It is expressed on the assumption that the electrons in the anode spot are mostly composed of thermal electrons. However, the composition of electrons accelerated from the ambient plasma in anode spot increases as the bias current increases. The size of the anode spot can be underestimated at high bias current operation, and it can act as an error in the estimation of total generation rate in the volume of anode spot. Thus, it can be used as predictive model of plasma properties in anode spot with respect to the variation of operating parameters that the calculated values well follow the trend of measured results with respect to bias current and the plasma properties of ambient plasma within 10% errors.

4.3.2. Validation of 0-D Particle Balance Model in ASPIS

With respect to the bias current, the variation of anode spot plasma properties including the its size are calculated by 0-D particle balance model and validated by comparison with the experimental results related to plasma properties. Based on this,

the operating criteria of the anode spot plasma ion source are summarized and it is compared the extracted ion beam current between experimental results and calculated results through the particle balance model with considered the ion loss to anode spot.

4.3.2.1. Operating Criteria of ASPIS for High Current Beam Extraction.

In order to extract high current ion beam from ASPIS, it needs to consider the area criteria of bias electrode to generate the anode spot in front of the bias electrode and the operational range of anode spot size to enhance the ion beam current and sustain it stably with ion beam extraction as well.

Before generated the anode spot, the area ratio of bias electrode to discharge chamber wall should be lower value than μ determined by the ion and electron mass ratio depending on gas species in order to generate the electron sheath in front of bias electrode. The area ratio criterion of bias electrode to discharge chamber wall, expressed as Eq. (4.28), is derived from the balancing of net loss current through the boundaries made of conductors.

$$A_{bias}/A_{wall} < \mu \left(\mu = \sqrt{2.3 \frac{m_e}{M_i}} \right) \quad (4.28)$$

Where A_{bias} and A_{wall} is area of bias electrode and discharge chamber wall, respectively. After generated the anode spot in front of the bias electrode, the anode spot should be sustained stably during the ion beam extraction for used as high current ion source.

Based on the experimental result of ion beam extraction, it is summarized that the optimum operating range of anode spot size is determined by the comparison with design parameters of ASPIS, such as the diameter of bias electrode and the beam extraction aperture size. It is defined the annular width of bias electrode as $w = (D_{bias} - a_{ext}) / 2$. Anode spot size should be satisfy in ranges expressed as Eq. (4.29).

$$\begin{aligned}
 a_{ext} < L_{as} \leq D_{bias} & \quad (a_{ext} < w) \\
 w < L_{as} \leq D_{bias} & \quad (w \leq a_{ext})
 \end{aligned}
 \tag{4.29}$$

4.3.2.2. Anode Spot Plasma Properties Variations with Ion Beam Extraction

Figure 4.9. is represented the calculation results of plasma properties of anode spot plasma, double layer potential and estimated beam current density from anode spot with fixed diameter of beam extraction aperture as 2 mm in diameter. And $1.2 \times 10^{17} \text{ m}^{-3}$ of plasma density and 3 eV of electron temperature are worked as the constraints of ambient plasma properties inferred from the beam current, 100 μA extracted from the ambient plasma sustained by 200W of RF power and 50 mTorr of Argon. Increasing the diameter of bias electrode, the double layer potential is decreased to create bigger anode spot to expand the surface area of anode spot. By considering beam extraction effect, the anode spot can't be sustain in front of bias electrode, whose diameter is bigger than 7 mm, because the calculated double layer potential is lower

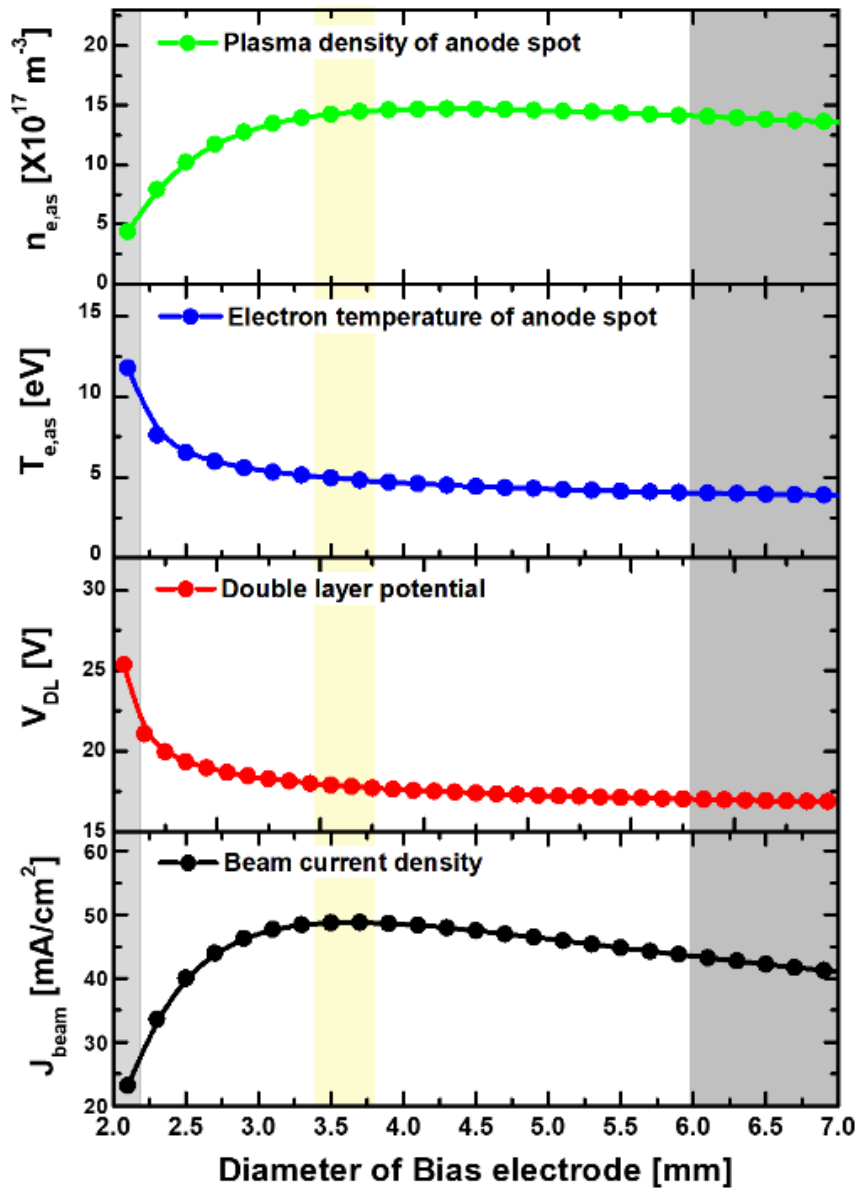


Figure 4. 9. The estimated values that the plasma properties and extracted beam current density tendency with varied the diameter of bias electrode from 2.1 mm to 7 mm in case of fixed the extraction aperture as 2 mm in diameter.

than ionization potential of argon. In case that the diameter of bias electrode is smaller than 2.3 mm is not satisfied the Eq. (2.2) that the anode spot size is too small to extract ion beam from anode spot. Therefore, the appropriate range of bias electrode's diameter is from 2.3 mm to 7 mm. the plasma properties of anode spot is typically kept in range of $1.5 \times 10^{18} \text{ m}^{-3}$ and 5 eV. By using the bias electrode whose diameter is varied from 2.3 mm to 3.5 mm, the estimated beam current density and plasma density of anode spot is increased. But by using the bigger bias electrode than 3.5 mm in diameter the plasma density and electron temperature and double layer potential of anode spot is decreased, it is induced the extracted beam current be lower. By installing the bias electrode of 3.5 mm in diameter with extraction aperture as 2 mm- ϕ , the maximum extractable beam current density is 50 mA/cm². Comparison between measured maximum beam current density (188 mA/cm²) and calculated beam current density(50 mA/cm²), their absolute values are not fit well, but the beam current trend with varying the bias electrode area is similar each other. Adopting 3mm of bias electrode helps to achieve ion beam current at same experimental conditions of ambient plasma. It means that the optimum bias electrode sizes are existed on each extraction aperture sizes in order to achieve maximum beam current from same plasma properties of ambient plasma.

4.4. Expectation of ASPIS's Operating Parameters Range

It is general way to expand the aperture size in order to extract high current ion from plasma. But ASPIS has the limitations on extraction aperture size that it can't be larger than the diameter of bias electrode, and it is also considered the balancing between electron and ion lost through the boundaries of anode spot, such as bias electrode and the surface of anode spot. It is expected that the optimum extraction aperture is determined by the balancing between the ion loss through the surface area and the electron loss through the bias electrode. **Figure 4.10** shows that the estimated extractable ion beam current is varied by the diameter of aperture size with the bias electrode fixed its diameter. The diameter of bias electrode are varied as 3, 4 and 5 mm that each cases of varied the diameter of bias electrode are expressed as black-square, red-circle and green-triangle dot in **Fig. 4.10**, respectively. It is assumed that the plasma density is about $1 \times 10^{17} \text{ m}^{-3}$ with 5 eV of electron temperature estimated from the extracted ion beam current at the ambient plasma sustained at 50 mTorr of operating pressure and 200 W of RF power. Assuming that the ion beam is extracted at anode spot sustained with 0.5 A of bias current, the extracted ion beam current can be obtained as the maximum beam current in which area ratio of the bias electrode to the extraction aperture (A_{bias} / A_{ext}) is close to 2. As the area ratio is less than 2, the area of the bias electrode is too small to cover the sufficient electron loss so that the electron can be accumulated inside anode spot. As a result, the plasma density of

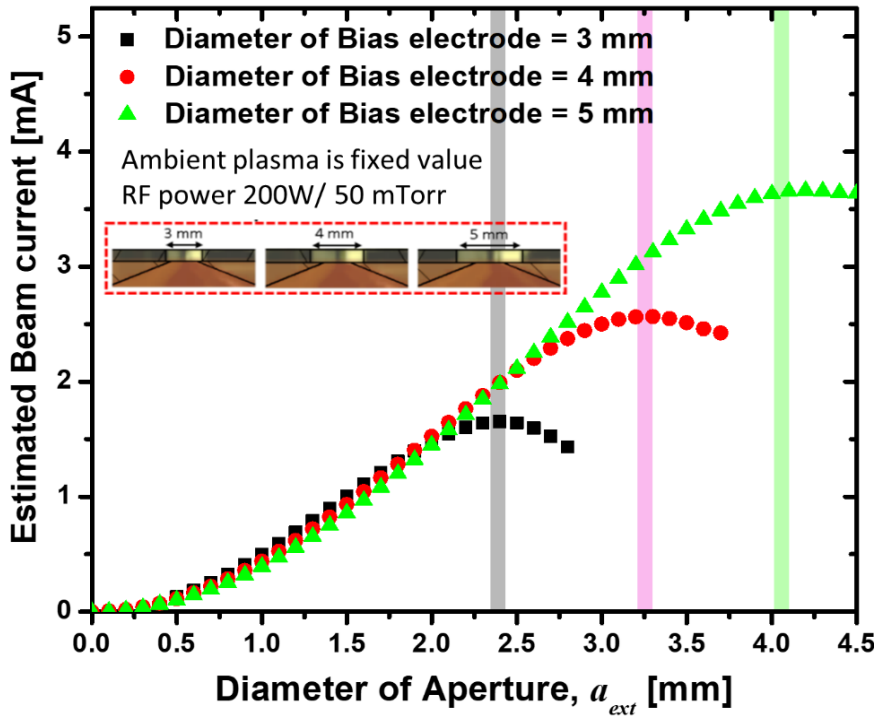


Figure 4. 10. The estimated ion beam currents are estimated with varied the extraction aperture size at fixed diameter of bias electrode as 3, 4, and 5 mm.

anode spot can be lower than the case the area ratio is close to 2 since the space potential of anode spot as well as the double layer potential are reduced and the total ionization reaction rate in anode spot is decreased.

And the controllable range of operating parameter of ASPIS is also estimated by solving the particle balance model with considering the ion beam extraction. As mentioned in the previous section 4.3.2.2., the diameter of the bias electrode most suitable for the extraction of the maximum beam is estimated about 3.5 mm with fixed extraction aperture of 2 mm in diameter as shown in Fig. 4.10. Figure 4.11. shows

the operating range of ASPIS according to the variations of anode spot size under various operating conditions of working pressure and bias current. In the ASPIS with current status, the bias current can be operated up to 0.7 A with fixed RF power as 200 W. Based on this, it is estimated the size variations of the anode spot according to the bias current operating pressure and their operational range is shown in **Fig. 4.11** through suggested operating criteria of ASPIS. Assuming that the controllable pressure range is 10-100 mTorr in current ASPIS system, the bias current is

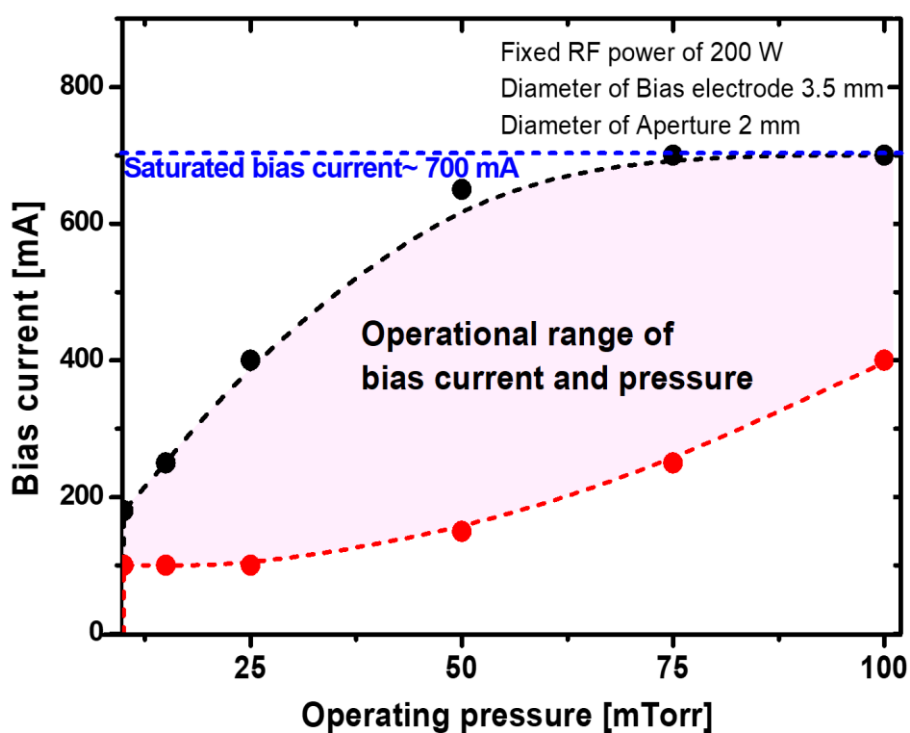


Figure 4. 11. The operational range of bias current and operating pressure are determined by the comparison among the anode spot size, diameter of bias electrode (3.5 mm) and aperture size (2 mm).

determined according to the size of the anode spot. As operated at low pressure, ASPIS is only operated at low bias current. Because the anode spot operated at high bias current with low pressure, the anode spot is formed as unstable cylindrical shape that anode spot becomes unstable by ion beam extraction. As operated at high pressure, the anode spot must be operated at a high bias current because the anode spot affects the beam extraction with comparable size. In this manner, the optimum operating pressure is about 50 mTorr with utilized all bias current range, 200 -700 mA, when the design parameter of ASPIS is fixed condition: the diameter of the bias electrode is 3.5 mm and the extraction aperture size is 2 mm.

Figure 4. 12. shows the estimated extractable ion beam current and maximum operating pressure with varied the extraction aperture size from 1 mm to 5 mm. The magenta dotted line of **Fig. 4.12.** is expressed the maximum operating pressure that the diameter of bias electrode is satisfied the area ratio as 2, and the black-diamond dots show the experimentally checked operating pressures that the anode spots are sustained during ion beam extraction. The blue dotted lines explains the extractable ion beam current with assumption as same plasma density of anode spot and blue -square dots represents the measured ion beam current with bias current of 600 mA. The measured and estimated values are follows same trends with varied the extraction aperture. In order to extract the ion beam current with maintaining the anode spot at enlarged extraction aperture, the ASPIS should be operated at low pressure. As supply a sufficient amount of electrons to anode spot at low pressure, it

can be easily expected that the RF power should be increased for enhancing the plasma density of ambient plasma. As marked with a hatch on the right side of the **Fig. 4.12**, it is difficult to generate the ambient plasma by ICP within 50 mTorr as the bias electrode has a large extraction hole than 4 mm with current status of ASPIS. Therefore, the design of ASPIS should be modified with a larger volume of discharge tube than the current ASPIS in order to extract the ion beam current with tens of mA level since the extraction aperture size as well as the diameter of bias electrode must be enlarged.

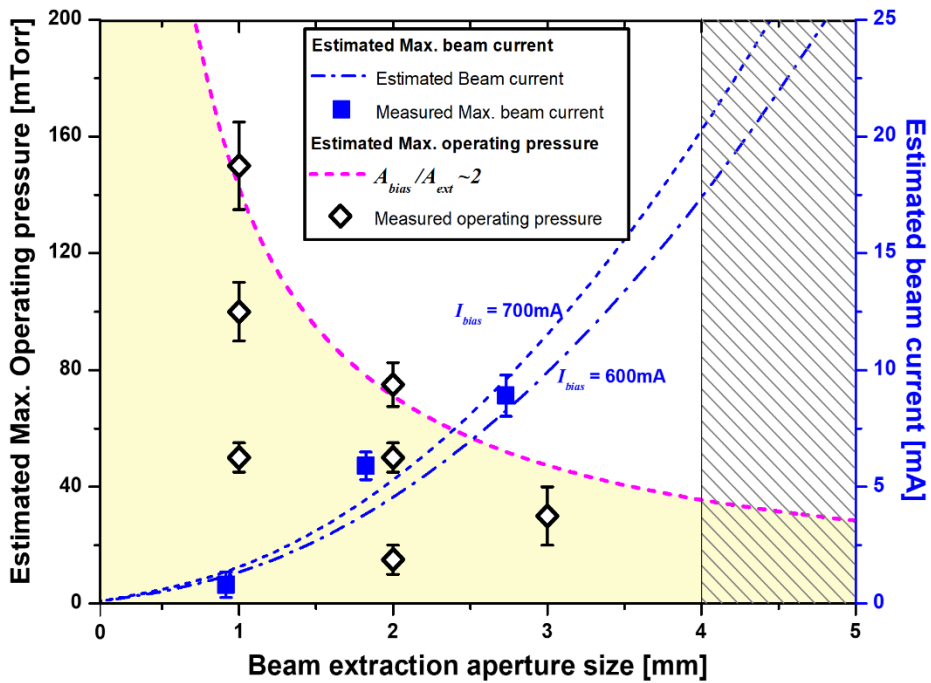


Figure 4. 12. The estimated operating pressure and extractable beam current are varied with the beam extraction aperture size. The extractable beam current is estimated with assumption that the bias current is constant.

5. Summary and Conclusion

At Seoul National University, it has been developed the high brightness ion source utilized the anode spot plasma for Nano-applications that has strong point to generate the localized high density plasma with high power efficiency and it has been successfully used as an ion source for FIB (Focused Ion Beams) and Nano-MEIS(Nano-Medium Energy Ion Scattering). In order to expand its application fields, such as ion implantation, we will examine the operational conditions of Anode Spot Plasma Ion Source (ASPIS) for high current ion beam extraction. It is expected that the plasma properties as well as its sustainment will be affected by ion beam extraction from it. This study is focused on the correlation between the size variations of the anode spot and the operating variables of ASPIS. It is also figured out the effective factors to maintain the anode spot in presence of ion beam extraction.

The most important consideration of anode spot plasma ion source used as high current source is the sustainment of anode spot with ion beam extraction since high current ion beam extraction acts as an additional ion loss in terms of maintaining the anode spot. As using a larger diameter of extraction aperture, extracted ion beam currents are more affected to the size variation of the anode spot and the beam current is not followed the increases with linearity according to operating parameters such as bias current and operating pressure. In addition, the length of anode spot is also an essential factor in sustainment of anode spot in presence of ion beam extraction. In

order to derive the optimum operating conditions of anode spot with ion beam extraction, its size should be larger than the diameter of beam extraction aperture and also be smaller than the diameter of the bias electrode.

It is estimated the anode spot size variations expressed in terms of operating parameter of ASPIS and the plasma properties of ambient plasma based on the correlation between the plasma parameters and operating parameters. Expanded the surface area of anode spot are enhanced the ionization rate inside anode spot in order to compensate the particle loss, such as ion beam extraction, to anode spot.

Based the experimental results, the characteristics of anode spot plasma considered with ion beam extraction is understood by developed the particle balance of anode spot. To focus on the generation and loss of ion at anode spot, the particle balance model is the particle balance model is applied to analyze the anode spot with existence of ion beam extraction. The size of the bias electrode and the extraction aperture were changed, it was found that the maximum beam current could be extractable at the area ratio of bias electrode to extraction aperture as 2. and it is also predictable to the size variation of anode spot with respect to bias current that the operating parameter as well as design parameter of ASPIS is suggested with target current and operating pressure.

In this study, it is confirmed that the operation condition of ASPIS is restricted by the particle equilibrium condition of the anode spot in order to be used as high current ion source. Within the constraint condition, however, it exists

appropriate conditions that the anode spot is sustained in presence of ion beam extraction. It is determined by the size of the anode spot and the surrounding design parameters, such as diameter of bias electrode and aperture and ASPIS can be operated under various conditions to achieve the target ion beam current since the size of the anode spot can be controlled through the operating parameters. In order to apply the anode spot plasma ion source as a large area ion source beyond the high current ion source, this research will be used as a key index to suggest guidelines for ion source design.

Bibliography

- [1] C. W. Kimblin, "Anode voltage drop and anode spot formation in dc vacuum arcs", *Journal of Applied Physics*, **40** 1744 (1969).
- [2] G. A. Dyuzhev, G.A. Lyubimov and S. M. Shkol'nik, "Conditions of the anode spot formation in a Vacuum Arc," *IEEE Transactions on Plasma Science*, Vol. PS-11, No. 1,(1983).
- [3] A. Anders and M. Kuhn, "Characterization of a low-energy constricted-plasma source," *Review of Scientific Instruments* **69** (3), 1340 (1998).
- [4] Y.-S. Park and Y. S. Hwang, "Enhancement in ion beam current with layered-gloves in a constricted dc plasma ion source," *Review of Scientific Instruments* **81** (2), 02B309 (2010).
- [5] Y. Lee, K.-J. Chung, Y.-S. Park and Y .S. Hwang, "Investigation of helium ion production in constricted direct current plasma ion source with layered-gloves," *Review of Scientific Instruments* **85** 02C105 (2014).
- [6] I. Langmuir, "The interaction of electron and positive ion spaces charges in cathode sheaths," *Physical Reviews* **33** (6), 954 (1929).
- [7] S. D. Baalrud, N. Hershkowitz and B. Longmier, "Global nonambipolar flow: Plasma confinement where all electrons are lose to one boundary and all positive

- ions to another boundary”, *Physics of Plasmas* **14** (4) 042109 (2007).
- [8] E.V. Barnat, G. R. Laith and S. D. Baalrud, “Response of the plasma to the size of an anode electrode biased near the plasma potential”, *Physics of Plasmas* **21** 103512 (2014).
- [9] L. Schiesko, M. Carrere, G. Cartry and J. M. Layet, "Experimental study and modeling of the electron-attracting sheath: The influence of secondary electron emission," *Physics of Plasmas* **15** (7), 073507 (2008).
- [10] B.Scheiner, S.D. Baalrud, B. T. Yee, M. M. Hopkins and E. V. Barnat, “Theory of the electron sheath and presheath,” *Physics of Plasmas* **22**, 123520 (2015).
- [11] Y.-S. Park, “Study on Breakdown Conditions of Local Discharges in Plasma Sheath”, M.S. Thesis, Seoul National University (2007).
- [12] L. Conde, C. F. Fontan and J. Lambas, “The transition from an ionizing electron collecting plasma sheath into an anodic double layer as a bifurcation”, *Physics of Plasmas* **13** 113504 (2006).
- [13] B. Song, N. D'Angelo and R. L. Merlino, "On anode spots, double layers and plasma contactors," *Journal of Physics D: Applied Physics* **24** (10), 1789 (1991).
- [14] B. Song, N. D'Angelo and R. L. Merlino, "Stability of a spherical double layer produced through ionization," *Journal of Physics D: Applied Physics* **25** (6), 938 (1992).

- [15] Y.-S. Park, Y. Lee, K.-J. Chung and Y. S. Hwang, "Characterization of plasma ion source utilizing anode spot with positively biased electrode for stable and high-current ion beam extraction," *Review of Scientific Instruments* **82** (12), 123303 (2011).
- [16] Y.-S. Park, Y. Lee, K.-J. Chung and Y. S. Hwang, "Operating conditions for the generation of stable anode spot plasma in front of a positively biased electrode," *Review of Scientific Instruments* **85**, 02A508 (2014).
- [17] S. Baalrud, B. Longmier and N. Hershkowitz, "Equilibrium states of anodic double layers," *Plasma Sources Science and Technology* **18**, 035002 (2009).
- [18] M. Sanduloviciu and E. Lozneau, "On the generation mechanism and the instability properties of anode double layers," *Plasma Physics and Controlled Fusion* **28** (3), 585 (1986).
- [19] M. Sanduloviciu, C. Borcia and G. Leu, "Self-organization phenomena in current carrying plasmas related to the non-linearity of the current versus voltage characteristic," *Physics Letters A* **208** (1-2), 136 (1995).
- [20] C. Ionitã, D.-G. Dimitriu and R. W. Schrittwieser, "Elementary processes at the origin of the generation and dynamics of multiple double layers in DP machine plasma," *International Journal of Mass Spectrometry* **233** (1-3), 343 (2004).
- [21] M. Sanduloviciu, V. Melnig and C. Borcia, "Spontaneously generated temporal

- patterns correlated with the dynamics of self-organized coherent space charge configurations formed in plasma," *Physics Letters A* **229** (6), 354 (1997).
- [22] L. Conde and L. Leon, "Multiple double layers in a glow discharge," *Physics of Plasmas* **1** (8), 2441 (1994).
- [23] L. Conde and L. Leon, "Visual observation of multiple double layers", *IEEE TRANSACTIONS ON PLASMA SCIENCE*, VOL. 27, NO. 1, (1999)
- [24] M. A. Lieberman and A. J. Lichtenberg, *Principle of Plasma Discharges and Materials Processing*, 2nd edition (New Jersey: Wiley-Interscience, 2005).
- [25] Y.-S. Park, "Characterization of High Density Anode Spot Plasma", Ph.D Thesis, Seoul National University (2013).
- [26] R. L. Stenzel, J. Gruenwald, B. Fonda, C. Ionitã and R. Schrittwieser, "Transit time instabilities in an inverted fireball. II. Mode jumping and nonlinearities," *Physics of Plasmas* **18** (1), 012105 (2011).
- [27] T. An, R. L. Merlino and N. D'Angelo, "Cylindrical anode double layers ('firerods') produced in a uniform magnetic field," *Journal of Physics D: Applied Physics* **27**, 1906 (1994).
- [28] R. L. Stenzel, C. Ionita and R. Schrittwieser, "Dynamics of fireballs," *Plasma Sources Science and Technology* **17** (3), 035006 (2008).

- [29] B. R. Weatherford, E. V. Barnat and J. E. Foster, "Two-dimensional laser collision-induced fluorescence measurements of plasma properties near an RF plasma cathode extraction aperture," *Plasma Sources Science and Technology* **21**, 055030 (2012).
- [30] Y. J. Kim, D. H. Park, H. S. Jeong and Y. S. Hwang, "New method of high brightness ion extraction based on bias electrode," *Review of Scientific Instruments* **77** (3), 03B507 (2006).
- [31] Y.-S. Park, Y. Lee, Y.-J. Kim, M.-J. Park, D. W. Moon, K.-J. Chung and Y. S. Hwang, "Brightness enhancement of plasma ion source by utilizing anode spot for nano-applications," *Review of Scientific Instruments* **83** (2), 02B313 (2012).
- [32] Y. Lee, K.-J. Chung and Y. S. Hwang, "Feasibility study on high current ion extraction from anode spot plasma for large area ion implantation," *Current Applied Physics* **15**, 1599 (2015).
- [33] J. Orloff, M. Utlaut and L. Swanson, 『*High resolution focused ion beams: FIB and Its applications*』 (Kluwer Academic/ Plenum Publisher New York, 2002).
- [34] I. G. Brown, 『*The Physics and Technology of Ion Sources*』 (WILEY-VCH, Germany, ed. 2nd, 2004).
- [35] H. Zhang, 『*Ion Sources*』 (Springer, New York, 1999).

- [36] R. Miyano, S. Izumi, R. Kitada, M. Fujii, S. Ikezawa and A. Ito, “Influence of electron beam on profile of sheath potentials in electron-beam-excited plasma apparatus”, *Plasma Sources Science and Technology* **6**, 551 (1997).
- [37] S. B. Jeon, “Tunable external RF choke filter design for single Langmuir probe in RF discharges”, M. S. Thesis, Hanyang University (2016).
- [38] F.F. Chen, “Langmuir probe analysis for high density plasmas”, *Physics of Plasmas* **8**, 3029 (2011).
- [39] N. Hershkowitz, “How Langmuir probes work”, in 『*Plasma Diagnostics*』 Vol. 1 Discharge Parameters and Chemistry. Edited by O. Auciello and D. L. Flamm (New York: Academic, 1989)
- [40] D. N. Ruzic, 『*Electric probes for low temperature plasmas*』 AVS Monograph Series, New York, 1994.
- [41] H. D. Jung, M. J. Park, S. H. Kim and Y. S. Hwang, “Development of a High-Current Helicon Ion Source with High Monatomic Fraction for Application of Neutron Generator”, *IEEE Transaction Plasma Science* **35** 1476 (2007).
- [42] B. K. Jung, J. J. Dang, Y. H. An, K.-J. Chung and Y. S. Hwang, “Development of a novel radio-frequency negative hydrogen ion source in conically converging configuration”, *Review of Scientific Instruments* **85**, 02B112 (2014).

[43] Y.-S. Park, H.T. Kim and Y. S. Hwang, “Design of compact microwave plasma ion sources for focused ion beam”, Proceeding of KSME, Jeju, Korea (2008).

[44] D. G. Dimitriu, M. Aflori, C. Ionitã and R. W. Schrittwieser, “Common physical mechanism for concentric and non-concentric multiple double layers in plasma”, *Plasma Physics and Controlled Fusion* **49** 237 (2007).

Abstract in Korean

고전류 인출을 위한 양전극 국부 플라즈마 이온원 개발

이 윤 아

에너지시스템공학부

(핵융합 및 플라즈마 공학 전공)

서울대학교 대학원

주변부 플라즈마(Ambient plasma)에 노출된 도체에 양 전압을 인가하였을 때, 도체 앞에 형성되는 작고 밝은 플라즈마가 발생하는데 이를 양전극 국부 플라즈마(Anode spot plasma)라 하고 주변부 플라즈마와 이중 쉬스(Double layer)로 경계를 이루고 있다. 이 경계를 통해 가속되어 들어오는 전자가 중성 입자와 이온화 반응으로 양전극 국부 플라즈마가 유지되며, 이는 낮은 입력 전력에 비해 높은 플라즈마 밀도를 갖는다고 알려져 있다. 서울대학교에서 양전극 국부 플라즈마 자체 특성 연구를 진행하였을 뿐만 아니라, 이를 이용한 고휘도 이온원(High brightness)을

성공적으로 개발하여 집속 이온빔(FIB, Focused Ion Beams) 장비나 Nano-MEIS(Nano-Medium Energy Ion Scattering) 장비의 이온원으로 활용하였다. 그러나 최근 고전류-대면적 플라즈마 이온원의 필요성이 이온 주입 분야에서 각광받는 가운데, 양전극 국부 플라즈마 이온원(Anode Spot Plasma Ion Source, ASPIS)의 인출구를 넓혀, 고전류 플라즈마 이온원으로 개발하고자 한다. 인출구를 확장함으로써 인해 이온빔 인출이 양전극 국부 플라즈마의 특성 및 유지에 영향을 미칠 것이라 예상된다. 외부 운전 변수에 따른 이온빔 전류 변화 및 양전극 국부 플라즈마 특성 변화를 바탕으로 이온빔 인출을 고려한 양전극 국부 플라즈마의 입자 평형 모델을 통해 고전류 인출을 위한 양전극 국부 플라즈마 이온원의 설계 변수 및 운전 변수의 범위를 제시하고자 한다.

이온빔 인출구의 직경을 mm 단위로 확장시킨 양전극 국부 플라즈마 이온원에서 운전 변수에 따른 빔 전류 변화 및 양전극 국부 플라즈마의 유지 조건에 대해 연구하였다. 바이어스 전극의 중심에 위치한 인출구의 직경을 2 mm로 고정하고 주변부 플라즈마에 노출된 바이어스 전극의 직경을 바꾸었을 때, 운전 압력 및 바이어스 전류 변화에 따른 이온빔 전류 변화를 측정하였다. 바이어스 전극의 노출 면적의 직경이 3 mm 일 때, 최대 인출 전류는 6.4 mA로 양전극 국부 플라즈마가 없었을 때보다 최대 40배 이상 증가하였다. 기존 양전극 국부 플라즈마 이온원에서 이온빔 전류 변화는 바이어스 전류에 비례한다고 알려졌다. 그러나 같은 바이어스 전류에서, 바이어스 전극의 노출 면적과 인출구 면적 비율을 변화에 따라 이온빔 전류 또한 변화할 뿐만 아니라 바이어스 전극의 노출 직경이 클수록 최적 운전 압력은 감소하였다. 바이어스 전류를 증가시켰

을 시, 이온 빔 전류는 비선형적으로 증가하는 구간이 발생하는 데, 이는 양전극 국부 플라즈마의 크기가 바이어스 전류에 따라 변화하기 때문이다. 따라서 양전극 국부 플라즈마의 크기와 바이어스 전극 노출 직경의 비율은 최적 빔 인출 조건을 결정할 뿐만 아니라, 양전극 국부 플라즈마의 유지 조건으로 제시될 수 있으며, 바이어스 전류와 더불어 양전극 국부 플라즈마의 주요 운전 변수로 고려되어야 한다.

이에 운전 압력 및 바이어스 전류 변화에 따른 양전극 국부 플라즈마의 크기 및 플라즈마 특성 변화를 측정 및 분석하였다. 운전 압력이나 바이어스 전압의 증가는 주변부 플라즈마의 밀도나 중성 입자의 밀도를 증가시키는 요인으로 작용한다. 운전 압력이나 바이어스 전압을 증가시켰을 시 공통적으로 이중 쉬스 전압은 감소하고, 바이어스 전류는 증가한다. 그러나 양전극 국부 플라즈마는 각 운전 변수 변화에 따라 다른 양상을 보이는 데, 운전 압력이 증가할 시에는 그 크기가 감소하지만, 바이어스 전압 증가 시에는 팽창한다. 양전극 국부 플라즈마는 운전 변수의 변화로 인해 발생한 외부 변수의 변화를 상쇄시키기 위해 국부 플라즈마의 자체 부피를 조절하여 내부 총 이온화율을 일정하게 유지하기 때문이다. 양전극 국부 국부 플라즈마 내에서의 이온 생성 및 손실의 평형 조건을 바탕으로 양전극 국부 플라즈마 크기를 운전 변수와 주변부 플라즈마 특성 변수로 표현하여, 양전극 국부 플라즈마의 크기와 운전 변수와 상관관계를 파악하였다.

이온 빔 인출을 고려한 양전극 국부 플라즈마의 입자 평형 모델을 제시하였다. 양전극 국부 플라즈마를 해석하는 데 있어서 그 동안 전자를 중심으로 살펴보았지만, 이온원으로써 양전극 국부 플라즈마를 활용할 시

에는 이온의 생성 및 손실 또한 중요하기에 전자와 이온의 생성과 손실을 모두 고려할 수 있는 입자 평형 모델을 도입하였다. 인출 구가 없었을 시, 바이어스 전류 변화에 따른 플라즈마 특성을 측정 결과와 비교하였을 뿐만 아니라, 인출 구가 있었을 시 양전극 국부 플라즈마에서 빔 인출을 고려한 예측 결과와 빔 인출 실험 결과와도 비교하여 양전극 국부 플라즈마의 입자 평형 모델을 검증하였다. 이를 바탕으로 바이어스 전극 및 인출구의 크기를 변화하였을 시, 인출 구와 바이어스 전극 면적 비율이 약 2 정도에서 최대 빔 전류를 인출 가능함을 도출하였다. 또한 실험을 통해 구한 양전극 국부 플라즈마 이온원의 유지 조건을 고려하여, 운전 압력과 바이어스 전류 변화에 따른 양전극 국부 플라즈마의 크기를 예측함으로써, 고전류 이온원으로 양전극 국부 플라즈마 이온원이 이용될 시 설계 변수에 따른 운전 변수의 범위를 제시하였다.

본 연구를 통해 양전극 국부 플라즈마 이온원에서 고전류 이온원으로 활용하는 데 있어서, 양전극 국부 플라즈마의 크기와 바이어스 전극의 직경 및 인출 홀의 비율에 따라 양전극 국부 플라즈마의 유지 조건 및 운전 조건을 제시하였다. 이를 바탕으로 고전류 이온원을 넘어 대면적 이온원으로 양전극 국부 플라즈마를 적용하는 데 있어서 본 연구는 이온원 설계의 가이드 라인을 제시하는데 주요 지표로 활용될 것이다.

Keywords; 양전극 국부 플라즈마, 양전극 국부 플라즈마 이온원, 고전류 이온 빔, 양전극 국부 플라즈마 크기, 이중 쉬스, 입자평형모델,

학 번: 2010-21043